الجمهورية الجزائرية الديمقراطية الشعبية
وزارة التعليم العالي و البحث العلمي

Université Abou Bekr Belkaid
Tlemcen Algérie

جامعة أبي بكر بلقايد
تلمسان الجزائر

Faculty of Nature and Life Sciences, Earth and Universe Sciences

Department of Biology - Natural Products Laboratory (LAPRONA)

THESIS

Submitted in partial fulfillment of the requirements for the degree of Doctor of Philosophy (LMD) in Biology

Specialization: **Nutrition and Health**

Presented by:

BOUTRIF Otmane

Topic

Chemical Characterization and Biological Activities of Alkaloids from *Anabasis articulata*

Presented publicly on: 08/ 06/ 2026

In front of the jury composed of:

President:	Mrs. BELARBI Meriem	Professor	University of Tlemcen
Examiners:	Mr. BELYAGOUBI Larbi	Professor	University of Tlemcen
	Mr. BENAMAR Houari	Professor	University of Oran
	Mrs. ZITOUNI Hanane Saida	MCA	University of Oran

Supervisor:

Mrs. BELYAGOUBI-BENHAMMOU Nabila Professor University of Tlemcen

Academic Year 2025 - 2026

ACKNOWLEDGEMENTS

This research was conducted at the Natural Products Laboratory (LAPRONA), Department of Biology, Faculty of Nature and Life Sciences, Earth and Universe Sciences (SNV-STU) at Abou Bekr Belkaïd University of Tlemcen.

I wish to express my profound gratitude to Professor BELYAGOUBI-BENHAMMOU Nabila, who supervised this thesis with exemplary scientific rigor. Her expertise, constant availability, sound advice, and high-quality guidance were instrumental in the success of this project. I extend to her my sincere appreciation.

I address my sincere thanks to Mrs. BELARBI Meriem, Professor at the University of Tlemcen, Faculty SNV-STU, Department of Biology, for the honor she bestows upon me by chairing the jury of this thesis. I thank her warmly for her support, availability, and the constant interest she demonstrates in scientific research.

My warm thanks go to Mr. BELYAGOUBI Larbi, Professor at the University of Tlemcen, Faculty SNV-STU, Department of Biology, for his valuable assistance, judicious advice, and for agreeing to examine this work.

I also thank Mr. BENAMMAR Houari, Professor at the University of Oran, for welcoming me into his laboratory. I express my deep appreciation for his scientific support and for accepting to evaluate this work as an examiner.

My thanks also extend to Mrs. ZITOUNI Hanane Saida, Assistant Lecturer in Pharmacy at the University of Oran, for agreeing to examine the content of this thesis.

I also wish to thank Mr. CHABANE SARI Daoudi and Mrs. HADDOUCHI-CHAOUECH Farah, Professors at the University of Tlemcen, Faculty SNV-STU, Department of Biology, for their assistance and valuable advice throughout this work.

I warmly thank the entire team at the Natural Products Laboratory (LAPRONA) where I conducted this research, as well as my colleagues: Dr. ABBOU Fayza, Dr. BENMAHIEDDINE Assia, Dr. HACI Imadeddine, Imane, Meriem, Nabila, Wafaa, Asma,

Dounia, not forgetting Wahiba -may Allah have mercy on her- for their help, kindness, and collaboration. My gratitude extends to the laboratory engineers and technicians for their services and valuable contributions.

My profound thanks go to Mr. GISMONDI Angelo, Professor at the University of Rome 'Tor Vergata', for his dedication and enlightened counsel from the beginning to the completion of this work, as well as to his entire team at the Botany Laboratory of the Department of Biology.

I sincerely thank Mr. Erdi Can AYTAR, Research Assistant at the Department of Horticulture, University of Usak, Turkey, for his valuable contribution to the molecular modeling section of this work. His expertise and collaboration were of great value to this research.

Finally, I express my appreciation to all those who contributed, directly or indirectly, to the development of this work.

DEDICATIONS

It is through the grace of الله, Almighty God, who gave me the courage, strength, and perseverance necessary to accomplish this work, that I dedicate this thesis:

To my dearest parents, for their unconditional love and countless sacrifices. Your unwavering support, precious advice, constant encouragement, and prayers have been the cornerstone of my success throughout my academic journey. Without your dedication, patience, and the trust you placed in me, this work would never have been possible. No words can express all my gratitude and appreciation. May Allah grant you a long life, health, and happiness. I love you infinitely.

To my dear wife, my confidante, and my source of inspiration. Your presence by my side, your unwavering support and your constant encouragement have been essential to the completion of this work. You followed every step of this journey with care and kindness. I hope to make you proud and to show you every day my gratitude for all that you bring to my life.

To my dear brother Mohamed, thank you for always being there, for being a friend as much as a brother. To my two dear sisters, thank you for your affection and support. To my nephews Nada and Iyad, you brighten our lives. I love you all enormously.

To my in-laws, thank you for your warm welcome, your steadfast support, and your comforting presence. Your encouragement has been a precious source of motivation. May God protect you and shower you with happiness.

To all my family, to all my friends, and to all those who contributed, directly or indirectly, to the development of this work. Your presence in my life has made all the difference.

Otmane

ملخص

يكشف هذا البحث عن الإمكانيات العلاجية لـ *Anabasis articulata* من خلال الاستكشاف الكيميائي النباتي والدوائي المنهجي لأجزاء الهوائية. خضع المستخلص الخام وأربعة أجزاء مميزة (A، B، C، D) لتقييم دقيق في المختبر من خلال اختبارات متعددة لمضادات الأكسدة (DPPH-، TAC و ABTS، FRAP واختبارات تثبيط الحراري BSA)، واختبارات تثبيط ألفا-أميليز، بالإضافة إلى تقييم مضاد للالتهابات في الجسم الحي نموذج مخلب الفأر المُستحث بالكاراجينان. تم فحص 36 جزءًا فرعيًا مستمَدًا من الجزء C الذي بالفلوريدات للمتحقق من أنشطتها البيولوجية باستخدام تقييم DPPH المضاد للأكسدة، وتم تحليها باستخدام تقنية كروماتوغرافيا GC / SM لتحديد محتواها من الفلوريدات. ثم التعرف لأول مرة على ستة فلوريدات تنتمي إلى ثلاث عائلات هي رباي هيدروكسيروزينولين، فيتينيتيامين، وإندول-فلوريدات. في ثبات، أظهر المستخلص الخام أعلى نشاط مضاد للأكسدة في اختبارات TAC و FRAP ومن اللافت النظر أن الجزء **C** أظهر تأثيرات مضادة للالتهابات بشكل ملحوظ، محققاً أقصى قدر من التثبيط عند جرعة 150 ملغم/كم من وزن الجسم، متجاوزًا بذلك ديكلوفيناك (50 ملغم/كم من وزن الجسم) المستخدم كمادة ضابطة. أظهرت المستخلصات تأثيرات مضادة للالتهابات ومضادات السكرية (BSA) وتثبيطًا ملحوظًا للنشاط الحاسوبية باستخدام ثلاثة أهداف بروتينية رئيسية (BRMS1 و COX-2، EDA-A2) لإزايق ألفا-أميليز، مما يُبرز إمكاناتها المضادة للالتهابات ومضادات السكري. أكدت دراسات الالتحام الجزيئي الحاسوبية باستخدام 2-ميثيل-1,2,3,4-تيترادرو-بيتا-كاربونيل، وديهيدروسالسوليدين، وكاريوجين أكثر أهمية بناءً على أدنى قيمة للارتباط (Ki).

تصنع هذه النتائج الشاملة *Anabasis articulata* كمصدر واعد لمركبات الطويلة النشطة بيولوجيًا للتطبيقات العلاجية، وخاصةً في إدارة الإجهاد التأكسدي، والحالات الالتهابية، وداء السكري، مما يدعم تطوير استراتيجيات جديدة للأمراض الالتهابية.

الكلمات المفتاحية: *Anabasis articulata* ، القلويدات، الأنشطة البيولوجية، GC/MS، الإرساء الجزيئي.

Abstract

This investigation unveils the therapeutic potential of *Anabasis articulata* through systematic phytochemical and pharmacological exploration of its aerial parts. The crude extract and four distinct fractions (A, B, C, and D) underwent rigorous in vitro assessment via multiple antioxidant assays (DPPH, ABTS, FRAP, and TAC), BSA heat denaturation inhibition, and α-amylase inhibition tests, complemented by *in vivo* anti-inflammatory evaluation using the carrageenan-induced rat paw edema model. A total of 36 sub-fractions derived from the alkaloid-rich fraction C were screened for biological activities using DPPH antioxidant evaluation and analyzed by Gas Chromatography-Mass Spectrometry to characterize their alkaloid content. Six alkaloids belonging to three families—tetrahydroisoquinolines, phenethylamines, and indole-alkaloids—were identified for the first time in *A. articulata*. The crude extract demonstrated the highest antioxidant activity in FRAP and TAC assays, while the alkaloid-rich fraction C excelled in DPPH and ABTS tests. Remarkably, fraction C exhibited significant anti-inflammatory effects, achieving maximum inhibition at 150 mg/kg body weight, surpassing diclofenac (50 mg/kg BW) used as a positive control. The extracts also showed protective effects against BSA denaturation and notable α-amylase inhibition, highlighting their anti-inflammatory and antidiabetic potential. *In silico* molecular docking studies with three key protein targets (COX-2, EDA-A2, and BRMS1) confirmed the anti-inflammatory activity, with 2-Methyl-1,2,3,4-tetrahydro-beta-carboline, Dehydrosalsolidine, and Carnegine exhibiting the most significant activity based on lowest binding and Ki values. These comprehensive findings position *A. articulata* as a promising source of bioactive alkaloid compounds for therapeutic applications, particularly in managing oxidative stress, inflammatory conditions, and diabetes, supporting the development of new therapeutic strategies for inflammation-based pathologies.

Keywords: *Anabasis articulata*, Alkaloids, Biological activities, Gas Chromatography-Mass Spectrometry (GC-MS), Molecular docking.

Résumé

Cette investigation révèle le potentiel thérapeutique d'*Anabasis articulata* à travers une exploration phytochimique et pharmacologique systématique de ses parties aériennes. L'extrait brut et quatre fractions distinctes (A, B, C et D) ont été soumis à une évaluation rigoureuse *in vitro* via de multiples essais antioxydants (DPPH, ABTS, FRAP et TAC), l'inhibition de la dénaturation thermique de la BSA et des tests d'inhibition de l'α-amylase, complétés par une évaluation anti-inflammatoire *in vivo* utilisant le modèle d'œdème de la patte de rat induit par la carragénine. Un total de 36 sous-fractions dérivées de la fraction C riche en alcaloïdes ont été criblées pour leurs activités biologiques en utilisant l'évaluation antioxydante DPPH et analysées par chromatographie en phase gazeuse couplée à la spectrométrie de masse (CG-SM) pour caractériser leur contenu en alcaloïdes. Six alcaloïdes appartenant à trois familles—tétrahydroisoquinoléines, phénéthylamines et alcaloïdes indoliques—ont été identifiés pour la première fois dans *A. articulata*. L'extrait brut a démontré l'activité antioxydante la plus élevée dans les essais FRAP et TAC, tandis que la fraction C riche en alcaloïdes a excellé dans les tests DPPH et ABTS. Remarquablement, la fraction C a exhibé des effets anti-inflammatoires significatifs, atteignant une inhibition maximale à 150 mg/kg de poids corporel, surpassant le Diclofénac (50 mg/kg PC) utilisé comme contrôle positif. Les extraits ont également montré des effets protecteurs contre la dénaturation de la BSA et une inhibition notable de l'α-amylase, soulignant leur potentiel anti-inflammatoire et antidiabétique. Des études d'amarrage moléculaire in silico avec trois cibles protéiques clés (COX-2, EDA-A2 et BRMS1) ont confirmé l'activité anti-inflammatoire, avec le 2-Méthyl-1,2,3,4-tétrahydro-bêta-carboline, la Déhydrosalsolidine et la Carnégine présentant l'activité la plus significative sur la base des valeurs de liaison et Ki les plus faibles.

Ces résultats exhaustifs positionnent *A. articulata* comme une source prometteuse de composés alcaloïdes bioactifs pour des applications thérapeutiques, particulièrement dans la gestion du stress oxydatif, des conditions inflammatoires et du diabète, soutenant le développement de nouvelles stratégies thérapeutiques pour les pathologies à base inflammatoire.

Mots-clés : *Anabasis articulata*, Alcaloïdes, activités biologiques, Chromatographie en Phase Gazeuse-Spectrométrie de Masse (CG-SM), Docking moléculaire.

Scientific production

- **International publications**
  - **Plant Biosystems (2024)**

    Title: Antioxidant and *in vivo* anti-inflammatory properties of alkaloid-rich fractions from the aerial parts of the Algerian *Anabasis articulata*.

    Authors: Otmane Boutrif, Nabila Belyagoubi-Benhammou , Assia Benmahieddine, Fayza Abbou, Gabriele Di Marco, Alessia D'Agostino, Antonella Canini and Angelo Gismondi.
  - **Plant Biosystems (2024)**

    Title: Enzyme inhibitory, antioxidant and anti-inflammatory activities of *Anabasis articulata* phenolic-rich extract; *in vitro, in vivo,* and *in silico* studies

    Authors: Dounia Ben Menni, Nabila Belyagoubi-Benhammou, Imane Abdelli, Sohayb Bekkal Brikci, Assia Benmahieddine, Hanane Ben Menni, **Otmane Boutrif**, Angelo Gismondi, Gabriele Di Marco, Alessia D'Agostino, Antonella Canini, Houari Benamar, Mohammad Saeed Kharazmi, Miguel Angel Prieto Lage and Seid Mahdi Jafari.
  - **Plant Biosystems (2026)**

    Title: *In vitro* and *in silico* evaluation of antioxidant, antidiabetic, and anti-inflammatory activities of alkaloids from *Anabasis articulata*

    Authors: Otmane Boutrif, Nabila Belyagoubi-Behnhammou, Erdi Can Aytar, Fayza Abbou, Imane Ghellai and Angelo Gismondi.
- **International Communications**

Sixth MGIBR International Workshop of Aromatic, Medicinal and condiment plants Virtues and development prospects, held in 21-22 December 2020, Tlemcen university, Algeria : Evaluation de l'activité antioxydante des fractions d'alcaloïdes d'*Anabasis articulata.*

Otmane Boutrif, Nabila Belyagoubi-Benhammou, Assia Benmahieddine, Dounia Ben Menni, Fawzia Atik Bekkara.

- **National Communications**

National Association of Algerian Teachers and Researchers, The 6th edition of PhD students day held in 05 march 2019 Oran university, Algeria: Étude phytochimique et activité antioxydante de l'extrait brut et ses fractions de l'algue brune *Sargassum vulgare* récoltée du littoral Ouest-Algérien (Île De Rachgoun).

Otmane BOUTRIF, Nabila BENHAMMOU-BELYAGOUBI.

List of tables

Table 1. Characteristics of crude extract of the aerial part of *A. articulata* and their obtained fractions……22

Table 2. Phytochemical screening of the crude extract of the aerial part of *A. articulata* and its obtained fractions……24

Table 3. Alkaloids of *A. articulata* subfractions characterised through GC-MS with their retention time (min)……..30

Table 4. Antioxidant activities of the extracts of *A. articulata* obtained by four *in vitro* assays (DPPH, ABTS, FRAP, and TAC). Selected standard antioxidants (i.e. ascorbic acid, BHA, and trolox) were also subjected to the same analyses……..34

Table 5. Results of DPPH radical scavenging activity test carried out on the 36 subfractions (SF) of *A. articulata*. ……..…….35

Table 6. ADMET values estimated for *A. articulata* alkaloids……50

Table. 7 Results of the binding interactions between alkaloidal compounds and selected target proteins……..……53

Table 8. Predicted interactions in docked conformations between *A. articulata* alkaloids and human selected proteins……...…….54

List of figures

Figure 1. Photograph of *Anabasis articulata* (personal photo)……3

Figure 2. *A. articulata* crude extract (E) and relative fractions (A-D) separated on TLC. a) Exposure of TLC to Dragendorff's reagent; b) visualization of the TLC plates under UV light (365 nm)……26

Figure 3. Column Chromatography under UV light (365 nm)……....27

Figure 4. *A. articulata* subfractions separated by TLC. a) Visualization under normal light; b) exposure to 365 nm UV light; c) exposure to 250 nm UV light; d) reaction with Dragendorff's reagent…….……..28

Figure 5. *A. articulata* crude extract, fractions and subfractions separated on TLC and subjected to reaction with DPPH. (A): Crude extract and derived fractions, (B and C): Subfractions…….32

Figure 6. IC_{50} values of α amylase inhibition potential of *A. articulata* extracts. The data are represented as mean SEM, n = 3. Statistical significance was determined by one-way ANOVA followed by Tukey's post hoc test. *p < 0.05, **p < 0.01, ***p < 0.001, **ns**: not significant (p > 0.05) vs Acarbose as positive control…….42

Figure 7. Percentage of inhibition of BSA denaturation by *A. articulata* extracts at concentrations ranging from 0.25 to 2 mg/mL. Diclofenac was used as a reference standard. Statistical significance was expressed with respect to the respective Diclofenac sample……44

Figure 8. IC_{50} values (mg/mL) relative to the anti-inflammatory activity of *A. articulata* extracts and Diclofenac (standard drug) assessed by the BSA denaturation test. Significance was shown for the samples vs. Diclofenac. Fraction D showed negligible and indeterminable activity……..…44

Figure 9. Percentage of edema volume after treatment with control (tween 80), *A. articulata* alkaloidal extracts at 50, 100, 150, and 200 mg/Kg BW, and diclofenac (standard). The monitoring was performed every hour for 6 hours. Values are means ± SD of independent experiments (n = 5 animals per group). *p < 0.05; **p < 0.01; ***p < 0.001, compared to the control……..….47

Figure 10. Anti-inflammatory effect of *A. articulata* alkaloids (inhibition percentage) at 50, 100, 150 and 200 mg/kg during the time, in comparison with Diclofenac treatment. (n = 5 animals per group)……..……..48

Figure 11. Blood brain barrier and human intestinal absorption predictions of the selected phytochemical compounds……..…….51

Figure 12. Interactions of Carnegine with target 5IKQ: A) Aromatic surface representation B) H-Bond distribution, C) 2D ligand interaction, D) 3D representation of docked poses…….57

Figure 13. Interactions of Dehydrosalsolidine with target 1RJ8: A) Aromatic surface representation B) H-Bond distribution, C) 2D ligand interaction, D) 3D representation of docked poses…….57

Figure 14. Interactions of Salsoline with target 1RJ8: A) Aromatic surface representation B) H-Bond distribution, C) 2D ligand interaction, D) 3D representation of docked poses……..58

Figure 15. Interactions of 2-Methyl-1,2,3,4-tetrahydro-beta-carboline with target 5IKQ: A) Aromatic surface representation B) H-Bond distribution, C) 2D ligand interaction, D) 3D representation of docked poses…….58

Figure 16. Interactions of 2-Methyl-1,2,3,4-tetrahydro-beta-carboline with target 1RJ8: A) Aromatic surface representation B) H-Bond distribution, C) 2D ligand interaction, D) 3D representation of docked poses…….59

Figure 17. Interactions of 2-Methyl-1,2,3,4-tetrahydro-beta-carboline with target 4AUV: A) Aromatic surface representation B) H-Bond distribution, C) 2D ligand interaction, D) 3D representation of docked poses……59

List of abbreviations

$A_{0.5}$: Concentration required to achieve an absorbance of 0.5

ABTS: 2,2'-azinobis-3-ethylbenzothiazoline-6-sulfonic acid / 2,2'-azinobis-(3-ethylbenzothiazoline-6-sulfonate)

AAE: Ascorbic Acid Equivalent

ADMET: Absorption, Distribution, Metabolism, Excretion, and Toxicity

AMPK: AMP-activated protein kinase

ARE: Antioxidant Response Element

BBB: Blood-Brain Barrier

BHA: 3-tert-butyl-4-hydroxyanisole

BRMS1: Breast Cancer Metastasis Suppressor 1

BSA: Bovine Serum Albumin

BW: Body Weight

CAEAC: Caffeic Acid Equivalent Antioxidant Capacity

CAT: Catalase

COX: Cyclooxygenase

COX-1: Cyclooxygenase-1

COX-2: Cyclooxygenase-2

CYP: Cytochrome P450

CYP1A2: Cytochrome P450 1A2 isoform

CYP2C9: Cytochrome P450 2C9 isoform

CYP2C19: Cytochrome P450 2C19 isoform

CYP2D6: Cytochrome P450 2D6 isoform

CYP3A4: Cytochrome P450 3A4 isoform

DCM: Dichloromethane

DM: Dry Matter

DNSA: 3,5-dinitrosalicylic acid

DPPH: 2,2-diphenyl-1-picrylhydrazyl

EAA: Equivalent Ascorbic Acid

EC_{50}: Half-maximal Effective Concentration

EDA-A2: TNF family member (Ectodysplasin A2)

ET: Electron Transfer

EY: Extraction Yield

FQ: Fit Quality

FRAP: Ferric Reducing Antioxidant Power

GC-MS: Gas Chromatography-Mass Spectrometry

GI: Gastrointestinal

GLUT4 : Glucose Transporter 4

GPx: Glutathione Peroxidase

HAT: Hydrogen Atom Transfer

HCl: Hydrochloric Acid

HSD: Honest Significant Difference (Tukey's test)

IC_{50}: Half-maximal Inhibitory Concentration

IL-1β: Interleukin-1 beta

IL-6: Interleukin-6

iNOS: inducible Nitric Oxide Synthase

Ki: Inhibition Constant

LD_{50}: Median Lethal Dosage

LELP: Ligand Efficiency-dependent Lipophilicity

LLE: Ligand Lipophilic Efficiency

LOX: Lipoxygenase

MAPK: Mitogen-Activated Protein Kinase

MBC: Minimal Bactericidal Concentration

MeOH: Methanol

MIC: Minimal Inhibitory Concentration

MS: Mass Spectrometry

NF-κB: Nuclear Factor kappa B

NO: Nitric Oxide

Nrf2: Nuclear factor erythroid 2-related factor 2

NSAIDs: Nonsteroidal Anti-inflammatory Drugs

OECD: Organization for Economic Co-operation and Development

P-gp: P-glycoprotein

PDB: Protein Data Bank

PGE_2: Prostaglandin E2

PPAR-α: Peroxisome Proliferator-Activated Receptor-alpha

Rf: Retention factor

ROS: Reactive Oxygen Species

SD: Standard Deviation

SDF: Structure Data File

SE: Standard Error

SEM: Standard Error of the Mean

SMILES: Simplified Molecular-Input Line-Entry System

SOD: Superoxide Dismutase

TAC: Total Antioxidant Capacity

TCA: Trichloroacetic Acid

TE: Trolox Equivalent

TLC: Thin-Layer Chromatography

TNF-α: Tumor Necrosis Factor-alpha

TPSA: Topological Polar Surface Area

UV: Ultraviolet

WHO: World Health Organization

Summary

ACKNOWLEDGEMENTS

DEDICATIONS

ملخص

Abstract

Résumé

Scientific production

List of tables

List of figures

List of abbreviations

General introduction……..……..1

Materials and methods

1. Botanical material collection and identification ……10

2. Processing and preparation……...10

3. Chemicals……..10

4. Preparation of the crude extract and extraction of alkaloids……11

5. Yield calculations……..11

6. Phytochemical screening……...……11

6.1. Detection of phenolic compounds……..……...12

6.2. Detection of alkaloids ……..……13

7. Chromatographic methods ……..13

7.1. Column chromatography……13

7.2. Thin-layer chromatography (TLC) analysis……...14

7.3. GC-MS ……..……14

8. Biological study……14

8.1. Antioxidant activity evaluation……..14

8.1.1. DPPH thin-layer chromatography (TLC) bioautography assay……..15

8.1.2. DPPH radical scavenging assay……..15

8.1.3. Scavenging of the ABTS•+ radical……15

8.1.4. Ferric reducing antioxidant power (FRAP)……16

8.1.5. Total antioxidant capacity (TAC) ……..16

8.2. Investigation of α-amylase inhibitory activity ……..……17

8.3. Inhibition of bovine serum albumin heat denaturation assay…….……...18

8.4. *In vivo* investigations……18
8.4.1. Experimental animals……..18
8.4.2. Acute toxicity test……...19
8.4.3. *In vivo* anti-inflammatory activity ……..19
8.5. *In silico* evaluation ……20
8.5.1. ADMET and drug-likeness assessment……..20
8.5.2. Molecular docking studies……..20
9. Statistical analysis……...21
Results and discussion
1. Yield and fractionation……..22
2. Phytochemical screening……...23
- Dragendorff's detection ……. ……25
3. Column chromatography observation……..27
4. TLC analysis results interpretation……..27
5. GC-MS analysis……...……29
6. Antioxidant activity……...……31
6.1. DPPH thin-layer chromatography (TLC) bioautography assay……...……..32
6.2. DPPH radical scavenging test……...…….32
6.3. $ABTS^{\bullet+}$ cation radical scavenging test……..……37
6.4. Ferric reducing antioxidant power (FRAP)…….……..……39
6.5. Total antioxidant capacity (TAC) ……...……..40
7. Antidiabetic activity……..42
8. Inhibition of bovine serum albumin denaturation ……...…….43
9. *In vivo* investigations of toxicity.……..46
10. *In Vivo* anti-inflammatory activity ……46
11. ADMET properties ……..……..……49
12. Result of molecular docking ……..……...51
Conclusion and perspectives ……62
References ……...64
Appendices

General introduction

The use of medicinal plants has witnessed remarkable growth in recent years, driven primarily by their cultural significance, widespread availability, and economic accessibility (Ekor, 2014). Medicinal plants are widely regarded as a valuable and promising source of bioactive compounds, many of which possess significant therapeutic potential. A substantial number of plant-derived drugs have been discovered through the study of traditional remedies and indigenous knowledge systems, highlighting the critical importance of ethnobotanical research in modern pharmaceutical development (Heinrich et al., 2021). Despite remarkable advancements in synthetic chemistry, certain natural compounds derived from plants remain irreplaceable due to their unique molecular structures, complex biological activities, and often superior safety profiles compared to synthetic alternatives (Atanasov et al., 2015). These natural substances continue to play a critical role in drug development, offering solutions to complex health challenges that synthetic compounds cannot fully address, thereby underscoring the enduring relevance of medicinal plants in both traditional and contemporary healthcare systems (Newman and Cragg, 2016). In developing nations, particularly across Africa, medicinal plants continue to serve as the cornerstone of primary healthcare, with approximately 80% of the population relying on them for essential medical needs (World Health Organization, 2013). The World Health Organization estimates that over 25% of modern pharmaceutical agents contain at least one active ingredient derived from plant sources (Rates, 2001).

Algeria's diverse ecosystems, spanning Mediterranean coastal regions, Atlas Mountains, steppes, and Saharan zones, harbor an exceptionally rich medicinal flora with over 600 documented species employed in traditional medicine (Benaiche et al., 2019; Belhouala & Benarba, 2021). The country's ethnobotanical heritage represents a convergence of Berber, Arab, and Mediterranean medicinal traditions that continue to serve both rural and urban communities. Traditional preparation methods demonstrate remarkable consistency across regions, with decoctions and infusions representing 60-70% of all preparations, typically using dried or fresh leaves for digestive disorders (35-40% of citations), respiratory ailments (25-30%), and dermatological conditions (15-20%) (Baziz et al., 2020; Bouafia et al., 2021). Comprehensive multiregional surveys consistently identify Lamiaceae (mint family), Asteraceae (daisy family), and Chenopodiaceae (goosefoot family) as the most frequently cited medicinal plant families, accounting for approximately 30-40% of all medicinal species documented across different regions (Baziz et al., 2020; Belhouala & Benarba, 2021; Aouir et al., 2025) noting *Artemisia herba-alba* (white wormwood), *Marrubium vulgare* (white

horehound), and *Rosmarinus officinalis* (rosemary), which are extensively used for respiratory and digestive ailments (Belhouala & Benarba, 2021; Bouafia et al., 2021).

Chenopodiaceae family contributes important medicinal species such as *Anabasis articulata*, traditionally used for diabetes, hypertension, and inflammatory conditions across North African arid regions (Batanouny, 1999; Boulos, 2000; Belyagoubi-Benhammou et al., 2019). This family represents a distinct group of halophytic plants adapted to Algeria's saline and arid environments, predominantly found in salt depressions, coastal marshes, and desert margins (Youcef et al., 2012; Lombardi et al., 2022). More broadly, the genus *Anabasis* L., belonging to this family, comprises 28 halophytic and xerophytic species primarily distributed across Central and Southwest Asia and around the Mediterranean basin, colonizing deserts, rocky terrains, and sandy wadis (O'Leary and Glenn, 1994; Lauterbach et al., 2019). The remarkable adaptation mechanisms of *Anabasis* species to extreme environmental conditions have attracted considerable scientific interest, particularly regarding their unique secondary metabolite production as survival strategies (Goura et al., 2025). Indeed, these salt-tolerant species have developed unique phytochemical profiles contributing to their therapeutic properties. Specifically, Chenopodiaceae species share characteristic phytochemical features including predominantly quercetin, kaempferol, and isorhamnetin-based flavonoids, unique betacyanin pigments, triterpene and steroid saponins, and osmoprotective alkaloids (Afiomah and Iwuozor., 2020; Hemmami et al., 2023; Cherrada et al., 2024). Notably, environmental stress conditions enhance secondary metabolite production in these halophytes, with plants growing in high-salinity environments showing elevated flavonoid and phenolic content (Cherrada et al., 2024). Among the notable species within this family, *Chenopodium botrys* and *C. murale* contain flavonoid glycosides, essential oils, and betacyanins with anti-inflammatory and antimicrobial properties (Morteza-Semnani., 2015). Similarly, *Suaeda fruticosa* is rich in flavonoids, phenolic acids, and triterpene saponins with antioxidant activities (Munir et al., 2014). Additionally, *Salsola* species (*S. vermiculata* and *S. kali*) contain isorhamnetin derivatives and saponins with potential antidiabetic effects (ElNaggar et al., 2022). Consequently, the therapeutic potential of Chenopodiaceae plants is supported by documented antidiabetic properties through enzyme inhibition and insulin sensitization, broad-spectrum antimicrobial activity, including against antibiotic-resistant strains, and anti-inflammatory effects with cytokine modulation supporting traditional wound healing applications (Cherrada et al., 2024). However, despite their considerable medicinal value, these plants face significant conservation challenges, including habitat degradation, climate change, overexploitation, and pollution, necessitating urgent implementation of in-situ

conservation, sustainable harvesting protocols, and community engagement strategies (Kaur et al., 2022; Hemmami et al., 2023; Aftab et al., 2025).

Our particular interest within the *Anabasis* genus is *Anabasis articulata* (Forssk.) Moq., locally known as "El-Ajrem," "Eshnan," or "Ramth," is a highly resilient, salt-tolerant desert subshrub characterized by its distinctive morphological features. The plant presents as a low-growing bush with a thick, twisted rootstock and pale bluish-green coloration. Its branches are articulated and nearly leafless, exhibiting a notable adaptation mechanism whereby terminal branches die and fall at the plant's base during periods of extreme drought (Ozenda, 2004). The leaves are opposite with very short free portions, either obtuse or terminated by a whitish point. The flowers, ranging from white to pink, appear solitary in the axil of each leaf. The fruit is distinctive, surrounded by three wing-like structures formed by the enlargement of three sepals (Ozenda, 2004).

Figure 1. Photograph of *Anabasis articulata* (February 20019, flowering period, Beni Abbes region).

A. articulata has been widely used in traditional medicine across North African and Middle Eastern regions for treating various ailments. In Algerian folk medicine, the leaves and roots are consumed as infusions or decoctions, either alone or combined with other plant species, to treat diabetes, fever, headache, gastrointestinal disorders, inflammatory conditions, and skin diseases such as eczema (Hammiche and Maiza, 2006). The therapeutic properties of *A. articulata* are attributed to its richness in diverse classes of bioactive phytochemicals which investigations have revealed the presence of saponins, which have demonstrated strong antidiabetic effects (Kambouche et al., 2009); alkaloids including isoquinoline derivatives, indole alkaloids, and phenethylamine compounds, which possess potent antioxidant and

antimicrobial activities (Bellakhdar et al., 1991; Said et al., 2002; Belyagoubi-Benhammou et al., 2019); and sterols exhibiting antiradical, antityrosinase, anti-acetylcholinesterase, and anti-inflammatory properties (Ben Menni et al., 2022). Several scientific studies have documented the diverse biological activities of *A. articulata*. The phenolic components have demonstrated significant antioxidant properties (Benhammou et al., 2013; Forni et al., 2019). Additional bioactivities include larvicidal effects (Sathiyamoorthy et al., 1997), hepatoprotective properties (Azza et al., 2014; Mohamed et al., 2014), and anti-inflammatory activities (Abdallah et al., 2014). Regarding anti-inflammatory mechanisms, Abdallah et al. (2014) documented the capacity of *A. articulata* to reduce prostaglandin E2 (PGE2) and tumor necrosis factor-alpha (TNF-α) levels and to inhibit cyclooxygenase-2 (COX-2) activity. Benzineb et al. (2019) demonstrated significant antimicrobial potential, while El Dine et al. (2019) showed that the n-butanol fraction exhibited strong agonistic activity toward the peroxisome proliferator-activated receptor-alpha (PPAR-α) in human hepatoma (HepG2) cells, suggesting potential applications in metabolic disorders. Most recently, Monteleone et al. (2024) highlighted the antiproliferative, antimetastatic, and anti-invasive actions of the *A. articulata* aqueous extract against the MDA-MB-231 breast cancer cell line.

Among the diverse array of plant secondary metabolites, alkaloids represent one of the most pharmacologically significant classes of natural compounds. These nitrogen-containing organic compounds are characterized by their basic properties and remarkable structural diversity (Aniszewski, 2007). Notably, alkaloids are widely distributed throughout the plant kingdom, with 27,683 alkaloids included in the Dictionary of Natural Products (Varela et al., 2023) representing approximately 20% of all known natural products (Thawabteh et al., 2019). Historically, alkaloids have played a pivotal role in the development of modern medicine, serving as the structural basis for numerous therapeutic agents, including morphine, codeine, quinine, atropine, and vinblastine (Cushnie et al., 2014; Newman & Cragg, 2020; Heinrich et al., 2021). Indeed, the biological activities of alkaloids are extraordinarily diverse, encompassing analgesic, anti-inflammatory, antimicrobial, anticancer, antidiabetic, and antioxidant properties (Zhang et al., 2015; Mondal et al., 2019; Heinrich et al., 2021; Ferreira et al., 2022) This remarkable pharmacological versatility stems from their ability to interact with multiple biological targets, including enzymes, receptors, ion channels, and nucleic acids (Matsuura & Fett-Neto, 2015; Atanasov et al., 2015).

Within the Chenopodiaceae family specifically, alkaloids include isoquinoline alkaloids, indole alkaloids, and phenethylamine derivatives, many of which exhibit potent biological

activities (Tundis et al., 2009; Shegebayev et al., 2023; Amtaghri et al., 2025). The alkaloid chemistry of *A. articulata* aligns with broader patterns observed across this family, where related genera such as Salsola and Hammada also produce structurally similar bioactive alkaloids with comparable pharmacological activities (Tundis et al., 2009; Bouaziz et al., 2016; Shegebayev et al., 2023). This convergent alkaloid production across halophytic Chenopodiaceae species suggests evolutionary adaptation to harsh environmental conditions while simultaneously providing chemical defense mechanisms and bioactive compounds of potential therapeutic value. More specifically, phytochemical investigations using gas chromatography-mass spectrometry (GC/MS) analysis have revealed that *A. articulata* contains diverse alkaloid classes, with anabasine (3-(2-piperidinyl)pyridine) identified as the predominant alkaloid, alongside significant quantities of nicotine and several minor related compounds, particularly in stems and aerial portions (Benhammou et al., 2013; Belyagoubi-Benhammou et al., 2019).

Consequently, the alkaloid-rich fractions from *A. articulata* have demonstrated remarkable biological activities that validate traditional therapeutic applications. These include potent antimicrobial effects against both Gram-positive and Gram-negative bacterial pathogens, significant antioxidant properties through free radical scavenging mechanisms, and notable enzyme inhibitory activities relevant to diabetes management (Benhammou et al., 2013; Belyagoubi-Benhammou et al., 2019; Al-Joufi et al., 2022). Furthermore, anti-inflammatory properties have been documented through various in vitro experimental models, supporting the traditional use of this species for inflammatory conditions (Makhlouf et al., 2024).

Given these promising findings, the therapeutic potential of alkaloids continues to drive intensive research efforts aimed at discovering novel bioactive compounds from underexplored plant species, particularly those with traditional medicinal uses (Atanasov et al., 2015; Newman & Cragg, 2020).

Among the various pathological conditions where plant-derived alkaloids show therapeutic promise, oxidative stress has emerged as a critical factor in the pathophysiology of numerous chronic diseases, including atherosclerosis, cancer, diabetes mellitus, rheumatoid arthritis, cardiovascular disorders, neurodegenerative diseases, and aging-related conditions (Phaniendra et al., 2015). Oxidative stress arises from an imbalance between pro-oxidant and antioxidant systems, resulting in excessive production of reactive oxygen species (ROS) that

cause damage to lipids, proteins, and nucleic acids (Sies, 2015). Accumulating evidence suggests that oxidative stress plays a crucial role in initiating and perpetuating inflammatory responses, thereby contributing to the development of chronic inflammation-associated diseases (Mittal et al., 2014). The interconnection between oxidative stress and inflammation creates a vicious cycle that perpetuates tissue damage and disease progression, making antioxidant interventions a promising therapeutic strategy (Hussain et al., 2016). In this context, plant-derived alkaloids have demonstrated significant antioxidant properties through multiple mechanisms. Specifically, alkaloids from various plant sources exhibit free radical scavenging activity, metal chelation capacity, and enhancement of endogenous antioxidant enzyme systems, including superoxide dismutase (SOD), catalase (CAT), and glutathione peroxidase (GPx) (Mirkov et al., 2020; Mahomoodally et al., 2022). Moreover, certain alkaloids have been shown to activate the Nrf2-ARE signaling pathway, a master regulator of cellular antioxidant responses, thereby upregulating the expression of cytoprotective genes (Zhang et al., 2013; Bhakkiyalakshmi et al., 2018). Furthermore, alkaloid-mediated reduction of oxidative stress has been associated with decreased inflammation markers, improved mitochondrial function, and protection against oxidative damage-induced cellular dysfunction in various experimental models (Mondal et al., 2019; Chen et al., 2023)—these multifaceted antioxidant mechanisms position alkaloids as valuable therapeutic candidates for managing oxidative stress-related pathologies.

Closely intertwined with oxidative damage, inflammation represents a complex biological response orchestrated by the immune system, characterized by vascular changes, increased vascular permeability, cellular infiltration, and the cardinal signs of redness, heat, swelling, and pain following tissue injury, infection, or noxious stimuli (Medzhitov, 2008; Ji et al., 2023). While acute inflammation serves a protective and reparative role, chronic inflammation contributes to the pathogenesis of numerous diseases, including arthritis, inflammatory bowel disease, atherosclerosis, and metabolic disorders (Furman et al., 2019). Currently available anti-inflammatory medications, particularly nonsteroidal anti-inflammatory drugs (NSAIDs) and corticosteroids, exhibit significant limitations including adverse effects and incomplete therapeutic efficacy in chronic inflammatory conditions (Sostres et al., 2010; Oray et al., 2016). Prolonged NSAID use has been associated with serious complications, most notably gastrointestinal ulceration and bleeding, cardiovascular events, hepatotoxicity, and renal dysfunction (Laine et al., 2008; Bindu et al., 2020). These limitations underscore the urgent need for alternative therapeutic agents with improved safety

profiles and efficacy. In this context, plant-derived alkaloids have emerged as promising anti-inflammatory agents through their ability to modulate multiple inflammatory pathways. Mechanistically, alkaloids exert anti-inflammatory effects by inhibiting pro-inflammatory enzymes such as cyclooxygenase (COX) and lipoxygenase (LOX), suppressing the production of inflammatory mediators including prostaglandins, leukotrienes, and nitric oxide (NO), and downregulating pro-inflammatory cytokines such as TNF-α, IL-1β, and IL-6 (Leite et al., 2014; Hashmi et al., 2018; Ferreira et al., 2022). Additionally, alkaloids interfere with key inflammatory signaling cascades, particularly the NF-κB and MAPK pathways, thereby preventing the nuclear translocation of transcription factors responsible for inflammatory gene expression (Luo et al., 2009; Yang et al., 2021). These multifaceted anti-inflammatory mechanisms position plant alkaloids as valuable candidates for developing safer and more effective therapeutic alternatives to conventional anti-inflammatory drugs. The anti-inflammatory activity of *A. articulata* alkaloids has been validated through in vivo experimental models, particularly using the carrageenan-induced rat paw edema test, a well-established acute inflammation model. These findings have been further supported by recent studies demonstrating that *A. articulata* fractions effectively reduce inflammatory responses through protein denaturation inhibition and membrane stabilization mechanisms (Makhlouf et al., 2024).

Building upon the previously discussed antioxidant and anti-inflammatory properties of alkaloids, these natural compounds also demonstrate remarkable antidiabetic potential, positioning them as multi-targeted therapeutic agents. Diabetes mellitus represents a major global health challenge, with type 2 diabetes accounting for approximately 90% of cases, characterized by insulin resistance and progressive pancreatic β-cell dysfunction (Kahn, 2003; Saeedi et al., 2019; American Diabetes Association, 2021). Currently, one established therapeutic approach involves inhibiting carbohydrate-digesting enzymes, particularly α-amylase and α-glucosidase, which hydrolyze complex carbohydrates into absorbable glucose, thereby delaying glucose absorption and reducing postprandial hyperglycemia (Bischoff, 1994). However, synthetic enzyme inhibitors such as acarbose are associated with adverse gastrointestinal effects including flatulence, diarrhea, and abdominal discomfort (Bischoff, 1994; Sales et al., 2012). Therefore, plant-derived alkaloids offer promising alternatives with improved safety profiles. In this regard, alkaloids exert their antidiabetic effects through multiple complementary mechanisms. Primarily, they inhibit α-glucosidase and α-amylase enzymes by binding to their active sites, thereby preventing carbohydrate breakdown (Kumar

et al., 2011; Salehi et al., 2019). Additionally, alkaloids enhance insulin secretion from pancreatic β-cells, improve insulin sensitivity in peripheral tissues, modulate glucose transporters (particularly GLUT4), and activate AMP-activated protein kinase (AMPK), a master regulator of cellular energy homeostasis (Salehi et al., 2019; Amssayef et al., 2023; Seal et al., 2024). Moreover, various alkaloid classes have demonstrated potent antidiabetic properties, including isoquinoline alkaloids such as berberine, which show glucose-lowering effects through AMPK activation (Yin et al., 2008; Xu et al., 2014), indole alkaloids with insulin secretagogue properties (Christodoulou et al., 2019), and piperidine alkaloids exhibiting α-glucosidase inhibitory activity (Kumar et al., 2013).

In addition to experimental validation, molecular docking has emerged as a powerful computational tool complementing biological assays by predicting binding interactions between alkaloids and their therapeutic targets at the molecular level (Kitchen et al., 2004; Meng et al., 2011; Ferreira et al., 2015).

Specifically, docking studies have elucidated the binding mechanisms of various alkaloid classes with diabetes-related enzymes, including berberine's interactions with α-glucosidase and α-amylase, revealing strong binding affinities that correlate with experimental enzyme inhibitory activities (Das et al., 2023). Similarly, computational analyses have demonstrated alkaloid interactions with insulin signaling proteins and AMPK, supporting their insulin-sensitizing effects (Behl et al., 2022), as well as their binding to COX and NF-κB proteins, confirming anti-inflammatory mechanisms (Reddi et al., 2021; Bar et al., 2022). Thus, the integration of molecular docking, ADMET predictions, and experimental validation provides a comprehensive framework for advancing alkaloid compounds from traditional medicinal plants toward evidence-based therapeutic development (Rocha et al., 2018).

Despite these preliminary findings and the ethnomedicinal importance of *A. articulata*, comprehensive pharmacological studies investigating the biological activities of its alkaloid constituents, particularly their antioxidant, anti-inflammatory, and antidiabetic properties, remain limited. This underscores the need for systematic scientific investigation to validate traditional uses and elucidate the molecular mechanisms underlying the therapeutic potential of this plant species. The present study was designed to achieve the main objective to address the knowledge gap concerning the alkaloid phytochemical composition of *A. articulata* and to assess, for the first time, its anti-inflammatory and antidiabetic potential using an integrative strategy that combines in vitro and in vivo biologicals tests with molecular docking investigations, thereby providing scientific validation for its traditional applications.

And to achieve this, we will follow the following steps:

- Extraction and fractionation of bioactive compounds from *A. articulata* aerial parts using sequential solvent extraction with organic solvents of varying polarity
- Qualitative identification of alkaloid compounds in plant fractions using thin-layer chromatography (TLC) coupled with Dragendorff's reagent detection and gas chromatography-mass spectrometry (GC-MS) analysis
- Comprehensive evaluation of in vitro antioxidant capacity using multiple complementary assays including DPPH radical scavenging, ABTS radical cation decolorization, ferric reducing antioxidant power (FRAP), and total antioxidant capacity (TAC) assays
- Assessment of antidiabetic potential through α-amylase enzyme inhibition assays using the chromogenic dinitrosalicylic acid (DNSA) method
- Investigation of in vitro anti-inflammatory activity using the protein denaturation inhibition assay with bovine serum albumin (BSA) as a model system
- Assessment of acute toxicity and safety profiles of the alkaloid-rich fraction in accordance with OECD guidelines
- Evaluation of in vivo anti-inflammatory effects using the carrageenan-induced paw edema model in experimental rats
- Molecular docking studies to predict binding interactions between identified alkaloid compounds and relevant protein targets implicated in inflammation and oxidative stress
- ADMET profiling of identified alkaloids to evaluate their drug-likeness and pharmacokinetic properties

Materials and methods

1. Botanical material collection and identification

This study was conducted in the Natural Products research laboratory (LAPRONA) at the University of Tlemcen.

The plant material (roots, stems, and leaves) was harvested in early February 2019 in Beni Abbès region, within the Béchar Province (Western Algeria). The harvested plant species was identified by the Plant Ecology Laboratory at the Department of Biology, University of Tlemcen, under the supervision of Professor Hassiba BOUDGHEN STAMBOULI.

Anabasis articulata specimens have been archived with the identification number "L. 754" in the herbarium of the Natural Products Laboratory (LAPRONA), Faculty of Natural and Life Sciences, Earth and Universe, Abou-Bekr Belkaid University Tlemcen, Algeria.

2. Processing and preparation

The aerial parts of *A. articulata* were utilized for all analytical procedures. This plant fraction was selected based on its documented use in traditional medicine, suggesting a high concentration of bioactive compounds of interest. Prior to analysis, the plant material underwent thorough washing followed by a 15-day shade-drying process to prevent photochemical degradation. Immediately before each analytical procedure, the dried material was manually ground using an agate mortar to avoid thermal degradation of heat-sensitive compounds that might occur with mechanical grinding devices.

3. Chemicals

Petroleum ether, ethanol, methanol, chloridric acid, hexane, acetone, ammonium hydroxide, chloroform, 2,20-azinobis-3-ethylbenzothiazoline- 6-sulfonic acid (ABTS), 2,2-diphenyl-1 -picrylhydrazyl (DPPH), potassium persulfate, 3-tert-butyl-4-hydroxyanisole (BHA), trolox (6-hydroxy-2,5,7,8-tetramethylchroman-2-carboxylic acid), sulfuric acid, sodium phosphate, ammonium molybdate, ascorbic acid, ferricyanide, trichloracetic acid, ferric chloride, trichloroacetic acid (TCA), bovine serum albumin (BSA), Tris-HCL, α-amylase (from porcine pancreas, EC 3.2.1.1), 3,5-dinitrosalicylic acid (DNSA), NaOH, NaCl, carrageenan and diclofenac sodium salt were purchased from Sigma (St. Louis, USA). Tween 80 was provided by Pharmalliance (Algiers, Algeria). All remaining chemicals used in this work were of analytical grade and were also purchased from Sigma.

4. Preparation of the crude extract and extraction of alkaloids

Eight hundred grams of *A. articulata* powder were defatted with petroleum ether for 24 hours. After filtration and air-drying, the defatted powder was resuspended under agitation in 1.2 L of ethanol at room temperature for 72 hours. The crude ethanolic extract (E) was obtained by filtering the mixture through Whatman filter paper and removing the solvent using a rotary evaporator at 40°C.

The extraction of alkaloids procedure followed the protocol of Benamar et al. (2016) with minor modifications. Briefly, the crude extract **(E)** was resuspended in 200 mL of 2 M HCl for 30 min and then filtered. The aim of adding HCl is because of the properties of alkaloid which is base. Therefore, it should be extracted in the acid solvents according to Harbourne, J., (1996) and Parbuntari (2018). The insoluble residue retained on the filter was extracted with 250 mL of acetone to yield the acetone fraction **(A)**. Meanwhile, the acidic filtrate was washed twice with 200 mL of n-hexane to isolate the fraction **(B)**. The acid phase was then basified to pH 9.8 by adding 100 mL of 25% NH4OH. Subsequent liquid-liquid extractions were performed twice with CHCl3: MeOH (3:1, v/v) and once with pure CHCl3, yielding the chloroform fraction **(C)**, enriched in alkaloids. The remaining alkaline aqueous phase constituted the final fraction **(D)**. All extracts were evaporated and stored at 4°C until further use in *in vitro* and *in vivo* studies.

5. Yield calculations

The extraction yield (EY) of all extracts and fractions was determined using the following formula:

$$EY\ (\%) = (M_0 / M_1) \times 100$$

Where: EY: Extraction yield; M_0: Mass (in grams) of the dry residue obtained after evaporation; M_1: Mass (in grams) of the initial plant material.

6. Phytochemical screening

A comprehensive phytochemical screening was conducted on the extracts derived from *A. articulata*. The objective was to detect and characterize the diverse families of secondary metabolites present in the plant's aerial parts. The screening involved well-established qualitative assays, including coloration reactions, precipitation tests, and UV-light-based fluorescence analysis. All protocols were performed in accordance with the standardized methods outlined by Harborne (1998) and Trease et Evans, (2002), ensuring reliability and consistency in the identification of bioactive.

6.1. Detection of phenolic compounds

The alkaloids and the phenolic compounds, including tannins, flavonoids, saponins, and coumarins were qualitatively analyzed using specific colorimetric assays as described below:

- **Flavonoids**

For the identification of flavonoids, 1 mL of the extract was placed in a test tube, followed by the addition of 1 mL of concentrated hydrochloric acid (HCl) along with a few fragments of magnesium metal was added. The appearance of a pink, red, or yellow coloration was considered indicative of flavonoid content within the sample.

- **Tannins**

To detect the presence of tannins, 1 mL of the extract under analysis was transferred into a test tube, followed by the addition of 0.25 mL of a 1% aqueous solution of ferric chloride ($FeCl_3$). The mixture was incubated at room temperature for 15 minutes. The formation of a greenish or bluish-black coloration indicates the presence of tannins.

- **Saponins**

The presence of saponins was evaluated using a foam test. Ten milliliters of the sample extract were introduced into a test tube and agitated for 15 seconds. After resting for 15 minutes, the formation of a stable foam layer exceeding 1 cm in height was considered indicative of saponin content.

- **Coumarins**

Coumarins were identified using a UV fluorescence assay. Two test tubes, each containing 1 mL of the extract, were prepared. While the first tube served as a control, 0.1 mL of 10% ammonium hydroxide (NH_4OH) was added to the second tube. A single drop from each tube was applied to filter paper and observed under UV light at 366 nm. Intense fluorescence under UV illumination confirmed the presence of coumarins.

6.2. Detection of alkaloids

The identification of alkaloids in the fractions and the crude extract using the Dragendorff test was confirmed by the formation of a brownish or yellowish precipitate. This precipitate results from the formation of a complex potassium-alkaloid compound. During the

preparation of the Dragendorff reagent, bismuth nitrate is dissolved in hydrochloric acid to prevent hydrolysis, as bismuth salts are highly susceptible to hydrolysis, which can produce BiO^+ ions. Altemimi et al (2017).

❖ **Dragendorff's detection**

The TLC detection is a powerful analytical technique that combines chromatographic separation with biological activity detection. The crude extract (E) and its four derived fractions (A, B, C and D) were subjected to Dragendorff's reagent-based test to screen for the presence of alkaloids. This method is widely used for the specific detection of nitrogen-containing compounds, particularly alkaloids, due to its ability to form orange or reddish-brown precipitates upon reaction with tertiary amines. Pascual et al (2002), Fathoni et al (2021).

7. Chromatographic methods

7.1. Column chromatography

The fraction C (3g) was further purified using column chromatography. A silica gel stationary phase (40–63 μm particle size, Merck) was employed, fully packed into a glass column with dimensions of 2.5 cm internal diameter and 55 cm length. The mobile phase consisted of a gradient elution system designed to optimize the separation of alkaloids based on their polarity. The elution gradient began with pure dichloromethane (DCM), followed by stepwise increases in methanol (MeOH) concentration: DCM–MeOH ratios of 100:0, 80:20, 60:40, 50:50, 40:60, 20:80, and finally 0:100. After the DCM–MeOH gradient, the column was further eluted with 600 mL of a solvent mixture composed of toluene–acetone–ethanol–ammonia (4:4:6:1, v/v/v/v). This final solvent system was specifically chosen to enhance the elution of highly polar alkaloids that may not have been fully recovered in earlier steps. The entire elution process yielded 36 distinct sub-fractions, which were collected sequentially in labeled vials.

7.2. Thin-layer chromatography (TLC) analysis

All collected sub-fractions were subjected to thin-layer chromatography (TLC) for qualitative analysis. TLC plates coated with silica gel (Merck, 60 F254) were used as the stationary phase, and the mobile phase composition was optimized to match the polarity range of the compounds under investigation. Following development, the TLC plates were first examined under ultraviolet (UV) light at wavelengths of 250 nm and 365 nm to detect

fluorescent or UV-absorbing compounds. Subsequently, the plates were sprayed with Dragendorff's reagent. Visualization under visible light after spraying allowed for the identification of orange-brown spots indicative of alkaloid content. Retention factor (Rf) values were calculated for each detected compound to assess their relative mobility and guide further purification steps.

All samples were stored at 4 °C protected from light and moisture to prevent degradation of thermally labile or light-sensitive compounds to further analysis.

7.3. GC-MS

The sample preparation involved resuspension in 2 mL of HPLC-grade methanol (MeOH, ≥99.9% purity) with continuous agitation (200 rpm) for 6 hours at ambient temperature (25±2°C). Following extraction, samples were centrifuged at 12,000 × g for 10 minutes (Eppendorf 5430 R, Hamburg, Germany) to obtain a particle-free supernatant. Aliquots (2 µL) of the clarified extract were injected in splitless mode into a Shimadzu QP2010 Ultra GC-MS system (Kyoto, Japan) equipped with an SH-Rtx-5MS fused-silica capillary column (30 m length × 0.25 mm internal diameter × 0.25 µm film thickness; 5% phenyl/95% dimethylpolysiloxane stationary phase). The temperature program began with an initial hold at 50°C for 2 minutes, followed by a 3°C/min ramp to 200°C (held for 2 minutes), then a 4°C/min ramp to 300°C (held for 5 minutes). Ultra-high purity helium (99.999%) carrier gas was maintained at a constant flow rate of 1.0 mL/min throughout the analysis. Mass spectrometry detection employed electron impact ionization at 70 eV, scanning from 100 to 700 m/z, with the ion source at 250°C and interface at 280°C. A 6-minute solvent cut time was applied. Compounds were identified using the NIST 14 library (Solution software), with only matches showing ≥85% similarity considered valid.

8. Biological study

8.1. Antioxidant activity evaluation

In vitro assessment of the antioxidant potential of the extracts was conducted using a bioautography assay and four well-established spectrophotometric methods, selected for their reliability, reproducibility, and rapid implementation. All assays were performed in triplicate to ensure result reliability, with appropriate positive controls included in each experimental run. The following standardized protocols were employed:

8.1.1. DPPH thin-layer chromatography (TLC) bioautography assay

The antioxidant potential of *A. articulata* crude extract, its four derived fractions and all the subfractions was assessed through thin-layer chromatography (TLC) coupled with 2,2-diphenyl-1-picrylhydrazyl (DPPH•) radical scavenging bioautography. Samples (50 µg/spot) were applied to silica gel 60 F254 aluminum-backed TLC plates and developed in an appropriate solvent system. Post-chromatography, plates were uniformly sprayed with 0.25% (w/v) methanolic DPPH• solution and incubated for 30 minutes under dark conditions at ambient temperature (25 ± 2°C). Antioxidant compounds were visualized as distinct yellow zones against a purple background, resulting from the reduction of DPPH• to its corresponding hydrazine form. The appearance, intensity, and Rf values of these decolorized spots provided qualitative information about both the presence and relative polarity of antioxidant constituents within each sample (Cuendet et al. 1997; Hostettmann et al. 1997; Hostettmann 1999).

8.1.2. DPPH radical scavenging assay

The antioxidant effects of various *A. articulata* samples (fractions and subfractions) were evaluated using the DPPH• assay method described by Sanchez-Moreno et al. (1998). For each test, 50 µL of extract at different concentrations (4, 2, 1, 0.5, 0.25, 0.125, and 0.0625 mg/mL) was added to 1.950 mL of freshly prepared methanolic DPPH• solution (0.025 g/L). After 30 minutes of incubation in darkness at room temperature, absorbance was measured at 515 nm using a spectrophotometer. A negative control was prepared by mixing 50 µL methanol with 1.950 mL of the DPPH• solution at the same concentration. Ascorbic acid served as the reference antioxidant (positive control).

The percentage inhibition of DPPH• radicals was calculated using the following formula:

$$\% \text{ Inhibition} = ((A_{blank} - A_{sample}) / A_{blank}) \times 100 \quad \ldots\ldots\ldots\ldots\ldots\ldots\ldots\ldots \quad (1)$$

Where: A_{blank} is the absorbance of the blank; A_{sample} is the absorbance of the sample.

The variation in inhibition percentages as a function of extract concentrations allowed for the determination of the half-maximal inhibitory concentration (IC_{50}).

8.1.3. Scavenging of the ABTS•+ radical

The scavenging activity of the ABTS•+ radical cation (2,2'-azinobis-(3-ethylbenzothiazoline-6-sulfonate)) was assessed using the method outlined by Re et al. (1999). To prepare the ABTS•+ solution, 5 mL of a 7 mM ABTS solution was mixed with 5 mL of 2.45 mM

potassium persulfate. The resulting mixture was incubated in the dark at ambient temperature for 12–16 hours to ensure complete generation of the radical cation.

Different concentrations of each plant extract (0.0625 to 8 mg) or Trolox which served as the reference standard (40 µL) were combined with 160 µL of the diluted ABTS solution and incubated for 10 minutes. The absorbance was then measured at 734 nm. The ability to scavenge the ABTS radical cation was calculated using the same percentage inhibition formula (1) described earlier for the DPPH assay.

The results were expressed as IC_{50} values, which were extrapolated from the percentage inhibition curve.

8.1.4. Ferric reducing antioxidant power (FRAP)

The ferric reducing power was determined using the method described by Oyaizu (1986). Different concentrations of the extracts, ranging from 0.0625 to 4 mg/mL, were mixed with 2.5 mL of phosphate buffer (0.2 M, pH 6.6) and 2.5 mL of a 1% aqueous solution of potassium ferricyanide ($K_3Fe(CN)_6$). The mixture was incubated at 50°C for 20 minutes. After incubation, 2.5 mL of 10% trichloroacetic acid (TCA) was added to the mixture, which was then centrifuged at 3000 rpm for 10 minutes. The upper layer of the solution (2.5 mL) was collected and mixed with 2.5 mL of distilled water and 0.5 mL of freshly prepared 0.1% ferric chloride ($FeCl_3$).

The results were expressed as $A_{0.5}$ values, which represent the concentration of the extract required to achieve an absorbance of 0.5 against a blank sample, defining the reducing ability of the chelator (Jayaprakash et al., 2001). The $A_{0.5}$ values were determined from linear regression curves of absorbance plotted against the different concentrations of each extract. BHA and ascorbic acid were used as standards.

8.1.5. Total antioxidant capacity (TAC)

The total antioxidant capacity (TAC) was assessed according to the protocol outlined by Prieto et al. (1999). The assay is based on the reduction of molybdenum (VI) (in the form of molybdate ions, MoO_4^{2-}) to molybdenum (V) (MoO_2^{+}) in the presence of the sample extract. This reduction leads to the formation of a characteristic green-colored phosphate/Mo (V) complex, which is measured under acidic pH conditions. A volume of 0.3 mL of each extract was combined with 3 mL of a reagent solution containing 0.6 M sulfuric acid, 28 mM sodium phosphate, and 4 mM ammonium molybdate. The reaction mixtures were sealed in tubes and incubated at 95°C for 90 minutes. Following incubation and subsequent cooling, the

absorbance of the solutions was measured at 695 nm. A blank reference, prepared using 3 mL of the reagent solution and 0.3 mL of methanol, was treated identically to the test samples and used as a baseline for comparison.

The calibration curve was prepared using ascorbic acid as the reference standard, with concentrations varying between 50 and 600 µg/mL (Apendice 1). The total antioxidant capacity (TAC) was quantified and reported in terms of milligrams of ascorbic acid equivalent per gram of dry matter (mg AAE/g DM) of the extract. This procedure was repeated three times to ensure reliable and reproducible results.

8.2. Investigation of α-amylase inhibitory activity

This method evaluates the inhibitory effect of crude extracts from the studied plant and their fractions on α-amylase activity. Under alkaline conditions and heat, the oxidation of free aldehyde groups from sugars simultaneously reduces the yellow-orange 3,5-dinitrosalicylic acid (DNSA) into red-orange 3-amino-5-nitrosalicylic acid, which absorbs at 540 nm. The intensity of the coloration is proportional to the amount of reducing sugars present in the reaction medium (Thalapaneni et al., 2008).

For this study, porcine pancreatic α-amylase (E.C.3.2.1.1) was used which has a similar structure to human α-amylase. The enzyme solution used in this assay was prepared at 3.9 U/mL (corresponding to 1.3 U/mL in the reaction medium) by dissolving 3 mg of lyophilized enzyme in 10 mL of phosphate buffer (0.02 M, 6.7 mM NaCl, pH 6.9).

The substrate used was soluble starch: 1 g of soluble starch was dissolved in 100 mL of phosphate buffer solution under stirring at 50–70°C.

For the chromogenic 3,5-dinitrosalicylic acid (DNSA) solution, 30 g of sodium potassium tartrate was dissolved in 20 mL of preheated (60°C) 2N NaOH under stirring. Separately, 1 g of DNSA was dissolved in 40 mL of preheated distilled water. The two solutions were then mixed under agitation to obtain a clear yellow-orange reagent. The final volume was adjusted to 100 mL with distilled water. The resulting reagent was stored protected from light at 4°C.

The inhibitory effect was determined using the method described by Thalapaneni et al. (2008). A mixture of 200 µL of sample and 200 µL of sodium phosphate buffer (20 mM, pH 6.9, containing 6.7 mM NaCl) with α-amylase solution was incubated at 37°C for 10 minutes. After incubation, 200 µL of starch solution (1%) was added. The mixture was then incubated again at 37°C for 15 minutes, followed by the addition of 400 µL of DNSA reagent. The solution was heated in a water bath at 100°C for 5 minutes, and the absorbance was measured at 540 nm using a UV/visible spectrophotometer. An Acarbose solution (Glucobay® 50),

used as a standard at different concentrations, was prepared in phosphate buffer (pH 6.9, 0.02 M).

The inhibition percentage (I%) was calculated using formula (1).

The α-amylase inhibitory activity was expressed as IC_{50} values (µg/mL), determined from logarithmic regression curves of inhibition percentages.

8.3. Inhibition of bovine serum albumin heat denaturation assay

The anti-denaturation potential of test extracts was assessed using bovine serum albumin (BSA) as a model protein, following the method of Kandikattu et al. (2013). This approach mimics inflammatory conditions where protein denaturation occurs. Briefly, 1 mL of each extract was combined with 1 mL of 0.2% BSA solution in 50 mM Tris-HCl buffer (pH 6.6), which provides optimal physiological conditions for protein stability. After 15 min of incubation at 37°C to allow protein-extract interactions, samples were subjected to heat-induced denaturation at 72°C for 5 min to accelerate structural unfolding. Following gradual cooling to room temperature to stabilize the protein conformation, absorbance was measured at 660 nm to quantify denaturation levels. Diclofenac, a known anti-inflammatory agent, served as the reference inhibitor for comparative analysis. The percentage inhibition of protein denaturation was calculated using formula :

$$\% \text{ Inhibition} = ((A_{control} - A_{sample}) / A_{control}) \times 100$$

Where: $A_{control}$ represents the absorbance of denatured BSA without inhibitor, and A_{sample} denotes the absorbance of test samples. This quantitative approach not only allows precise evaluation of the extracts' capacity to stabilize BSA against thermal denaturation but also provides insights into their potential anti-inflammatory mechanisms. The higher the inhibition percentage, the stronger the protective effect against protein denaturation.

8.4. *In vivo* investigations

8.4.1. Experimental animals

This study utilized adult Wistar rats of both sexes, aged 8 weeks and weighing 150–200 g. The animals were obtained from the Pasteur Institute (Algiers, Algeria) and housed in well-ventilated polypropylene cages (maximum 4 rats per cage) under controlled conditions: temperature (23 ± 2 °C), 12-hour light/dark cycle, and ad libitum access to water and standard rodent diet. Prior to experimentation, the rats underwent a 7-day acclimatization period to stabilize physiological conditions. For specific experimental procedures, animals were fasted overnight with free access to water. All protocols strictly adhered to the Guide for the Care

and Use of Laboratory Animals and were approved by the Institutional Animal Ethics Committee (1205/c/08/CPCSEA, approval date: 21.04.08).

8.4.2. Acute toxicity test

Acute toxicity studies were conducted following the Economic Co-operation and Development (OECD) guidelines (Test No. 425, 2008). The experiment involved five groups of three rats each, where four treatment groups received oral administration of plant fraction C at doses of 50, 100, 150, and 200 mg/kg body weight respectively, while the control group received an equivalent volume of saline buffer. Toxicological effects, including both acute and chronic toxicities, were evaluated based on mortality rates and behavioral modifications observed over a 14-day period (24 hours to 14 days post-administration). All gross pathological changes were systematically recorded for each individual animal throughout the study period.

8.4.3. *In vivo* anti-inflammatory activity

The anti-inflammatory activity was assessed using the carrageenan-induced paw edema method described by Winter et al. (1962), which represents the most widely used protocol for screening anti-inflammatory drugs against acute inflammation. Thirty rats were randomly divided into six equal groups: Group I served as the negative control receiving only 15% Tween 80 via oral gavage, Group II functioned as the positive control treated with diclofenac sodium (50 mg/kg body weight), while Groups III-VI received 15% Tween 80 containing plant fraction C (alkaloids) at doses of 50, 100, 150, and 200 mg/kg body weight, respectively. Acute inflammation was induced by injecting 0.1 mL of 0.5% carrageenan solution into the sub-plantar region of the right hind paw one-hour post-treatment in all experimental groups. Paw thickness measurements were obtained using calipers measuring method before and immediately after carrageenan injection, with subsequent edema volume monitoring conducted hourly from the 1st to 6th hour following carrageenan administration. The percentage of increase or reduction of paw edema was calculated according to the following formulas:

$$\text{Percentage of edema increase (\%)} = (V_t - V_i / V_i) \times 100$$

$$\text{Percentage of edema inhibition (\%)} = (E_S - E_T / E_S) \times 100$$

Where: V_t is the paw volume of the rat after carrageenan injection; V_i is the paw volume of the rat before carrageenan injection; E_S is the edema increase rate of the standard group; E_T is the edema increase rate of the treated groups.

8.5. *In silico* evaluation

8.5.1. ADMET and drug-likeness assessment

To evaluate the pharmacokinetic and safety profiles of the selected phytochemicals, we conducted *in silico* predictions of their absorption, distribution, metabolism, excretion, and toxicity (ADMET) properties. The seventeen compounds were converted into SMILES (Simplified Molecular-Input Line-Entry System) notations and analyzed using SWISSADME, a validated computational platform for predicting drug-like properties. This analysis assessed critical parameters which included Lipinski's rule of five compliance (molecular weight, lipophilicity and hydrogen bond donors/acceptors), gastrointestinal absorption and blood-brain barrier permeability, metabolic stability (CYP450 enzyme interactions) and toxicity risks (mutagenicity, hepatotoxicity)

The results provide essential insights into the compounds' drug-likeness and potential for further development, supporting their selection for *in vitro* and in vivo studies (Cheng et al., 2012; Yang et al., 2019). This computational screening enhances efficiency in identifying promising candidates while minimizing costly late-stage failures in drug discovery.

8.5.2. Molecular docking studies

The 3D structures of meclofenamic acid bound to human cyclooxygenase-2 (PDB ID: 5IKQ), TNF family member EDA-A2 (PDB ID: 1RJ8), and the BRMS1 N-terminal region (PDB ID: 4AUV) were retrieved from the protein data bank (https://www.rcsb.org/). Pre-docking preparation included the removal of water molecules and cofactors, followed by the addition of hydrogen atoms using AutoDockTools (ADT). The 3D structures of the natural product compounds were obtained in SDF format from PubChem and converted into PDB format using Discovery Studio Visualizer for subsequent docking analysis.

Docking simulations were initiated by defining the grid center for each protein target using the AutoGrid program in AutoDockTools. The grid box dimensions were set to 40 points per axis, with a spacing of 0.375 Å. Binding affinity calculations were performed using AutoDock Vina (Trott and Olson, 2010). The docking procedure was configured to generate 10 binding poses per ligand, with an energy range set to 9 kcal/mol. To improve accuracy, the exhaustiveness parameter was adjusted to 1000. The docking results were visualized in both 2D and 3D formats using BIOVIA Discovery Studio Visualizer (BIOVIA, 2015). This systematic approach ensured reliable predictions of ligand-protein interactions and provided insights into the binding modes and affinities of the tested compounds.

9. Statistical analysis

The results were presented as mean ± standard error (SE) (n=3). Statistical analysis was performed by one-way analysis of variance (ANOVA) followed by followed by Tukey's and Student-Newman-Keuls and Tukey's (HSD) post hoc test for multiple comparisons ($P < 0.05$) using IBM SPSS statistics V22 software from IBM.

Results and discussion

1. Yield and fractionation

Extraction and isolation of bioactive components from plant materials play a vital role in the development of herbal therapeutic formulations. Polar and apolar solvents were used in the extraction steps performed in this study, to purify the whole phytocomplex and specific chemical fractions from *A. articulata* aerial portions. Regarding the isolation of alkaloids, we use the acid/base principle.

An ethanolic extract was prepared via maceration of the aerial parts (stems, leaves, and flowers) of *A. articulata*. This crude extract was subsequently subjected to liquid-liquid fractionation, which yielded several distinct fractions. The obtained extracts—specifically the crude ethanolic extract (E), acetone fraction (A), hexane fraction (B), chloroform fraction (C), and alkaline aqueous fraction (D)—differed in their color, physical aspect, and extraction yield. The physical properties and yields of the crude hydromethanolic extract and its derived fractions are presented in Table 1.

Table 1. Characteristics of crude extract of the aerial part of *A. articulata* and their obtained fractions.

Extract/fractions	Aspect	Color	Yield (%)
Crude extract (E)	Pasty	Dark green	1.47
Fraction (A)	Pasty	Dark green	0.48
Fraction (B)	Oily	Light green	0.0015
Fraction (C)	Pasty	Dark brown	0.38
Fraction (D)	Crystallized	Dark brown	0.58

Extraction yields across all fractions ranged between 0.0015% and 1.47% The percentage yield of the ethanol crude extract and the fractions A, B, and D was 1.47%, 0.48%, 0.0015%, and 0.58 % respectively, while for the alkaloidal portion (i.e., fraction C) it was 0.38%. The fractionation with n-hexane resulted in the lowest yield. These results differ notably from those reported by Benhammou et al. (2013), who obtained significantly higher yields for methanolic extracts from *A. articulata* stems (5.47 ± 0.54%) and alkaloids (5.95 ± 0.25%). Also, they are significantly lower than the values reported by Makhlouf et al. (2024), who obtained yields ranging from 7.6% to 42.2% for different fractions, the aqueous fraction (AqFA) showed the highest yield (42.2%), followed by the n-butanol fraction (nBFA) at

29.1%, and the ethanolic extract (EEAA) at 15.5%. These yields are considerably higher than our results, where the crude ethanolic extract (E) provided the highest yield at only 1.47%.

The difference in yields can be explained by several factors. According to Dhanani et al. (2017): (i) the extraction method used (maceration vs organic solvent extraction), (ii) extraction duration and conditions, (iii) geographical origin and environmental conditions during plant collection, and (iv) the plant part analyzed.

Compared to other Chenopodiaceae family members, such as *Atriplex halimus* (Benhammou et al., 2009) and *Arthrophytum scoparium* (19.87%) reported by Dehimi et al. (2020), results show higher extraction efficiency. This variation emphasizes that extraction yield percentage depends mainly on the extraction procedure, particularly temperature, compound polarity, solvent ratio, and extraction methods (Markom et al., 2007; Wijngaard et al., 2012).

These comparable yields across studies highlight the importance of standardized extraction protocols for reproducible bioactive compound recovery while maintaining their functional integrity (De La Guardia and Armenta, 2011; Hmidani et al., 2019). It is noteworthy that in the study by Benhammou et al. (2013), the ethyl acetate and butanolic fractions presented respective yields of 1.86 ± 0.64% and 0.8 ± 0.14%, values that are closer to our results for the acetone fraction (A) (0.48%) and chloroform fraction (C) (0.38%). This relative concordance suggests that despite methodological differences, certain trends in secondary metabolite distribution remain consistent.

The low yield of our hexane fraction (0.0015%) confirms previous observations indicating that *A. articulata* contains few lipophilic compounds (Kambouche et al., 2009; Maatalah et al., 2012). Conversely, the relatively high yield of the alkaline aqueous fraction (0.58%) in our study is consistent with the alkaloid richness reported by Benhammou et al. (2013) and Belyagoubi-Benhammou et al. (2019) and highlights the importance of these bioactive compounds in this species.

These yield variations emphasize the importance of optimizing extraction protocols to maximize the recovery of active principles while considering environmental and genetic factors that may influence the phytochemical composition of *A. articulata.*

2. Phytochemical screening

A phytochemical screening was conducted to identify the major chemical families present in the crude extract and its fractions from the aerial parts of *A. articulata* through qualitative characterization reactions. The results are summarized in Table 2.

Table 2. Phytochemical screening of the crude extract of the aerial part of *A. articulata* and its obtained fractions.

Chemical families	Crude (E)	Fraction A	Fraction B	Fraction C	Fraction D
Flavonoids	+	+	+	+	+
Tannins	+	+	-	+	-
Saponins	+	-	-	-	-
Coumarins	-	-	-	-	-
Alkaloids	+	+	+	+	+

(+) presence, (−) absence.

The phytochemical screening of *A. articulata* aerial results demonstrated that the plant is rich in secondary metabolites. The presence of flavonoids, tannins, saponins, and alkaloids was confirmed in the crude extract and its fractions. It reveals distinct distribution patterns of bioactive compounds. Flavonoids and alkaloids are universally present across the crude extract and all fractions (A-D). Tannins show selective partitioning, present only in the crude extract and fractions A and C while absent from fractions B and D. Saponins are detected exclusively in the crude extract but are lost in all fractions. Coumarins are completely absent from all samples, suggesting either natural absence or concentrations below detection limits. Flavonoids and alkaloids demonstrate universal presence across all samples (crude extract E and fractions A-D), indicating that these compounds are abundantly distributed throughout the plant material and remain stable during fractionation processes. This abundance is particularly significant for alkaloids, which aligns with the typical phytochemical profile of Chenopodiaceae family plants known for their rich alkaloid and flavonoids content (Amtaghri et al., 2025). *A. articulata* extracts have been shown to possess high levels of flavonoids and phenolic compounds, which are associated with strong antioxidant and antidiabetic activities (Al-Joufi et al., 2022; Al-Douri et al., 2022; Al-Snafi, 2023) and high levels of alkaloids showing according to Belyagoubi-Benhammou et al., 2019 a significant antioxidant and antimicrobial properties.

Tannins show selective partitioning, being present only in the crude extract and fractions A and C while absent from fractions B and D, suggesting specific solubility characteristics that influence their distribution during extraction. Preliminary phytochemical screening of *A. articulata* confirms the presence of tannins, contributing to its antimicrobial and therapeutic properties (Al-Snafi, 2023). They have been also detected in the aerial parts of *A. articulata*,

contributing to its antimicrobial and cytotoxic activities against tumor cell lines. (Gamal et al; 2021).

Saponins are detected solely in the crude extract but are lost in all fractions, indicating possible degradation, dilution, or volatility during the fractionation process. *A. articulata* is notably rich in saponins according to Al-Snafi (2023), specifically 30-noroleanane triterpenoid saponins, which have been isolated and structurally characterized in recent studies (El Dine et al 2019). The presence of these saponins underpins the plant's therapeutic potential particularly its antihyperglycemic properties and supports its continued ethnomedicinal use in Algeria (Kambouche et al., 2009).

Coumarins were not detected in either the crude extract or any fractions from the aerial parts of *A. articulata*, indicating their absence or extremely low levels. Other bioactive compounds, such as triterpenoids, were successfully isolated and characterized from *A. articulata*, suggesting the plant's pharmacological potential lies in constituents other than coumarins (Gamal et al; 2021). The lack of coumarins may be due to their natural absence in the aerial parts of this plant species or concentrations below the detection limit of the analytical method used. In contrast the study by Mohammed et al. (2013) and Abdulsahib et al. (2016) demonstrated that the stems of *A. articulata* contain measurable amounts of phenols, coumarins, alkaloids, and amino acids. The observed differences between studies relate primarily to the concentrations of these bioactive compounds.

This phytochemical profile provides valuable insight into the bioactive potential of different fractions for further pharmacological investigations. The results suggest that fractions A and C, containing both flavonoids, alkaloids, and tannins, may exhibit enhanced biological activities compared to fractions B and D, which lack tannins but retain the other major compound classes. Moreover, the flavonoid content in plants can be influenced by genetic variability, biological traits, and environmental conditions. Due to the presence of hydroxyl groups, phenolic compounds—including flavonoids—exhibit higher solubility in polar organic solvents (Aryal et al., 2019).

- **Dragendorff's detection**

The TLC analysis using Dragendorff's reagent reveals the alkaloid distribution pattern across the crude extract (E) and its four fractions (A, B, C, D) from *A. articulata* and subjected to UV light (Figure 2). Orange to reddish-brown spots indicated positive alkaloid detection through characteristic precipitates with tertiary amines. The crude extract showed multiple alkaloid spots at different Rf values, suggesting various alkaloid compounds with different

polarities. Fraction A displayed distinct spots indicating successful concentration of multiple alkaloids. Fraction B contained fewer spots, suggesting selective partitioning during extraction. Fraction C showed prominent, intense spots confirming concentrated alkaloid presence, correlating with phytochemical screening results. Fraction D exhibited different migration patterns, indicating alkaloids with distinct chemical properties. The varying spot intensities and Rf values demonstrate successful separation of alkaloid compounds based on physicochemical properties. This analysis confirms the universal alkaloid presence detected in qualitative screening and provides information about their chromatographic behavior and relative concentrations in each fraction.

These results align well with established literature on *A. articulata* alkaloid profiles. The Dragendorff's reagent analysis revealing multiple alkaloid spots with characteristic orange to reddish-brown coloration confirms the rich alkaloid diversity typical of the Chenopodiaceae family. The Anabasis genus contains alkaloids, such as anabasine, anabasamine, lupinine, jaxartinine (Amtaghri et al., 2025); which explains the multiple spots observed at different Rf values across fractions.

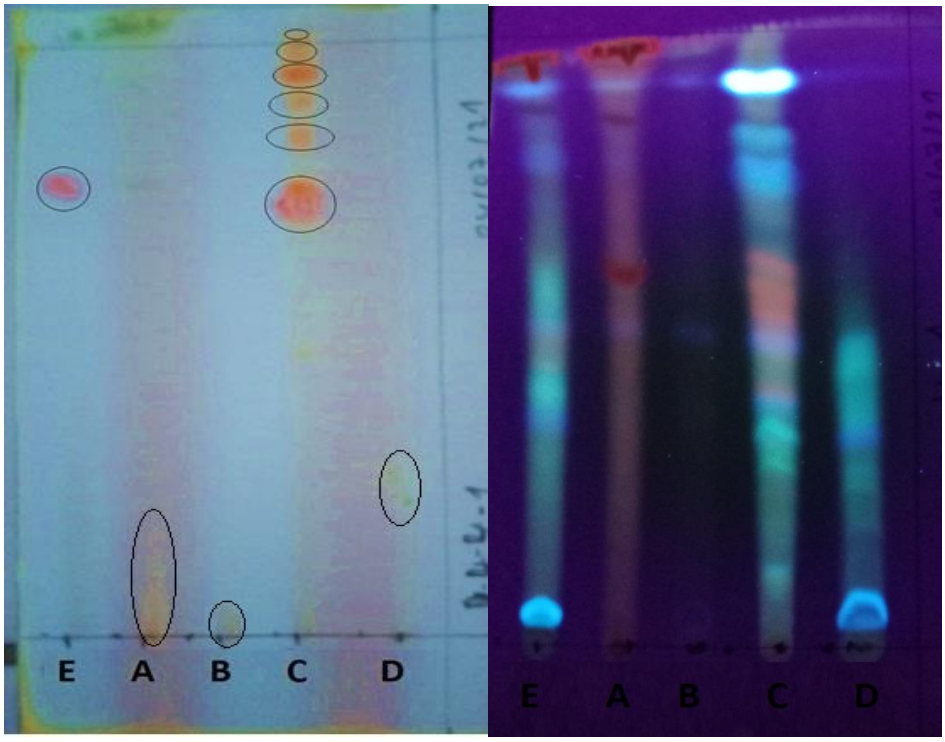

Figure 2. *A. articulata* crude extract (E) and relative fractions (A-D) separated on TLC. a) Exposure of TLC to Dragendorff's reagent; b) visualization of the TLC plates under UV light (365 nm).

3. Column chromatography observation

The Figure 3 shows the glass column under UV light (365 nm) exhibiting bright fluorescence characteristic of fraction C compounds. This intense fluorescence indicates the presence of highly conjugated aromatic systems typical of specific structures, demonstrating the successful isolation and concentration of fluorescent during the column chromatography process.

The successful separation of alkaloids through column chromatography and their distinct TLC migration patterns align with previous studies on polar and apolar solvents (Yubin et al., 2014), demonstrating the diversity of alkaloid polarities in the plant. Varying spot intensities across fractions A-D reflect different concentrations, supporting earlier findings on crude alkaloid extracts from aerial parts (Maatalah et al., 2012; Benhammou et al., 2019).

Figure 3. Column Chromatography under UV light (365 nm).

4. TLC analysis results interpretation

The TLC analysis of 36 sub-fractions from column chromatography of fraction C reveals comprehensive alkaloid separation patterns under different visualization conditions (Figure 4). Panel (a) shows plates under visible light, displaying natural compound coloration and baseline separation. Panel (b) demonstrates UV fluorescence at 365 nm, revealing multiple fluorescent compounds indicating aromatic alkaloids with conjugated systems. Panel (c)

displays plates under UV 250 nm, providing enhanced visualization of compounds not clearly visible at 365 nm with distinct separation patterns. Panel (d) presents Dragendorff's reagent treatment, showing characteristic orange to reddish-brown spots confirming alkaloid presence with varying intensities and Rf values.

The gradient elution system effectively separated alkaloids based on polarity differences: early fractions contained less polar alkaloids (eluted with higher DCM concentrations), while later fractions contained more polar alkaloids (eluted with higher MeOH concentrations and the final toluene-acetone-ethanol-ammonia mixture). Multiple visualization techniques confirm that fraction C contains a complex alkaloid mixture with diverse chemical properties, validating the column chromatography purification strategy and providing guidance for compound identification and further isolation procedures.

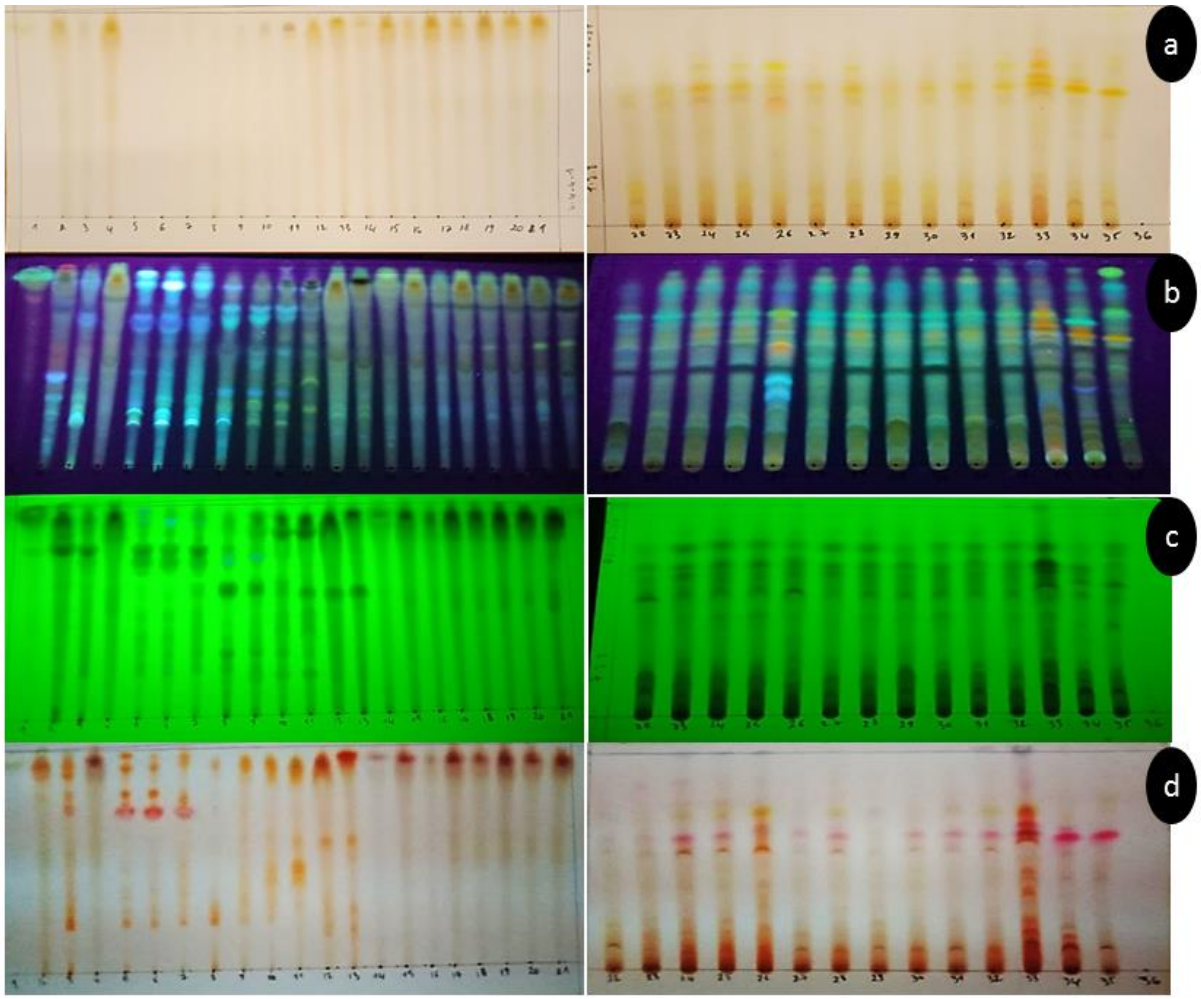

Figure 4. *A. articulata* subfractions separated by TLC. a) Visualization under normal light; b) exposure to 365 nm UV light; c) exposure to 250 nm UV light; d) reaction with Dragendorff's reagent.

The UV fluorescence at 365 nm and 250 nm wavelengths indicates aromatic alkaloids with extended conjugated systems, characteristic of many Chenopodiaceae alkaloids (Okhale et al., 2012; Abozeed et al., 2014; Bogucka-Kocka et al., 2017).

Given the complex phytochemical profile of *A. articulata* extracts containing various bioactive compounds, this multi-technique approach using sophisticated separation and detection methods is essential for complete alkaloid characterization. Comprehensive visualization through multiple detection methods—visible light, UV (365 nm and 250 nm), and Dragendorff's reagent—provides thorough profile characterization and validates the detection approach (Sreevidya et al., 2003; Kulp et al., 2011; Saini et al., 2024).

This systematic variation in mobile phase composition allows compounds with different polarities to elute at distinct times, enhancing resolution and enabling efficient separation of complex mixtures containing both hydrophilic and hydrophobic constituents. The system's effectiveness aligns with the known chemical diversity of *Anabasis* alkaloids (Yubin et al., 2014), confirming that fraction C contains a complex alkaloid mixture and validating the purification strategy for further compound identification and isolation.

5. GC-MS analysis

All 36 sub-fractions obtained from the column chromatographic separation of alkaloid-rich fraction C underwent GC-MS analysis, with the results presented in Table 3. The analysis identified six distinct alkaloid compounds distributed across only 11 sub-fractions, specifically sub-fractions 3 through 11, and sub-fractions 13 and 14. These alkaloids represent three major structural classes: tetrahydroisoquinolines including carnegine, dehydrosalsolidine, and salsoline; phenethylamines represented by hordenine; and indole alkaloids comprising gramine and 2-methyl-1,2,3,4-tetrahydro-β-carboline. The elution pattern of these compounds corresponded to their chemical properties and interactions with both the silica gel stationary phase and the gradient solvent system employed during column chromatography. The remaining 25 sub-fractions showed no detectable alkaloid content, indicating successful concentration and separation of the target compounds within specific fractions during the purification process.

Table 3. Alkaloids of *A. articulata* subfractions characterised through GC-MS with their retention time (min)

Subfractions	Alkaloids	Ret time (minutes)
1 - 2	No alkaloid detected	/
3	Carnegine Hordenine	45.002 48.140
4	Carnegine	45.025
5	Dehydrosalsolidine Carnegine	44.500 45.013
6	Carnegine	44.955
7	Dehydrosalsolidine Carnegine	44.442 44.967
8	Salsoline	42.913
9	Salsoline Carnegine	44.465 44.967
10	Salsoline Carnegine	44.418 44.932
11	Gramine	52.287
12	No alkaloid detected	/
13	2-Methyl-1,2,3,4-tetrahydro-.beta.-carboline	50.392
14	2-Methyl-1,2,3,4-tetrahydro-.beta.-carboline	50.485
15 - 36	No alkaloid detected	/

In 2019, 49 alkaloidal structures clustered in 16 different classes were identified for the first time in *A. articulata* (Belyagoubi-Benhammou et al., 2019). Unfortunately, to date, only few species of the genus *Anabasis* have been chemically investigated, with particular attention paid to *Anabasis aphylla* (Sadykov et al., 1960; Zakharov et al., 1974; Du et al., 2008).
Given the importance of expanding knowledge about alkaloids synthesized in these botanical species and their potential biological activity on human health, this new extraction protocol was applied to identify additional alkaloidal derivatives from *A. articulata*. All six identified alkaloids have been previously described in literature from other plants but, to the best of our knowledge, never in *A. articulata*. Their elution pattern corresponded to their chemical nature and affinity with the gradient solvents and stationary phase, while the remaining sub-fractions contained no alkaloids detected.

Carnegine has been registered by Bracca et al. (2004) in several Cactaceae, Chenopodiaceae and Boraginaceae families. It has been specifically identified in *Hammada articulata* (Moq.) O.Bolòs & Vigo (Chenopodiaceae) together with salsolidine and dehydrosalsolidine (Benkrief et al., 1990). Additionally, carnegine has been isolated from *Haloxylon scoparium* Pomel (Chenopodiaceae) crude extract, in association with 2-methyl-1,2,3,4-tetrahydrocarboline, salsolidine (El-Shazly et al., 2003; Jarraya et al., 2008; Bouaziz et al., 2016), isosalsoline,

dehydrosalsolidine, isosalsolidine, N-methylcorydaldine, tryptamine, and N-methyltryptamine (Haida et al., 2022). Since *A. articulata* belongs to the Chenopodiaceae family, our results align with previous findings, considering the typical association of the detected alkaloids.

Salsoline is a bicyclic monoterpene alkaloid typically synthesized in *Salsola* genus plant roots that are widely used in traditional Chinese medicine (Kuznetsova et al., 2005). Salsoline demonstrates antioxidant effects, helping reduce oxidative stress and protecting cells from free radical damage, making it a potential therapeutic agent for cancer, diabetes, infection, inflammation, depression, and neurodegeneration with no significant adverse effects (Ibrayev et al., 2022; Elwekeel et al., 2023). Its identification in our samples reflects the genetic relationship between *A. articulata* and *Salsola spp*. According to Murshid et al. (2022), the two genera are considered synonyms, while Tefarikis et al. (2022) proposed *A. articulata* and *Salsola soda* L. as strongly related species.

Gramine is an indole alkaloid characterized by bitter taste and toxicity at high doses. It has been found in several plants, including *Arundo donax* L., *Acer saccharinum* L., *Hordeum* L. *sp.*, *Phalaris* L., *Avena sativa* L. *and Lupinus luteus* L. (Cheeke et al., 1989; Corcuera, 1993).

Hordenine is a bioactive alkaloid largely distributed in several cacti and grass plants, such as *Hordeum* sp. (Appley et al., 2022). It has been studied for its potential therapeutic applications (Sobiech et al., 2020). Some studies demonstrated that hordenine can stimulate metabolism and cognitive function (Sommer et al., 2020). The pharmacological action of hordenine relates to its protective role against hyperglycemia, depression, anxiety, and inflammation (Bandala et al., 2023).

The possibility that the alkaloids documented in our samples represent degradation forms and/or intermediates for the synthesis of more complex phytochemicals cannot be excluded.

6. Antioxidant activity

The antioxidant activity of the crude extract of *A. articulata* (E), the four fractions derived from it (samples A, B, C and D), and the 36 subfractions obtained from fraction C was evaluated by different methods: DPPH-TLC bioautography, DPPH, ABTS, FRAP, and total antioxidant capacity (TAC). These tests are based on electron or hydrogen transfer, and the results are expressed in terms of IC_{50} and $A_{0.5}$.

6.1. DPPH thin-layer chromatography (TLC) bioautography assay

The evaluation of the antiradical properties of samples by incubation with DPPH reagent after separation on TLC revealed distinctive patterns of antioxidant activity (Figure 7). The crude extract (E) displayed multiple yellow spots against the purple DPPH background,

indicating the presence of several antioxidant compounds with different polarities. Fraction A (acetone fraction) showed moderate antioxidant activity with a few distinct spots, while fraction B (hexane fraction) exhibited minimal activity with very weak or absent decolorization zones.

Fraction C (chloroform alkaloid-rich fraction) demonstrated the most intense and numerous yellow spots, confirming its rich antioxidant content. The aqueous fraction D showed limited antioxidant activity with few visible spots.

The bioautography analysis of the 36 subfractions obtained from fraction C revealed varying degrees of antioxidant activity, with subfractions 8, 9, and several others (including fractions 3-7, 10, 17, 26, and 33) showing prominent yellow decolorization zones, indicating strong DPPH radical scavenging activity. This qualitative screening effectively identified the most promising subfractions for subsequent quantitative antioxidant evaluation.

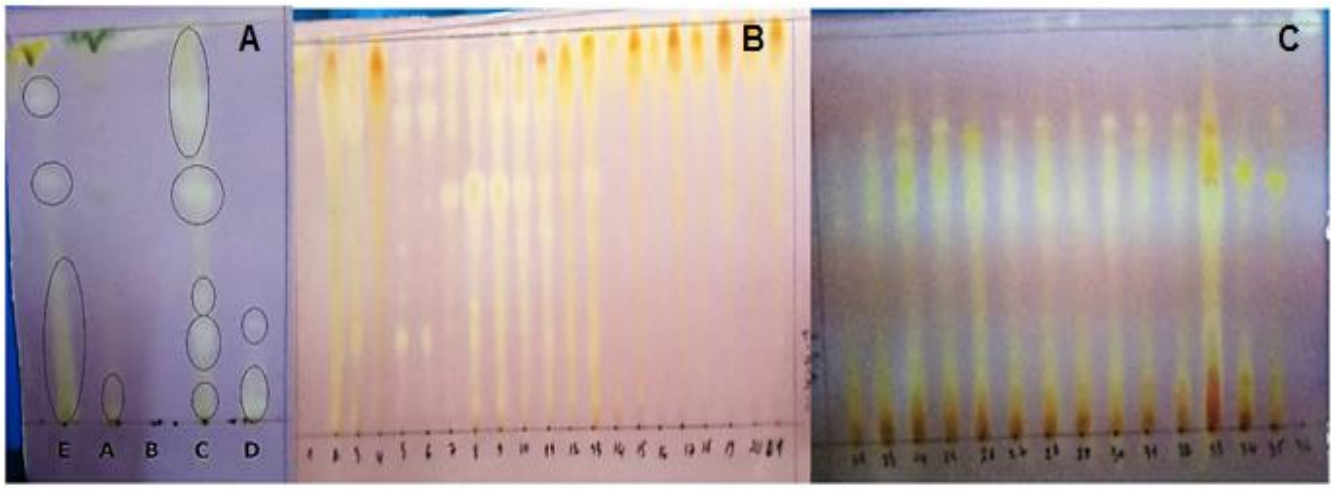

Figure 5. *A. articulata* crude extract, fractions and subfractions separated on TLC and subjected to reaction with DPPH. (A): Crude extract and derived fractions, (B and C): Subfractions.

6.2. DPPH radical scavenging test

The antiradical activity of *A. articulata* extracts and subfractions was evaluated using the DPPH· free radical scavenging method. The results obtained are expressed as percentages of inhibition of DPPH· free radical and IC_{50} values of the crude extract and its fractions (Appendice 2 and Table 4) tested from 0.25 to 4 mg/mL and IC_{50} values for the 36 subfractions (Table 5).

At the maximum concentration of 4 mg/mL, the crude extract shows an inhibition rate of 87.73%. Fraction A exhibits an inhibition of 42.27%, fraction B of 8.54%, fraction C of

74.91%, and fraction D of 9.32%. The inhibition percentages showed a dose-dependent decrease across all concentrations tested. At 2 mg/mL, the crude extract and fraction C demonstrated the highest activities with 54.74% and 55.65% inhibition, respectively, while fractions B and D remained poorly active (≤5.22%). At lower concentrations (1, 0.5, and 0.25 mg/mL), only the crude extract and fraction C maintained notable inhibition levels, ranging from 34.60% to 9.16% and 35.15% to 9.73% respectively.

The IC_{50} values obtained were calculated from logarithmic regression equations of the plotted curves. All active extracts of *A. articulata* exhibit significant antiradical activity in a dose-dependent manner. The best DPPH˙ free radical scavenging capacity was recorded with fraction C (alkaloids) and the crude extract with IC_{50} values of approximately 1.66 ± 0.015 mg/mL and 1.68 ± 0.006 mg/mL, respectively. This activity remains, however, lower than that of the reference antioxidant, ascorbic acid (IC_{50} = 0.138 ± 0.007 mg/mL), but remains significant. Fraction A shows moderate activity with an IC_{50} of 4.76 ± 0.212 mg/mL, while fractions B and D showed no detectable activity under the experimental conditions tested, with maximum inhibition percentages not exceeding 10% even at the highest concentration. The proximity of IC_{50} values between the crude extract and fraction C suggests that alkaloids constitute the main contributors to the antioxidant activity of *A. articulata*. These results confirm the antioxidant potential of this plant species, particularly of its alkaloidal compounds, and are consistent with qualitative bioautography observations where fraction C presented the most marked decolorization zones.

Table 4. Antioxidant activities of the extracts of *A. articulata* obtained by four *in vitro* assays (DPPH, ABTS, FRAP, and TAC). Selected standard antioxidants (i.e. ascorbic acid, BHA, and trolox) were also subjected to the same analyses.

	DPPH IC_{50} (mg/mL)	**ABTS IC_{50} (mg/mL)**	**FRAP A_{50} (mg/mL)**	**TAC (mg AAE/g DM)**
Crude extract (E)	1.68 ± 0.006[a]	1.00 ± 0.014[a]	0.54 ± 0.032[a]	114.13 ± 4.173[a]
Fraction A	4.76 ± 0.212[b]	1.97 ± 0.061[b]	1.37 ± 0.031[b]	74.10 ± 6.053[b]
Fraction B	NA	1.67 ± 0.088[c]	0.94 ± 0.023[c]	88.75 ± 4.057[c]
Fraction C	1.66 ± 0.015[a]	0.09 ± 0.002[d]	1.67 ± 0.128[d]	41.96 ± 5.691[d]
Fraction D	NA	2.41 ± 0.106[e]	4.98 ± 0.189[e]	14.23 ± 0.721[e]
Ascorbic acid	0.138 ± 0.007[c]	/	0.10 ± 0.002[f]	/
BHA	/	/	0.07 ± 0.000[f]	/
Trolox	/	0.05 ± 0.001[d]	/	/

NA: Not active in the investigated experimental condition; The data are represented as mean ± S SD of triplicate experiments. Values with the same letters superscript in the same column are not significantly different at $p < 0.05$ by Tukey's and Student-Newman-Keuls tests.

The antiradical activity of the 36 subfractions of *A. articulata* was evaluated using the DPPH· free radical scavenging method. The results obtained show significant variability in antioxidant activity depending on the subfractions tested, with IC_{50} values ranging from 0.694 mg/mL to 19.71 mg/mL (Table 5).

Among the active subfractions, the best antiradical activities were recorded with subfractions 8 and 9, presenting IC_{50} values of 0.694 ± 0.034 mg/mL and 0.812 ± 0.009 mg/mL respectively. These two subfractions contain mainly salsoline and carnegine as major alkaloids. Subfraction 33 also shows remarkable activity with an IC_{50} of 1.190 ± 0.014 mg/mL, although no specific alkaloid has been identified in it. Other subfractions show moderate activities, notably subfractions 6, 17 and 26 with IC_{50} values between 1.46 and 1.98 mg/mL. Subfraction 6, containing dehydrosalsolidine and carnegine, displays an IC_{50} of 1.493 ± 0.021 mg/mL. Subfractions 3, 4, 5, 25 and 32 present acceptable activities with IC_{50} values ranging from 2.32 to 2.69 mg/mL. In contrast, certain subfractions demonstrate weaker activities, particularly subfractions 11, 13, 19, 21, 24 and 27 with IC_{50} values between 3.15 and 3.99 mg/mL. Subfraction 22 presents the lowest activity among the active samples with an IC_{50} of 19.71 ± 1.889 mg/mL. Twelve subfractions (1, 2, 12, 14, 16, 28, 29, 30, 31, 35 and 36) showed no detectable activity under the experimental conditions tested.

Analysis of the correlation between alkaloid composition and antioxidant activity reveals that subfractions containing salsoline (subfractions 8, 9 and 10) generally present better antiradical activities. Carnegine, present in several active subfractions, also appears to contribute positively to antioxidant activity. However, it is notable that certain subfractions without identified alkaloids (such as subfractions 17, 26 and 33) maintain significant activity, suggesting the presence of other unidentified bioactive compounds.

Table 5. Results of DPPH radical scavenging activity test carried out on the 36 subfractions (SF) of *A. articulata*.

SF	IC_{50} (mg/mL)	Alkaloids
1	NA	/
2	NA	/
3	2.413 ± 0.037^{b}	Carnegine and hordenine
4	2.498 ± 0.109^{b}	Carnegine
5	2.69 ± 0.054^{c}	Dehydrosalsolidine and carnegine
6	1.493 ± 0.021^{a}	Dehydrosalsolidine and carnegine
7	2.979 ± 0.071^{c}	Carnegine
8	0.694 ± 0.034^{d}	Salsoline and carnegine
9	0.812 ± 0.009^{d}	Salsoline and carnegine
10	1.817 ± 0.132^{a}	Salsoline and carnegine
11	3.430 ± 0.266^{e}	Gramine
12	NA	/
13	3.988 ± 0.076^{e}	2-Methyl-1,2,3,4-tetrahydro-beta-carboline
14	NA	2-Methyl-1,2,3,4-tetrahydro-beta-carboline
15	5.413 ± 0.69^{f}	/
16	NA	/
17	1.981 ± 0.009^{a}	/
18	5.534 ± 0.252^{f}	/
19	3.730 ± 0.030^{e}	/
20	4.947 ± 0.302^{f}	/
21	3.151 ± 0.028^{c}	/
22	19.71 ± 1.889^{g}	/
23	5.346 ± 0.082^{f}	/
24	3.676 ± 0.035^{e}	/
25	2.368 ± 0.065^{b}	/
26	1.460 ± 0.008^{a}	/
27	3.869 ± 0.181^{e}	/
28-31	NA	/
32	2.3158 ± 0.068^{b}	/
33	1.190 ± 0.0139^{a}	/
34	4.451 ± 0.083^{f}	/
35-36	NA	/
AA	0.138 ± 0.007^{a}	/

For each subfraction, the alkaloids identified by GC-MS are also indicated. Different letters (a, b, c) indicate significant differences at $p<0.05$; NA: not active in the investigated experimental condition; AA: ascorbic acid used as positive control.

These findings are consistent with previous investigations of *A. articulata* antioxidant properties. Similarly, Benhammou et al. (2013) reported comparable activities for root crude extract and stem alkaloidal extract with IC_{50} values of 0.57 ± 0.03 mg/mL and 1.30 ± 0.02 mg/mL, respectively. Subsequently, Belyagoubi-Benhammou et al. (2019) found that pure basic alkaloidal extract exhibited high antiradical power (IC_{50}= 1.242 ± 0.168 mg/mL),

whereas total alkaloidal fraction showed weaker activity (IC_{50}= 5.350 ± 0.022 mg/mL). However, some studies have reported substantially higher activities. For instance, Abdallah et al. (2014) demonstrated DPPH inhibition at IC_{50}= 61 µg/mL, while Al-Joufi et al. (2022) showed crude extract and n-hexane fraction activities of 45 µg/mL and 90 µg/mL, respectively. More recently, investigations by Makhlouf et al. (2024, 2025) confirmed that ethanolic extract exhibited the best free radical scavenging activity IC_{50}= 0.074 ± 0.003 mg/mL), followed by chloroform and n-butanol extracts (IC_{50}= 0.082 ± 0.0012 mg/mL and 0.083 ± 0.0016 mg/mL). These variations highlight the significant influence of extraction methods and sample preparation protocols on antioxidant activity.

This activity extends across *Anabasis* species, as evidenced by related research. For example, Senhaji et al. (2020) demonstrated that *Anabasis aretioïdes* methanolic extract exhibited DPPH scavenging activity with IC_{50}= 52.91 ± 0.24 µg/mL. Additionally, El-Haci et al. (2013) reported free DPPH radical scavenging activities for ethyl acetate, methanolic, and chloroform extracts from Algerian *A. aretioïdes* aerial parts with IC_{50} values of 72.15 ± 1.04 µg/mL, 79.15 ± 4.23 µg/mL, and 86.73 ± 10.68 µg/mL, respectively. These results collectively indicate that antioxidant activity is a consistent characteristic throughout the genus.

Significantly, these fractions contained primarily salsoline and carnegine as major alkaloids. Based on these results, salsoline emerged as the most potent antioxidant alkaloid, likely due to its phenolic structure facilitating electron donation to DPPH radical. Indeed, the tetrahydroisoquinoline alkaloids salsoline, salsolidine, N-methylisosalsoline and carnegine exhibit very interesting phytopharmacological effects (Tundis et al., 2009).

Moreover, carnegine demonstrated remarkable synergistic potential, showing optimal antioxidant performance when combined with salsoline. This observation is strongly supported by literature evidence showing antioxidant and anticholinesterase activities of salsoline, salsolidine, N-methylisosalsoline, and carnegine isolated from Chenopodiaceae species (*Salsola oppositifolia*, *S. soda*, and *S. tragus*), thereby indicating high phytopharmacological and therapeutic potential for these alkaloids (Tundis et al., 2009).

The structural basis for this activity lies in tetrahydroisoquinoline alkaloids' oxygenated substituents, including hydroxyl, methoxy, or methylenedioxy groups, which consequently explain salsoline's electron-donating capability to DPPH radical (Shegebayev et al., 2023). Furthermore, Bouaziz et al. (2016) specifically demonstrated that carnegine exhibited the most potent antimicrobial and antioxidant activities, with minimal inhibitory concentration (MIC) and minimal bactericidal concentration (MBC) ranging from 0.125 to 0.5 mg/mL.

Interestingly, subfraction 33 also showed remarkable activity (IC_{50} = 1.190 ± 0.014 mg/mL) despite lacking identified alkaloids, thus suggesting contributions from other unidentified bioactive compounds.

The significant antiradical activity recorded in subfractions without detected alkaloids suggests important contributions from non-alkaloidal secondary metabolites to the overall antioxidant activity. This finding therefore indicates that *A. articulata*'s antioxidant potential extends beyond its alkaloid content, encompassing a broader spectrum of bioactive compounds (Kambouche et al., 2009; Abdulsahib al., 2016; Ben Menni et al., 2024: Makhlouf et al., 2024).

6.3. $ABTS^{\bullet+}$ cation radical scavenging test

The antiradical activity of the crude extract and fractions of *A. articulata* was also assessed using the $ABTS^{\bullet+}$ radical cation decolorization assay across a concentration range of 0.02-8 mg/mL. The results obtained are expressed as percentage of inhibition and IC_{50} values (Table 4, Appendice 3 and 4). Among all tested samples, fraction C (alkaloid-enriched fraction) exhibited the most potent scavenging activity with an IC_{50} value of 0.09 ± 0.002 mg/mL and 97.94% inhibition at the highest concentration (0.5mg/mL), demonstrating comparable efficacy to the reference standard Trolox (IC_{50} = 0.05 ± 0.001 mg/mL). The crude extract displayed substantial antioxidant capacity (IC_{50} = 1.00 ± 0.014 mg/mL at 8 mg/mL), while fractions B, A, and D showed progressively lower activities with IC_{50} values of 1.67 ± 0.088, 1.97 ± 0.061, and 2.41 ± 0.106 mg/mL, respectively.

Dose-response analysis revealed that at lower concentrations, fraction C retained notable inhibitory effects (71.62% at 0.125 mg/mL), whereas the crude extract and other fractions exhibited moderate inhibition percentage ranging from 23.00% to 48.16%. At lower concentrations (1 mg/mL), only fraction C and Trolox maintained significant radical scavenging capacity. Statistical analysis indicated that fraction C was approximately 11-fold more potent than the crude extract, strongly suggesting that alkaloid constituents represent the primary bioactive compounds responsible for the antioxidant properties of *A. articulata*.

The capacity of the aqueous (fraction D) and organic extracts (fractions A, B, C, and E) from *A. articulata* to scavenge ABTS radicals presented a trend similar to that revealed in the DPPH assay, demonstrating consistency across different radical systems. This similarity is attributed to the fact that both methods fundamentally measure the ability of compounds to donate hydrogen atoms or electrons (Brand-Williams et al., 1995; Miller and Rice-Evans, 1997; Gil et al., 2002; Leong and Shui, 2002; Prior et al., 2005). Although in the ABTS test

the reagent is soluble in both aqueous and organic solvents, which makes this assay more reliable compared to the DPPH one (Teow et al., 2007). This methodological advantage explains the detection of antiradical activity in fractions B and D (aqueous) in the ABTS test, which remained undetected in the DPPH assay due to solubility limitations.

The enhanced sensitivity and broader applicability of the ABTS assay support the theory that this method is more adequate than DPPH for studying food and medicinal plant extracts containing both hydrophilic and lipophilic molecules (Re et al., 1999; Floegel et al., 2011). The ABTS•+ radical cation can effectively assess the total antioxidant capacity by evaluating both electron transfer (ET) and hydrogen atom transfer (HAT) mechanisms, providing a more complete picture of the antioxidant potential (Huang et al., 2005; Prior et al., 2005).
This sustained activity profile suggests the presence of highly efficient radical scavenging compounds, likely alkaloids, which can effectively neutralize ABTS•+ radicals through electron donation mechanisms (Gil et al., 2002; Leong and Shui, 2002). The crude extract demonstrated considerable antioxidant capacity indicating a synergistic effect among various phytochemical components present in the whole extract.

The ranking of antioxidant potency (Fraction C > Crude extract > Fraction B > Fraction A > Fraction D) provides valuable insights into the distribution of bioactive compounds across different polarities. The superior performance of the chloroform fraction (Fraction C) aligns with previous reports highlighting the antioxidant potential of plant alkaloids, which are typically extracted in moderate polarity solvents (Cushnie and Lamb, 2014; Kumari et al., 2024). The intermediate activity of fractions A and B (IC_{50} values of 1.97 ± 0.061 and 1.67 ± 0.088 mg/mL, respectively) suggests the presence of complementary antioxidant compounds such as phenolic acids, flavonoids, or terpenoids that contribute to the overall antioxidant profile (Scalbert et al., 2005).

Comparative analysis with other species reveals interesting patterns in antioxidant activity. Djeridane et al., (2015) reported a value of 02.37 mM (Trolox equivalent antioxidant capacity) while Al-Joufi et al. (2022) reported significantly higher ABTS radical scavenging activity for *A. articulata* extracts from Pakistan, with IC_{50} values of 75 µg/mL and 71 µg/mL for acetate:n-hexane and pure n-hexane extracts, respectively. These values are considerably lower than our findings, potentially attributable to geographical variations, different extraction methodologies, or variations in alkaloid content influenced by environmental factors (Sultana et al., 2009; Ncube et al., 2015). Similarly, Senhaji et al. (2020) demonstrated potent ABTS antiradical activity in organic extracts of *A. aretioïdes* (48.99 ± 1.316 µg TE/mg, expressed in

Trolox equivalent capacity), further supporting the genus-wide distribution of antioxidant compounds.

The strong correlation observed between ABTS and DPPH results (where both assays detected activity) validates the reliability of our antioxidant assessment and confirms that the observed activities reflect genuine radical scavenging properties rather than assay-specific artifacts (Antolovich et al., 2002; Magalhães et al., 2008). This consistency across different radical systems supports the potential therapeutic applications of *A. articulata* alkaloid-rich fractions as natural antioxidant agents for preventing oxidative stress-related disorders.

6.4. Ferric reducing antioxidant power (FRAP)

The ferric reducing power of the crude extract and fractions of *A. articulata* was assessed using the FRAP assay across concentrations of 0.125-4 mg/mL reflecting the capacity of samples to reduce the Fe^{3+}-TPTZ complex to Fe^{2+}-TPTZ. Results are expressed as the variation of absorbances as a function of concentrations (Appendice 5) and $A_{0.5}$ values (Table 4).

The crude extract demonstrated superior reducing capacity ($A_{0.5}$ = 0.54 ± 0.032 mg/mL) with dose-dependent absorbance increases at 700 nm from 0.114 (0.125 mg/mL) to 2.183 (4 mg/mL). Fractions B and A exhibited moderate activities ($A_{0.5}$ = 0.94 ± 0.023 and 1.37 ± 0.031 mg/mL, respectively), while fractions C and D showed weaker reducing powers. Unlike DPPH and ABTS assays where fraction C predominated, the FRAP assay revealed crude extract superiority, suggesting synergistic effects among different bioactive compound classes in the ferric reduction mechanism.

This assay provides valuable insights into the electron-donating capacity of antioxidant compounds, which is fundamentally different from the radical scavenging mechanisms evaluated by DPPH and ABTS assays (Benzie and Strain, 1996; Pulido et al., 2000).

The electron-donating capacity of the extracts depends not only on the quantity of antiradical metabolites but also on the chemical structure of these molecules and their interaction capacity with radical species. The study of Benhammou et al. (2013) has reported that stem and root crude extracts from *A. articulata* possessed a great capacity to reduce Fe+3, presenting IC_{50} values of 0.36 and 0.66 mg/mL, in that order, whereas the relative purified fraction of alkaloids revealed an IC_{50} equal to 0.52 mg/mL. The strong performance of crude extracts compared to fractions suggests synergistic interactions between multiple bioactive compound classes present in the whole extract, indicating that the combination of phenolic

compounds, flavonoids, tannins, and other reducing agents work collectively to enhance the overall reducing power (Apak et al., 2007).

This evidence has indicated that both underground and aerial parts of this plant species contain good levels of antioxidants and that, probably, the major contribution is due to their content in alkaloids. Compared to the results reported in Benhammou et al. (2013), our data would suggest that the applied extraction method was able to select just some specific alkaloids, as also confirmed by the GC-MS analysis. These findings are supported also by those published by Belyagoubi-Benhammou et al. (2019), which demonstrate that various alkaloidal extracts from *A. articulata* are characterized by different antioxidant capacities. On the other hand, the antiradical potential measured by FRAP appeared coherent among the crude extracts.

While these values are higher than those reported by Ben Menni et al. (2022) for *A. articulata* aqueous extract and saponin extract (1.85 ± 0.41 mg/mL, 1.45 ± 0.51 mg/mL, respectively) and Djeridane et al. (2015), 4.71 M CAEAC (caffeic acid equivalent antioxidant capacity) while they remain significantly lower than the reference standards. The moderate reducing capacity observed aligns with findings from Makhlouf et al. (2024), where plant extracts demonstrated variable reducing power with IC_{50} values ranging from 0.188 to 0.9 mg/mL for different assays.

The electron-donating capacity of these fractions depends not only on the quantity of antioxidant metabolites present but also on their chemical structures and their specific interaction capacity with the ferric-TPTZ complex (Huang et al., 2005; Spiegel et al., 2020).

6.5. Total antioxidant capacity (TAC)

The TAC assay was expressed as ascorbic acid equivalents (mg AAE/g dry matter) (Table 4). The crude extract exhibited the highest total antioxidant capacity with 114.13 ± 4.173 mg AAE/g DM, followed by fraction B (88.75 ± 4.057 mg AAE/g DM) and fraction A (74.10 ± 6.053 mg AAE/g DM). Fraction C demonstrated moderate antioxidant capacity (41.96 ± 5.691 mg AAE/g DM), while fraction D showed the lowest capacity (14.23 ± 0.721 mg AAE/g DM).

Comparative analysis revealed that the crude extract possessed antioxidant capacity approximately 1.3-fold higher than fraction B and 8-fold higher than fraction D. These findings corroborate FRAP assay results, confirming that the crude extract outperforms all individual fractions in methods evaluating global antioxidant capacity. This pattern, distinct

from DPPH and ABTS assays, suggests that total antioxidant capacity results from synergistic interactions among diverse classes of bioactive compounds present in the crude extract.

In a similar study, Benhammou et al. (2013) provided detailed TAC analysis showing that methanolic extracts of stems (9.76 ± 0.13 mg AAE/g DM) and roots (10 ± 0.03 mg AAE/g DM) demonstrated superior antioxidant capacity compared to specific compound fractions. Among the individual compound classes tested, alkaloids showed the highest TAC values (2.86 ± 0.00 mg AAE/g DM for stems), followed by tannins (1.45 ± 0.04 mg AAE/g DM), saponins (1.30 ± 0.01 mg AAE/g DM), butanolic fraction (1.26 ± 0.05 mg AAE/g DM), and ethyl acetate fraction (1.28 ± 0.03 mg AAE/g DM). Interestingly, root extracts generally showed higher TAC values than stem extracts for most fractions, with tannins being particularly notable (2.50 ± 0.0 mg AAE/g DM in roots vs 1.45 ± 0.04 mg AAE/g DM in stems). Afterwards, Belyagoubi-Benhammou et al. (2019) reported that tetravalent alkaloids exhibited TAC values of 14.7 ± 0.2 mg AAE/g DM, higher than pure basic alkaloids (8.7 ± 0.5 mg AAE/g DM), but still substantially lower than our crude extract values. Ben Menni et al. (2022) also reported a TAC value of 0.40 ± 0.01 EAA/g MS for saponin extract and 13.51 ± 0.79 mg EAA/g MS for *A. articulata* aqueous extract, which is considerably lower than our crude extract but comparable to our fraction D (14.23 ± 0.7 mg AAE/g DM). This similarity suggests that fraction D may contain compounds with antioxidant profiles similar to those extracted by aqueous methods. Makhlouf et al. (2024) reported EC_{50} values ranging from 0.150 ± 0.0017 mg/mL (chloroform fraction) to 0.495 ± 0.0068 mg/mL (aqueous fraction), with intermediate values for n-butanol fraction, ethyl acetate fraction, and ethanolic extract fractions. These results demonstrate that different extraction solvents and fractionation methods yield varying antioxidant capacities, with chloroform-soluble compounds showing superior activity. The variation in EC_{50} values across fractions supports the influence of solvent polarity on extracting specific bioactive compounds with different antioxidant potentials.

The decreasing TAC pattern from crude extract to individual fractions, combined with the superior performance compared to literature values focusing on specific compound classes (alkaloids, saponins) (Brahim et al., 2015; Hayat et al., 2020), emphasizes the importance of synergistic interactions among diverse bioactive compounds in determining overall antioxidant capacity.

7. Antidiabetic activity

The antidiabetic activity of *A. articulata* was evaluated by measuring the inhibitory potential of its extracts on the α-amylase enzyme using the chromogenic DNSA method.

Figure 7 showed a proportional increase in the percentages of α-amylase inhibition with different concentrations of the aerial part extracts of *A. articulata*. The IC_{50} values were determined from the logarithmic regression equations of the curves illustrated in Appendice 6. The crude extract demonstrated dose-dependent inhibitory effects, achieving 57.58% inhibition at 0.25 mg/mL with an IC_{50} value of 103.9 ± 15.26 µg/mL, exhibiting comparable efficacy to acarbose (IC_{50} = 103.65 ± 1.56 µg/mL).

Among the fractions, fraction A showed progressive inhibition 59.45% (0.25 mg/mL), while fraction B demonstrated similar patterns with 61.26% inhibition at 0.25 mg/mL (IC_{50} = 110.67 ± 5.28 µg/mL). Fraction C exhibited moderate activity with 61.25% inhibition at 0.5 mg/mL (IC_{50} = 148.4 ± 3.35 µg/mL), whereas fraction D showed the weakest performance with only 36.74% inhibition at 0.5 mg/mL and an IC_{50} of 727.0 ± 9.54 µg/mL.

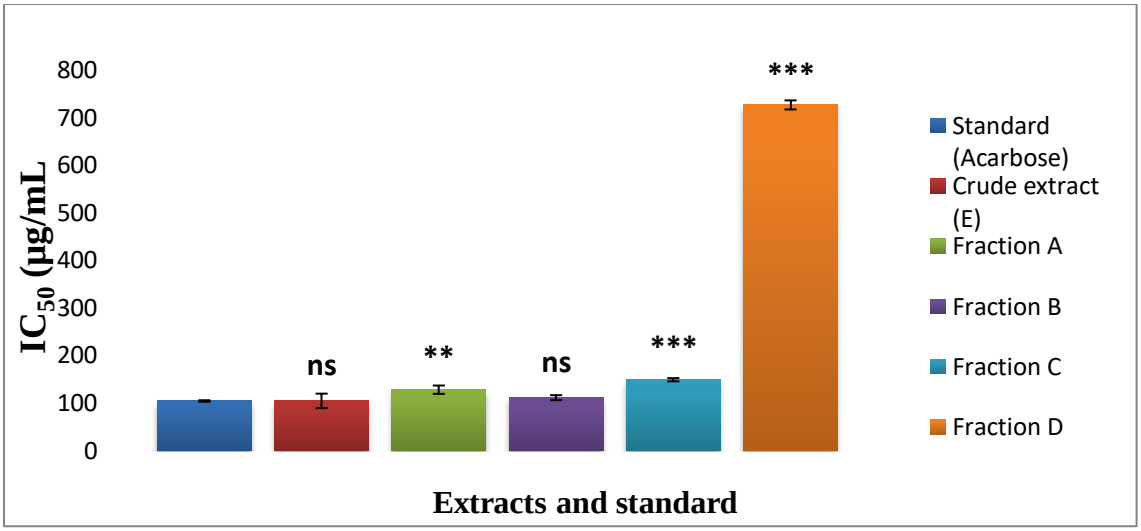

Figure 6. IC_{50} values of α amylase inhibition potential of *A. articulata* extracts. The data are represented as mean SEM, n = 3. Statistical significance was determined by one-way ANOVA followed by Tukey's post hoc test. *p < 0.05, **p < 0.01, ***p < 0.001, **ns**: not significant (p > 0.05) vs Acarbose as positive control.

Statistical analysis revealed the potency ranking: crude extract ≈ acarbose > fraction B > fraction A > fraction C >> fraction D. The crude extract's superior performance, maintaining consistent inhibitory activity across all tested concentrations, suggests synergistic interactions between multiple bioactive constituents, indicating substantial therapeutic potential equivalent to the clinically established antidiabetic agent acarbose.

The exceptional performance of the crude extract suggests the existence of a synergistic effect among the different bioactive compounds present in the complete plant matrix. Al-Joufi et al. (2022) have reported substantially lower IC_{50} values for *A. articulata*, with the crude extract showing an IC_{50} of 34 µg/mL. This discrepancy might be attributed to several factors, including geographical origin, seasonal collection, extraction methodologies, and protocol details that may affect the bioavailability or concentration of active substances responsible for the enzymatic inhibition. On the other hand, Jan et al. (2025) have identified four bioactive compounds in *A. articulata* demonstrating α-amylase inhibitory activity. Quercetin was found to possess the most potent effect, achieving 85.98% inhibition at 1000 µg/mL with an IC_{50} of 30 µg/mL. This could support the present findings about the fact that the investigated herb contains potent antidiabetic compounds, particularly in the lower molecular weight fractions. These findings align also with Djeridane et al. (2015), who reported that *A. articulata* exhibits non-competitive inhibition against both α-amylase and α-glucosidase with a Ki value of 146.00 µM for α-amylase. Their study demonstrated that *A. articulata* displayed a moderate inhibitory constant compared to other plant extracts like *Salsola baryosma* (Ki = 7.00 µM) and *Hammada elegans* (Ki = 15.00 µM), but showed a higher activity relative to standards such as ascorbic acid (Ki = 197.0 µM) and Rutin (Ki = 39.80 µM). The noncompetitive inhibition mechanism identified by Djeridane et al. (2015) suggests that *A. articulata* compounds bind to sites other than the active site, causing conformational changes that reduce enzyme efficiency without competing with the substrate. Furthermore, it is known that numerous alkaloids exert potent α-amylase inhibitory activity. Notably, two quinazoline alkaloids, vasicinol and vasicine, from *Adhatoda vasica* L. effectively inhibit intestinal α-glucosidase-mediated sucrose hydrolysis in rat models (Alamzeb et al., 2024). Complementary evidence from Tintu et al. (2012) has revealed that berberine, an isoquinoline alkaloid, can block *Aspergillus flavus* α-amylase through both enzymatic kinetic interference and molecular docking mechanisms.

8. Inhibition of bovine serum albumin denaturation

The *in vitro* anti-inflammatory activity of the crude extract and fractions was evaluated using the bovine serum albumin (BSA) heat denaturation assay, with diclofenac as a positive control. Results are expressed as a percentage of inhibition at different tested concentrations (0.0625 to 4 mg/mL) in Figure 7 and IC_{50} values in Figure 8.

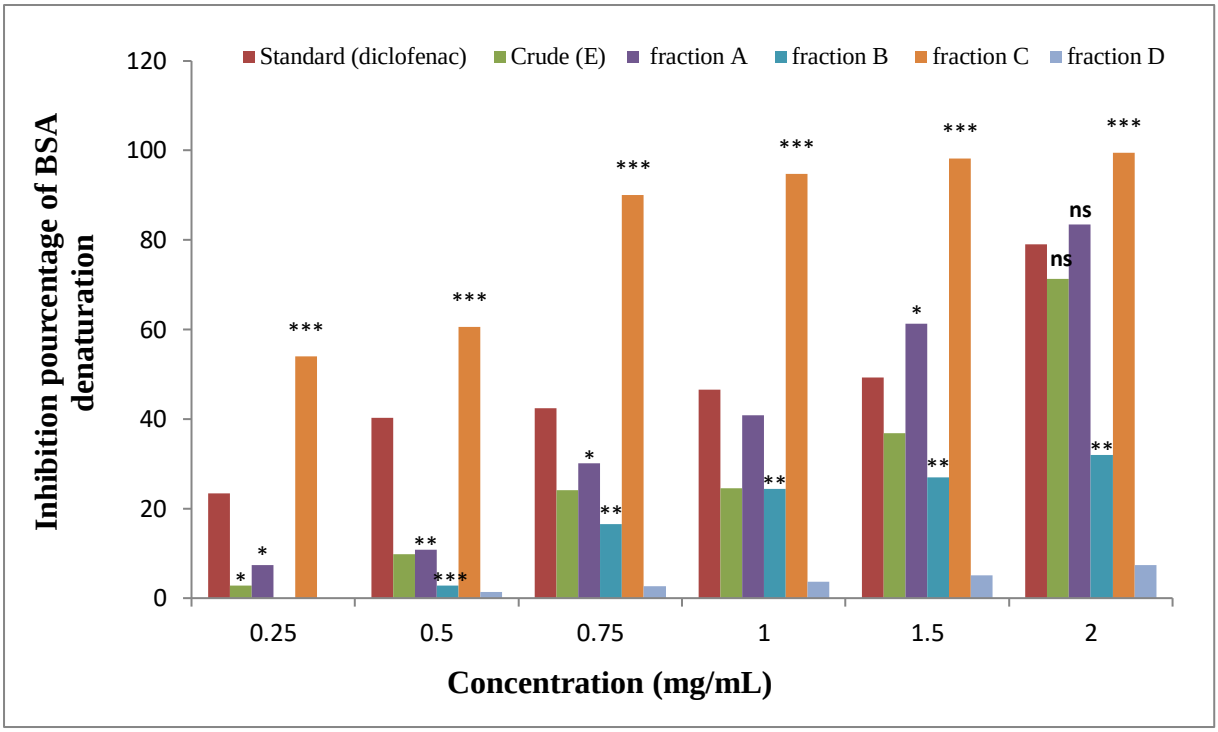

Figure 7. Percentage of inhibition of BSA denaturation by *A. articulata* extracts at concentrations ranging from 0.25 to 2 mg/mL. Diclofenac was used as a reference standard. Statistical significance was expressed with respect to the respective Diclofenac sample.

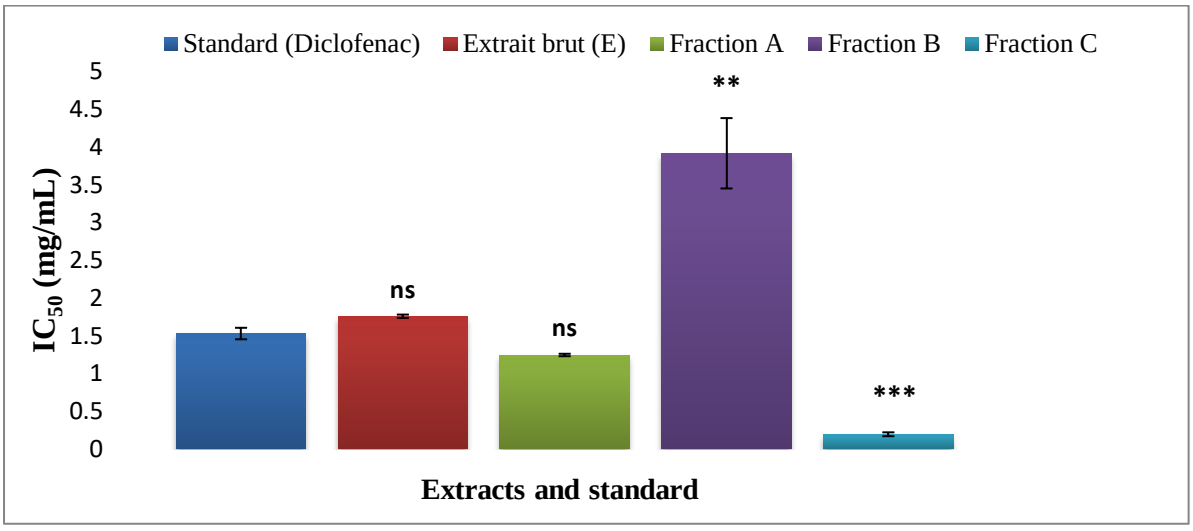

Figure 8. IC_{50} values (mg/mL) relative to the anti-inflammatory activity of *A. articulata* extracts and Diclofenac (standard drug) assessed by the BSA denaturation test. Significance was shown for the samples vs. Diclofenac. Fraction D showed negligible and indeterminable activity.

The crude extract (E) exhibited moderate anti-inflammatory activity with an IC_{50} of 1.75 ± 0.022 mg/mL, comparable to that of diclofenac (1.52 ± 0.0066 mg/mL). Fractionation revealed variable activities among the tested fractions. Fraction A showed slightly superior activity to the standard with an IC_{50} of 1.23 ± 0.016 mg/mL. Fraction B proved to be less active (IC_{50} = 3.91 ± 0.466 mg/mL), requiring higher concentrations to achieve significant inhibitory effects.

Remarkably, fraction C demonstrated exceptional anti-inflammatory activity with the lowest IC_{50} value (0.186 ± 0.025 mg/mL), representing approximately 8-fold higher activity than diclofenac. This fraction exhibited remarkable dose-dependent inhibition, reaching 99.49% inhibition at 2 mg/mL and maintaining significant activity even at the lowest tested concentrations (33.43% at 0.0625 mg/mL). Fraction D did not allow the determination of an IC_{50} within the tested concentration range.

Our results corroborate the works by Mekhlouf et al. (2024), which demonstrated that *A. articulata* extracts exhibit concentration-dependent anti-protein denaturation activity comparable to aspirin. Their study showed that flower and leaf extracts effectively prevented egg albumin denaturation, with inhibition rates ranging from 29.71% to 92.17% at concentrations of 0.0625–0.5 mg/mL. However, in the same BSA denaturation assay, other *A. articulata* extracts were reported to show a dose-responsive anti-inflammatory activity, achieving 59.18%–86.31% inhibition at higher concentrations (0.5–5 mg/mL), confirming the dose-responsive anti-inflammatory activity of this species.

The superior performance of fraction C suggests that alkaloid concentration plays a crucial role in anti-inflammatory efficacy. The mechanism would seem to involve directly the alkaloids, forming complexes with the albumin through non-covalent molecular interactions that stabilize protein structures during thermal stress, preventing their unfolding, aggregation and precipitation. However, the specific binding sites and interaction strengths in this context depended significantly on the chemical structures involved in the reaction and the specific properties of alkaloids (Nirmala et al., 2023; Ameena et al., 2023). The primary mechanisms involve hydrophobic interactions and bridging associations that maintain helical conformations, while alkaloids may also provide membrane stabilization effects, creating dual protection for both cellular membranes and proteins simultaneously (Bailey-Shaw et al., 2017).

The concentration-dependent activity observed across different *A. articulata* extracts, combined with the exceptional performance of alkaloid-rich fractions, highlights the therapeutic potential of these compounds as anti-inflammatory agents.

9. *In vivo* investigations of toxicity

Acute toxicity assessment encompasses not only mortality evaluation but also the detection of physiological and behavioral alterations in experimental animals (Katzung, 2014). Following oral administration of four different concentrations of the alkaloid-rich fraction C from *A. articulata* to distinct animal groups, no mortality, clinical signs of toxicity, significant changes in body weight, or alterations in food and water intake were observed throughout the experimental period when compared to control animals. These findings suggest that fraction C exhibits a favorable safety profile at the tested dose range.

The absence of acute toxicity signs indicates that the bioactive alkaloids present in fraction C do not induce immediate adverse effects, supporting the potential therapeutic application of this fraction. However, further chronic toxicity studies would be necessary to establish comprehensive safety parameters. To our knowledge, this represents the first report investigating the anti-inflammatory properties and safety profile of alkaloids derived from *A. articulata*, contributing novel insights to the phytochemical and pharmacological characterization of this species. These findings are consistent with the safety profile reported for other *A. articulata* preparations. Ben Menni et al. (2022) demonstrated that aqueous extract of *A. articulata* at 500 mg/kg body weight and saponin extract at 100 mg/kg body weight exhibited no acute toxicity, with treated animals showing normal physiological and behavioral parameters throughout the experimental period. Similarly, previous studies have shown that both decoction and ethanolic extracts of *A. articulata* flowers and leaves exhibited no acute toxicity even at considerably higher doses. Specifically, administration of doses up to 5000 mg/kg body weight produced no physical signs of toxicity, with animals maintaining normal breathing patterns and physiological functions throughout the monitoring period (Mekhlouf et al., 2024). According to OECD categorization guidelines, the median lethal dosage (LD_{50}) for these extracts was calculated to exceed 5000 mg/kg body weight, indicating that *A. articulata* compounds present minimal acute toxicity risk across different extraction methods and phytochemical fractions.

10. *In Vivo* anti-inflammatory activity

The *in vivo* anti-inflammatory activity of *A. articulata* alkaloid extract was assessed using the carrageenan-induced paw edema model in rats. Four different doses (50, 100, 150, and 200 mg/kg BW) were evaluated against diclofenac (50 mg/kg) as positive control and Tween 80 as vehicle control, with monitoring conducted over 6 hours (H0-H6) post-carrageenan injection (n = 5 animals per group).

Following carrageenan administration, all experimental animals developed edema with initial volumes ranging from 47.28 ± 4.23% to 55.74 ± 6.61% at H0, showing no significant inter-group differences (Figures 9 and 10). The control group exhibited a typical inflammatory response, with edema volume progressively increasing to reach maximum levels at H3, followed by gradual reduction from H4 onwards without returning to baseline values by H6.

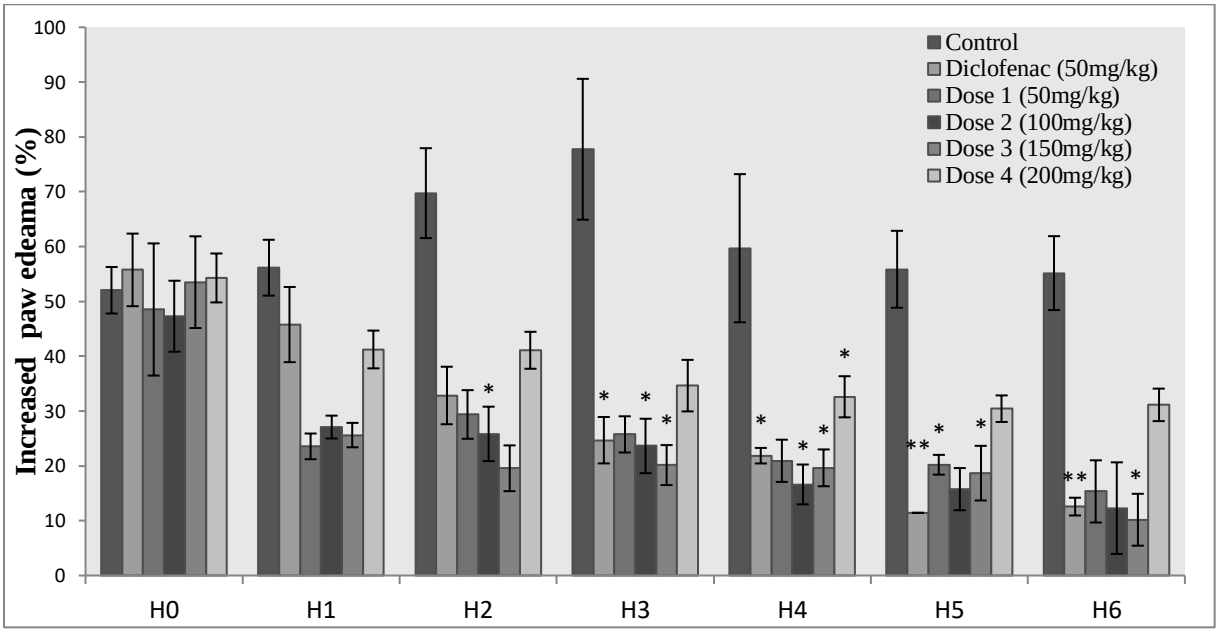

Figure 9. Percentage of edema volume after treatment with control (tween 80), *A. articulata* alkaloidal extracts at 50, 100, 150, and 200 mg/Kg BW, and diclofenac (standard). The monitoring was performed every hour for 6 hours. Values are means ± SD of independent experiments (n = 5 animals per group). *p < 0.05; **p < 0.01; ***p < 0.001, compared to the control.

Treatment with alkaloid extract and diclofenac demonstrated significant anti-inflammatory effects compared to the untreated control group. The percentage of paw edema inhibition was both dose- and time-dependent for the alkaloid doses of 50, 100, and 150 mg/kg BW, with inhibitory effects evident from H1 and reaching peak efficacy at H5, which was maintained through H6 (Figure 10). Dose 2 (100 mg/kg) and Dose 3 (150 mg/kg) exhibited remarkably similar inhibitory patterns, particularly from H5 onwards, suggesting a plateau effect at these concentrations.

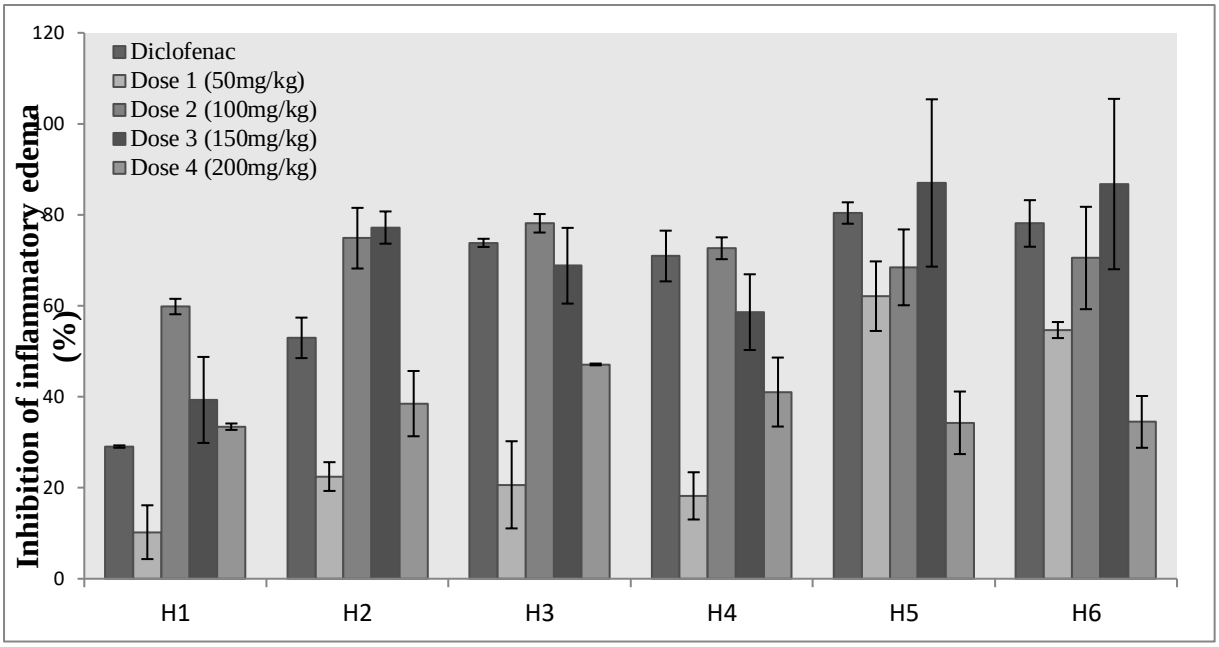

Figure 10. Anti-inflammatory effect of *A. articulata* alkaloids (inhibition percentage) at 50, 100, 150 and 200 mg/kg during the time, in comparison with Diclofenac treatment. (n = 5 animals per group).

The most significant anti-inflammatory activity was observed with Dose 3 (150 mg/kg BW), achieving a maximum inhibition of 86.99% at H5, which exceeded the efficacy of Diclofenac (80.39 ± 2.35%). Interestingly, Dose 4 (200 mg/kg BW) demonstrated reduced efficacy compared to the 150 mg/kg dose, showing a moderate inhibitory effect that peaked at 47.10 ± 0.19% at H3 before declining, suggesting a possible dose-response ceiling or potential adverse effects at higher concentrations.

These findings indicate that *A. articulata* alkaloid extract possesses potent anti-inflammatory properties with optimal efficacy at 150 mg/kg BW. The superior performance compared to diclofenac, combined with the sustained inhibitory effect lasting through the monitoring period, supports the therapeutic potential of this alkaloid-rich fraction. The biphasic dose-response relationship observed, with decreased efficacy at 200 mg/kg, warrants further investigation to elucidate the underlying mechanisms and establish optimal therapeutic dosing regimens.

Literature evidence demonstrates that sterol-rich extracts from Algerian *A. articulata* possess substantial anti-inflammatory potential, exhibiting edema inhibition percentages at 50 and 100 mg/kg BW that surpass those of diclofenac at 50 mg/kg (Ben Menni et al., 2022). Abdallah et al. ranked *A. articulata* as the second most potent anti-inflammatory species among thirteen plant species evaluated in their investigation (Abdallah et al., 2014). Their findings revealed that the n-butanol fraction achieved 68% edema reduction while inhibiting

both cyclooxygenase isoforms (COX-1 and COX-2). Comparative studies on alkaloids from *Matricaria pubescens* (Desf.) Sch.Bip demonstrated edema inhibition ranging from 17.95 to 88.89% at 200 mg/kg and from 13.39 to 79.01% at 100 mg/kg (Metrouh-Amir and Amir 2018).

The present investigation employed carrageenan-induced inflammation, a widely utilized *in vivo* acute screening model that produces reproducible inflammatory responses. According to Deng et al. (2011) and Tsai et al. (2015), this inflammatory process develops biphasically. The initial phase (1–2 h) involves release of chemical mediators including histamine, serotonin, and bradykinin, whereas the secondary phase (3–6 h) is characterized by elevated prostaglandins, leukotrienes, and free radicals, resulting in enhanced vascular permeability and neutrophil infiltration that promote edema formation through plasma fluid accumulation. Bai et al. (2021) identified the principal molecular targets mediating alkaloid anti-inflammatory activity as iNOS, cytokines, COX-2, prostaglandins, NF-κB, and MAPK. Consequently, *A. articulata* alkaloids likely exert their anti-inflammatory effects through modulation of one or more of these pathways. Additionally, alkaloids can influence leukocytes, neutrophils, and endothelial cells, thereby suppressing inflammation at the cellular level (Li et al., 2013; Wang et al., 2010). Haida et al. demonstrated that salsoline and carnegine, isolated from aerial and subterranean parts of Haloxylon scoparium Pomel, exhibited significant antioxidant activity potentially contributing to anti-inflammatory properties (Haida et al., 2022). Furthermore, β-carboline alkaloids identified in fraction C subfractions possess capacity to suppress nitric oxide, TNF-α, and IL-6 production, as well as inducible nitric oxide synthase expression and activity (Zhao et al., 2012). These mechanisms may constitute the scientific foundation for the anti-inflammatory activity observed in the *A. articulata* phytocomplex investigated herein.

11. ADMET properties

ADMET (Absorption, Distribution, Metabolism, Elimination, and Toxicity) properties of the alkaloidal phytochemical components found in *A. articulata* (i.e., carnegine, hordenine, dehydrosalsolidine, salsoline, gramine, and 2-methyl-1,2,3,4-tetrahydro-beta-carboline) were comprehensively evaluated (Table 6). Molar refractivity values, indicative of the molecules' polarizability and potential for biomolecular interactions, ranged from 50.75 (hordenine) to 68.48 (carnegine). The topological polar surface area (TPSA), a critical parameter for assessing the ability of molecules to cross biological membranes, varied between 19.03 Å² (gramine and 2-methyl-1,2,3,4-tetrahydro-beta-carboline) and 41.49 Å² (salsoline). Log P and

consensus Log $P_{o/w}$ values highlighted the lipophilicity of the components, a key factor influencing their bioavailability. All components exhibited high gastrointestinal (GI) absorption and were capable of crossing the blood-brain barrier (BBB). Regarding P-glycoprotein (P-gp) substrate potential, only 2-methyl-1,2,3,4-tetrahydro-beta-carboline was identified as a P-gp substrate (Figure 11). Evaluation of cytochrome P450 (CYP) enzyme inhibition revealed that while most components did not inhibit the isoforms CYP2C19, CYP2C9, or CYP3A4, some of them showed inhibitory activity against CYP1A2 and CYP2D6. Log Kp values for skin permeability ranged from -6.53 to -5.83 cm/s, indicating low dermal absorption for all components. The bioavailability score was consistently 0.55 for all molecules, and synthetic accessibility values ranged from 1.00 to 2.66, reflecting moderate ease of synthesis. The high GI absorption and BBB permeability of these molecules suggest their potential as therapeutic candidates for antioxidant, anti-inflammatory, and anticancer studies. Furthermore, their selective CYP enzyme inhibition profiles underline the need for further exploration regarding their drug metabolism and potential side effects. These findings provide valuable insights into the pharmacokinetic properties and toxicological profiles of *A. articulata* alkaloids, paving the way for their advanced research in therapeutic applications.

Table 6. ADMET values estimated for *A. articulata* alkaloids.

ADMET parameter	**Carnegine**	**Hordenine**	**Dehydrosalsolidine**	**Salsoline**	**Gramine**	**2-Methyl-1,2,3,4-tetrahydro-beta-carboline**
Molar Refractivity	68.48	50.75	63.87	59.11	55.77	62.54
TPSA	21.70 Å²	23.47 Å²	30.82 Å²	41.49 Å²	19.03 Å²	19.03 Å²
Log P	2.40	0.08	1.50	2.15	0.81	2.31
Consensus Log $P_{o/w}$	2.19	1.82	2.13	1.51	1.94	2.03
GI absorption	High	High	High	High	High	High
BBB permeant	Yes	Yes	Yes	Yes	Yes	Yes
P-gp substrate	No	No	No	No	No	Yes
CYP1A2 inhibitor	No	Yes	Yes	No	Yes	Yes
CYP2C19 inhibitor	No	No	No	No	No	No
CYP2C9 inhibitor	No	No	No	No	No	No
CYP2D6 inhibitor	Yes	No	No	No	No	No
CYP3A4 inhibitor	No	No	No	No	No	No
Log K_p (skin permeation)	-6.13 cm/s	-5.83 cm/s	-6.43 cm/s	-6.53 cm/s	-6.10 cm/s	-6.05cm/s
Bioavailability Score	0.55	0.55	0.55	0.55	0.55	0.55
Synthetic accessibility	2.52	1.00	2.66	2.26	1.44	1.90

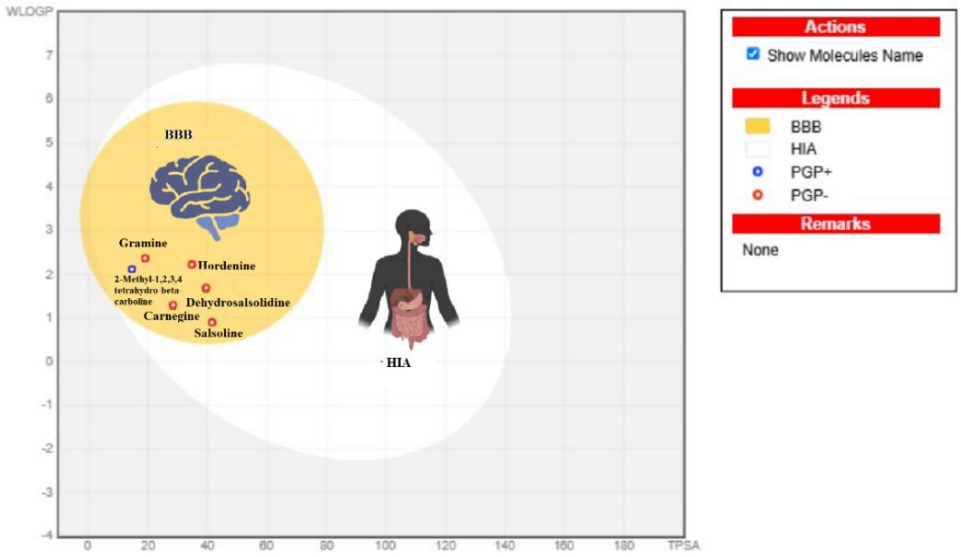

Figure 11. Blood brain barrier and human intestinal absorption predictions of the selected phytochemical compounds**.**

12. Result of molecular docking

The Table 7 presents the binding interaction results of the compounds (Carnegine, Hordenine, Dehydrosalsolidine, Salsoline, Gramine, and 2-Methyl-1,2,3,4-tetrahydro-beta-carboline) with specific target proteins (5IKQ, 1RJ8, and 4AUV), evaluated through various parameters, including binding energy (kcal/mol), ligand efficiency, fit quality (FQ), ligand lipophilic efficiency (LLE), ligand efficiency-dependent lipophilicity (LELP), estimated inhibition constant (Ki, µM), and pIC_{50} values. Carnegine demonstrated high binding energy across all proteins, with the strongest interaction observed with 5IKQ (-7.1 kcal/mol). The ligand efficiency was calculated as 0.216, with a fit quality of 0.591. The LLE and LELP values were 2.958 and 11.160, respectively, while the estimated Ki was 6.14 µM. However, lower binding energies and higher Ki values for 1RJ8 and 4AUV suggest protein-specific differences in binding affinity. Hordenine exhibited relatively lower binding energies, with a value of -5.7 kcal/mol for 5IKQ. The ligand efficiency (0.219) and fit quality (0.478) were moderate, while the LLE value (3.130) highlighted its lipophilic properties. However, the higher Ki value (47.8 µM) indicates weaker inhibitory activity compared to other compounds. Dehydrosalsolidine showed strong binding to 5IKQ (-7.0 kcal/mol) and a low Ki value of 1.51 µM, indicating potent inhibitory activity. The ligand efficiency was 0.250, with an FQ value of 0.595 and an LLE of 4.667, demonstrating its high binding capacity. However,

weaker interactions were observed with 1RJ8 and 4AUV, as evidenced by lower binding energies and higher Ki values. Salsoline demonstrated moderate binding energies, with the highest value of -6.7 kcal/mol for 5IKQ and a Ki of 19.7 µM. Its fit quality and LLE values were calculated as 0.565 and 3.116, respectively. However, its interaction with 4AUV was weaker, as indicated by a Ki value of 195 µM, suggesting lower efficacy for this target protein. Gramine exhibited binding energy of -6.6 kcal/mol and a Ki value of 12.9 µM with 5IKQ, indicating moderate inhibitory activity. The high LLE value (8.148) highlights its strong lipophilic nature. However, the increasing Ki values for other proteins suggest protein-specific variations in binding affinity. 2-Methyl-1,2,3,4-tetrahydro-beta-carboline showed the strongest binding energy (-7.3 kcal/mol) and the lowest Ki value (2.02 µM) for 5IKQ, indicating its high inhibitory potential. The ligand efficiency was 0.216, with an FQ of 0.609 and an LLE of 3.116, underscoring its strong interaction with this protein. However, slightly weaker binding was observed for other targets, such as 1RJ8, with relatively higher Ki values. This analysis highlights the varying binding affinities of the compounds for different target proteins and their potential applications in antioxidant, anti-inflammatory, and anticancer studies. Notably, Dehydrosalsolidine and 2-Methyl-1,2,3,4-tetrahydro-beta-carboline exhibited strong binding energies and low inhibition constants, making them promising candidates for further therapeutic exploration.

Table 7. Results of the binding interactions between alkaloidal compounds and selected target proteins.

	Protein	Binding Energy (kcal/mol)	Ligand efficiency	Fit quality (FQ)	Ligand lipophilic efficiency (LLE)	Ligand efficiency-dependent lipophilicity (LELP)	Estimated Inhibition constant {(Ki) (µM)}	pIC_{50}
Carnegine	5IKQ	-7.1	0.216	0.591	2.958	11.160	6.14	5.071
	1RJ8	-6.1	0.185	0.509	2.542	12.970	20.6	4.357
	4AUV	-5.4	0.164	0.451	2.250	14.630	123	3.857
Hordenine	5IKQ	-5.7	0.219	0.478	3.130	8.310	47.8	4.070
	1RJ8	-5.5	0.212	0.462	3.020	8.590	75.3	3.930
	4AUV	-5.4	0.208	0.454	2.970	8.750	122	3.860
Dehydrosalsolidine	5IKQ	-7.0	0.250	0.595	4.667	6.000	1.51	5.000
	1RJ8	-6.3	0.225	0.536	4.200	6.667	21.9	4.500
	4AUV	-5.8	0.207	0.493	3.867	7.250	61.8	4.143
Salsoline	5IKQ	-6.7	0.248	0.565	3.116	8.670	19.7	4.786
	1RJ8	-6.2	0.230	0.525	2.884	9.350	39.1	4.429
	4AUV	-5.9	0.218	0.493	2.745	9.870	195	4.214
Gramine	5IKQ	-6.6	0.244	0.556	8.148	8.670	12.9	4.714
	1RJ8	-6.1	0.226	0.515	7.530	9.350	20.4	4.357
	4AUV	-5.6	0.218	0.472	6.910	9.870	56.8	4.000
2-Methyl-1,2,3,4-tetrahydro-beta-carboline	5IKQ	-7.3	0.216	0.609	3.116	8.870	2.02	5.214
	1RJ8	-6.2	0.226	0.515	2.684	10.430	3.94	4.429
	4AUV	-6.7	0.239	0.560	2.904	9.660	19.8	4.786

The Table 8 presents detailed molecular docking interactions of the phytochemical compounds (Carnegine, Dehydrosalsolidine, Salsoline, and 2-Methyl-1,2,3,4-tetrahydro-beta-carboline) with specific protein targets (5IKQ, 1RJ8, and 4AUV). These compounds exhibited various binding interactions, including hydrogen bonds, carbon-hydrogen bonds, alkyl interactions, Pi-alkyl, and Pi-Pi interactions, with the active sites of the target proteins. The type of binding, the interacting amino acids, and the binding distances (Å) are detailed for each compound in Table 8. Carnegine displayed strong interactions with the 5IKQ protein, forming carbon-hydrogen bonds and alkyl interactions with amino acids such as MET523, VAL524, and ALA528. Pi-alkyl interactions were observed with aromatic amino acids like

TYR356, TYR386, and PHE519. These interactions enhanced the compound's affinity for hydrophobic regions of the protein. The binding distances, ranging from 2.34 Å to 5.24 Å, indicate stable interactions (Figure 12). Dehydrosalsolidine exhibited diverse interactions with the 1RJ8 protein. It formed hydrogen bonds with SER319, GLY268, and TYR310, with binding distances ranging from 1.89 Å to 3.01 Å. Additionally, it showed alkyl and Pi-alkyl interactions with hydrophobic amino acids such as VAL365 and ALA367, suggesting compatibility with the protein's hydrophobic regions. Pi-alkyl and Pi-Pi interactions with PHE317 enhanced the binding potential of its aromatic rings with the active site of the protein (Figure 13). Salsoline demonstrated the shortest hydrogen bond distance (1.53 Å) and a strong Pi-sigma interaction with the 1RJ8 protein. It formed hydrogen bonds with THR315, SER319, and PHE317, while showing alkyl interactions with VAL365 and ALA367. Pi-Pi stacked and Pi-alkyl interactions further strengthened the binding affinity of the compound for aromatic regions of the protein. These binding types suggest high affinity for the target protein (Figure 14). 2-Methyl-1,2,3,4-tetrahydro-beta-carboline exhibited a broad spectrum of binding interactions with the 5IKQ, 1RJ8, and 4AUV proteins (Figures 15, 16 and 17). It formed carbon-hydrogen bonds and Pi-alkyl interactions with amino acids such as SER353, LEU352, and VAL523 in the 5IKQ protein. For the 1RJ8 protein, Pi-cation and Pi-anion interactions were observed with GLU326 and LYS375, respectively. With the 4AUV protein, Pi-alkyl and Pi-Pi T-shaped interactions were noted with PHE71, VAL61, and MET64. These interactions suggest that the compound possesses flexible binding modes and can adapt to different protein targets.

Table 8. Predicted interactions in docked conformations between *A. articulata* alkaloids and human selected proteins.

Ligand	Protein	Amino acids	Interacting	Distance
Carnegine	5IKQ	:[001:H7 - B:MET523:O	Carbon Hydrogen Bond	2.34
		:[001:H11 - B:MET523:O	Carbon Hydrogen Bond	2.70
		B:VAL524 - :[001	Alkyl	4.74
		B:ALA528 - :[001:C13	Alkyl	4.48
		:[001 - B:LEU353	Alkyl	5.10
		:[001 - B:MET523	Alkyl	5.24
		:[001:C10 - B:VAL524	Alkyl	4.56
		:[001:C13 - B:VAL350	Alkyl	3.48
		:[001:C13 - B:LEU532	Alkyl	4.30
		B:TYR356 - :[001:C10	Pi-Alkyl	4.52

		B:TYR386 - :[001:C12	Pi-Alkyl	4.62
		B:PHE519 - :[001	Pi-Alkyl	4.81
		:[001 - B:VAL350	Pi-Alkyl	5.24
		:[001 - B:LEU353	Pi-Alkyl	5.21
		:[001 - B:VAL524	Pi-Alkyl	4.82
		:[001 - B:ALA528	Pi-Alkyl	4.05
Dehydrosalsolidine	1RJ8	A:SER319:HG - :[001:N1	Conventional Hydrogen Bond	2.16
		E:GLY268:HN - :[001:O1	Conventional Hydrogen Bond	2.76
		:[001:H2 - D:TYR310:OH	Carbon Hydrogen Bond	3.01
		:[001:H3 - E:LYS263:O	Carbon Hydrogen Bond	2.34
		:[001:H14 - E:VAL262:O	Carbon Hydrogen Bond	2.71
		:[001:H15 - E:LEU266:O	Carbon Hydrogen Bond	1.89
		A:GLN331:HE21 - :[001	Pi-Donor Hydrogen Bond	2.70
		A:VAL365 - :[001	Alkyl	4.67
		E:ALA367 - :[001	Alkyl	5.49
		E:ALA367 - :[001:C10	Alkyl	3.30
		E:ALA367 - :[001:C11	Alkyl	3.57
		:[001:C10 - E:LYS263	Alkyl	4.65
		:[001:C11 - A:VAL365	Alkyl	4.76
		:[001:C12 - E:VAL262	Alkyl	5.14
		:[001:C12 - E:LEU266	Alkyl	5.44
		A:PHE317 - :[001:C10	Pi-Alkyl	5.18
		A:PHE317 - :[001:C11	Pi-Alkyl	4.53
		D:TYR310 - :[001:C10	Pi-Alkyl	5.37
		:[001 - E:ALA367	Pi-Alkyl	4.34
Salsoline	1RJ8	:[001:H7 - E:THR315:O	Conventional Hydrogen Bond	1.53
		A:SER319:HB1 - :[001:O1	Carbon Hydrogen Bond	2.55
		A:SER319:HB1 - :[001:O2	Carbon Hydrogen Bond	2.51
		:[001:H5 - E:PHE317:O	Carbon Hydrogen Bond	2.44
		:[001:H13 - A:PHE317:O	Carbon Hydrogen Bond	2.08
		:[001:H14 - A:VAL365:O	Carbon Hydrogen Bond	2.50
		:[001:H9 - E:HIS366	Pi-Sigma	2.82
		A:PHE317 - :[001	Pi-Pi Stacked	5.21
		A:ALA367 - :[001:C10	Alkyl	3.73

		A:ALA367 - :[001:C11	Alkyl	3.07
		:[001:C11 - A:VAL365	Alkyl	3.95
		:[001:C11 - A:ILE369	Alkyl	4.81
		E:HIS366 - :[001:C6	Pi-Alkyl	4.67
		:[001 - A:VAL365	Pi-Alkyl	4.86
		:[001 - A:ALA367	Pi-Alkyl	4.71
		:[001 - E:ALA367	Pi-Alkyl	5.04
2-Methyl-1,2,3,4-tetrahydro-beta-carboline	5IKQ	A:SER353:HB2 - :[001:N1	Carbon Hydrogen Bond	2.68
		A:LEU352 - :[001	Alkyl	5.45
		A:VAL523 - :[001	Alkyl	3.65
		:[001 - A:LEU352	Pi-Alkyl	4.89
		:[001 - A:VAL523	Pi-Alkyl	3.78
		:[001 - A:ARG513	Pi-Alkyl	5.26
		:[001 - A:ALA516	Pi-Alkyl	4.25
		:[001 - A:VAL523	Pi-Alkyl	4.58
	1RJ8	:[001:H14 - E:GLU326:O	Carbon Hydrogen Bond	2.78
		D:LYS375:NZ - :[001	Pi-Cation	4.91
		E:GLU326:OE1 - :[001	Pi-Anion	4.49
		A:PRO328 - :[001	Alkyl	5.47
		E:VAL270 - :[001	Alkyl	5.05
		E:LYS363 - :[001	Alkyl	4.49
		D:HIS376 - :[001	Pi-Alkyl	5.48
		:[001 - E:VAL270	Pi-Alkyl	5.24
		:[001 - D:LYS375	Pi-Alkyl	4.68
		:[001 - E:VAL270	Pi-Alkyl	5.22
	4AUV	:[001:H14 - B:PHE71:O	Carbon Hydrogen Bond	2.90
		:[001 - E:PHE71	Pi-Pi T-shaped	4.82
		B:PHE71 - :[001	Pi-Alkyl	4.51
		E:PHE71 - :[001	Pi-Alkyl	5.13
		:[001 - A:VAL61	Pi-Alkyl	4.49
		:[001 - A:MET64	Pi-Alkyl	4.99
		:[001 - E:LEU74	Pi-Alkyl	4.65

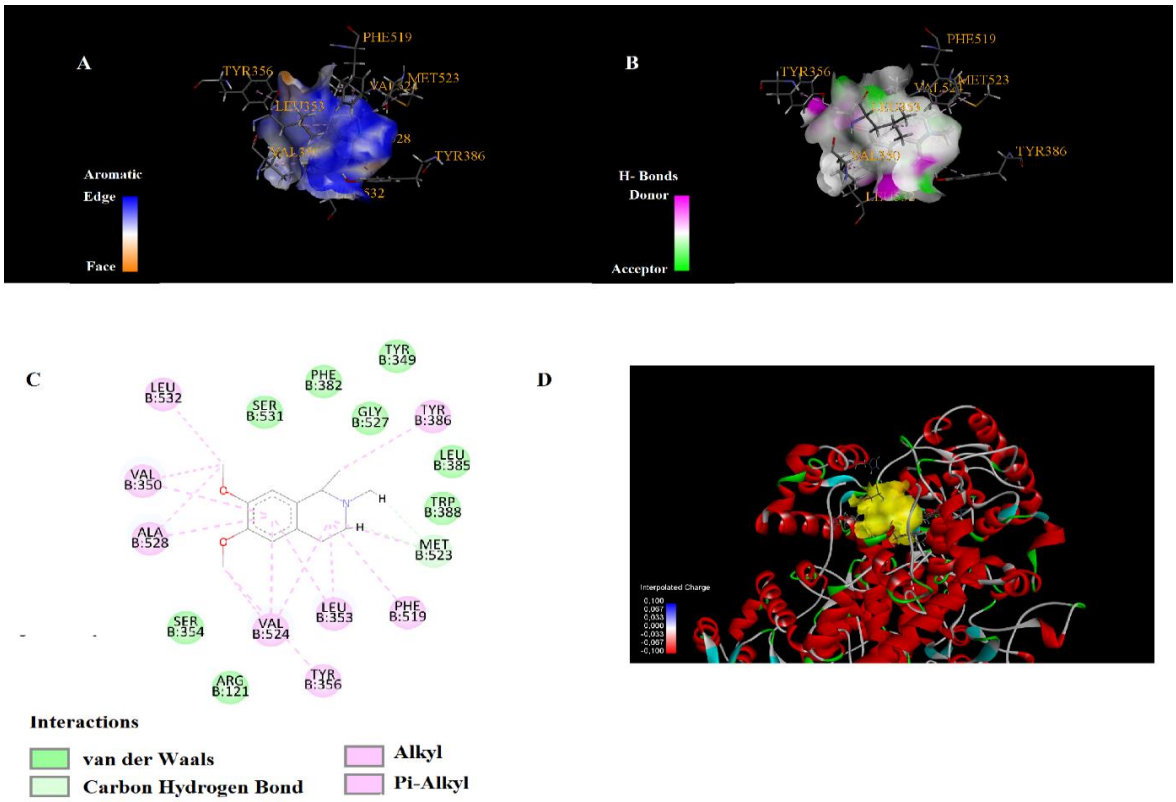

Figure 12. Interactions of Carnegine with target 5IKQ: A) Aromatic surface representation B) H-Bond distribution, C) 2D ligand interaction, D) 3D representation of docked poses.

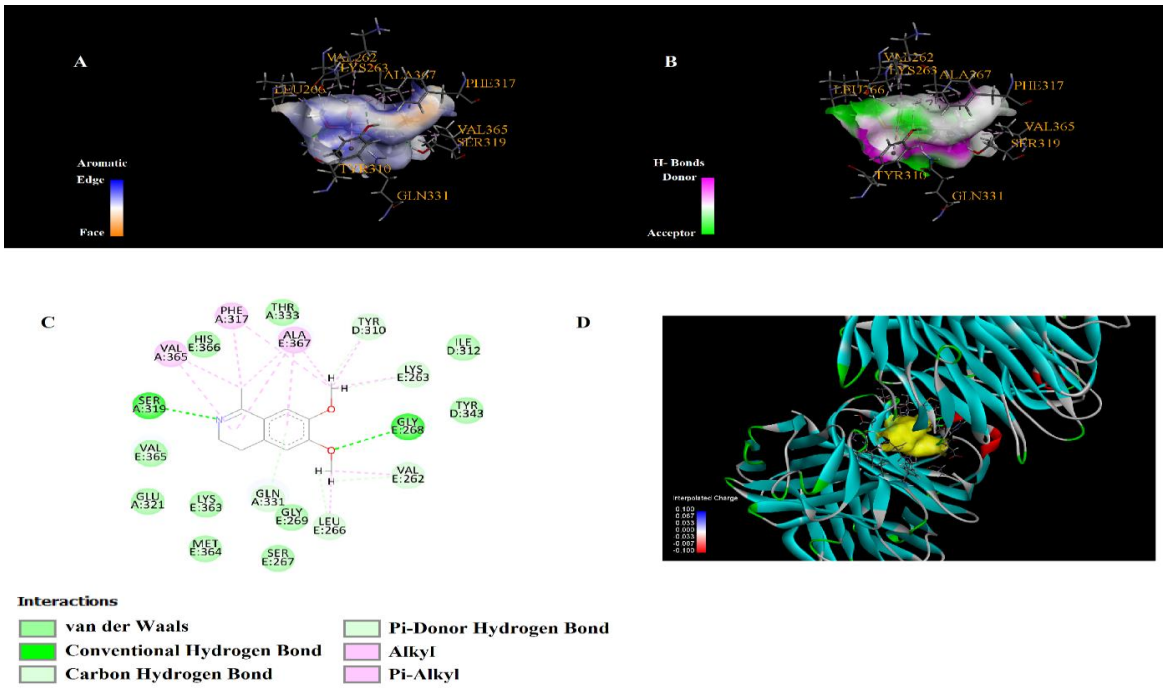

Figure 13. Interactions of Dehydrosalsolidine with target 1RJ8: A) Aromatic surface representation B) H-Bond distribution, C) 2D ligand interaction, D) 3D representation of docked poses.

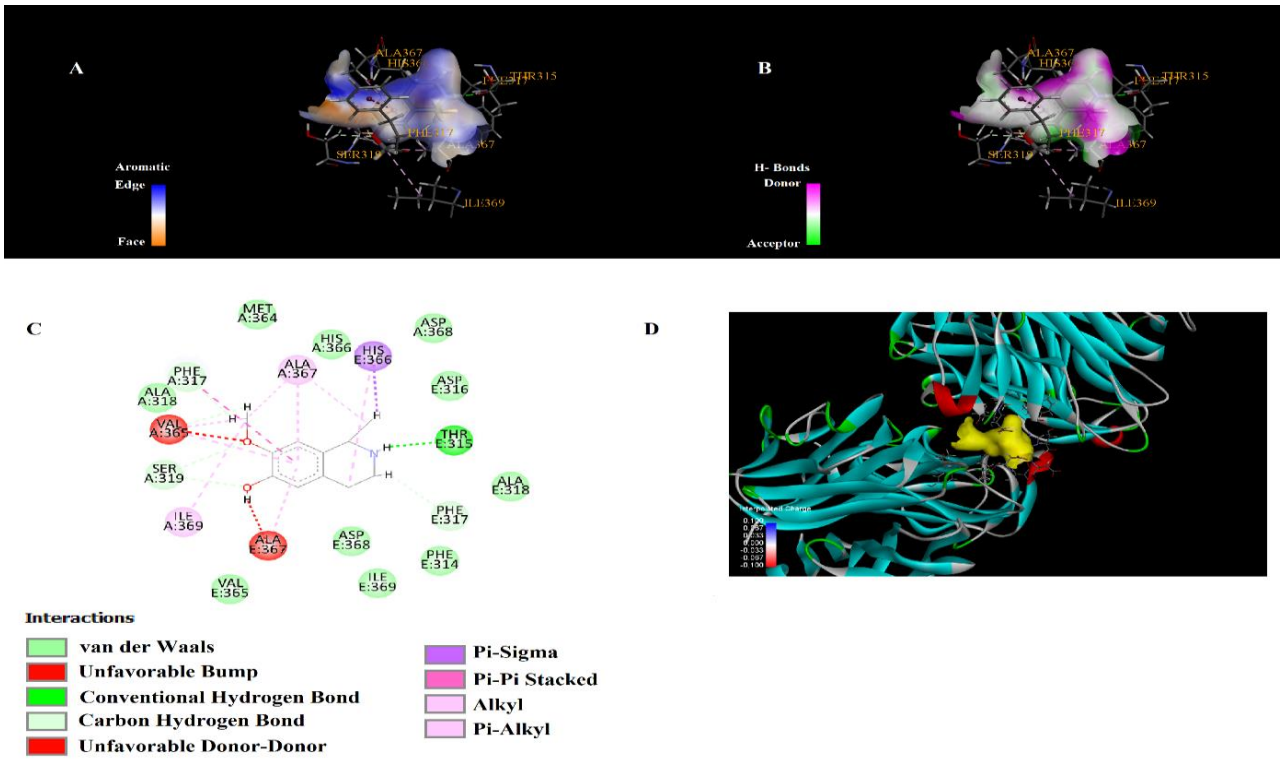

Figure 14. Interactions of Salsoline with target 1RJ8: A) Aromatic surface representation B) H-Bond distribution, C) 2D ligand interaction, D) 3D representation of docked poses.

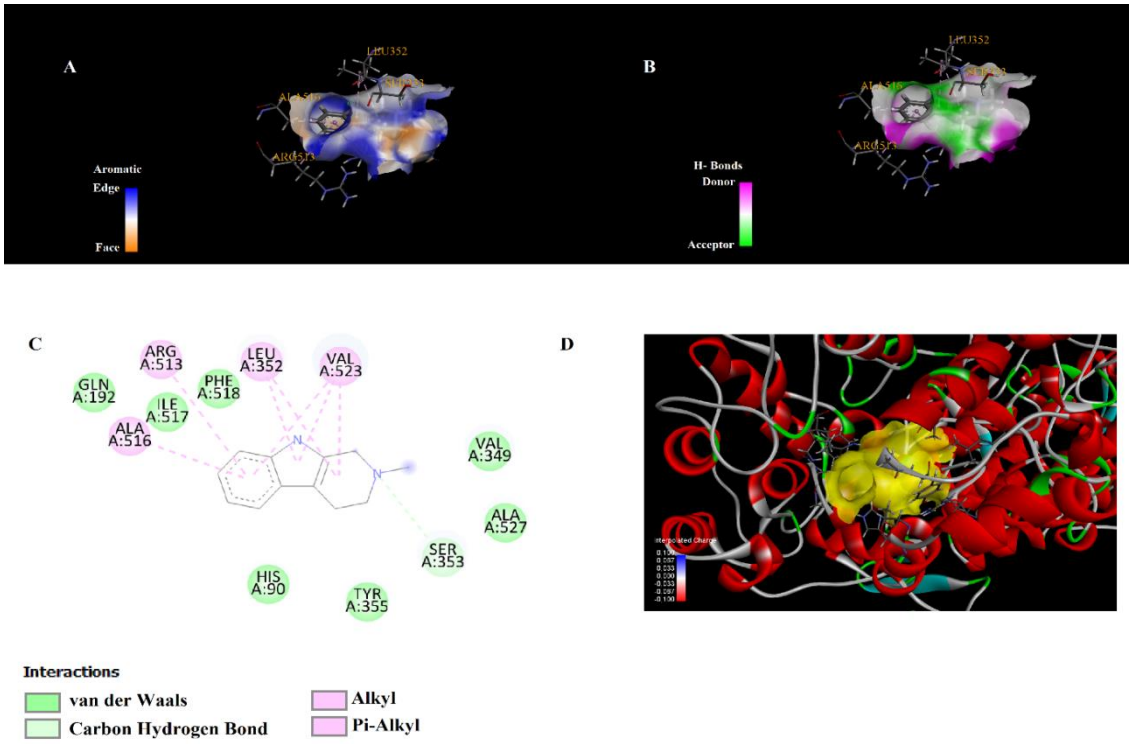

Figure 15. Interactions of 2-Methyl-1,2,3,4-tetrahydro-beta-carboline with target 5IKQ: A) Aromatic surface representation B) H-Bond distribution, C) 2D ligand interaction, D) 3D representation of docked poses.

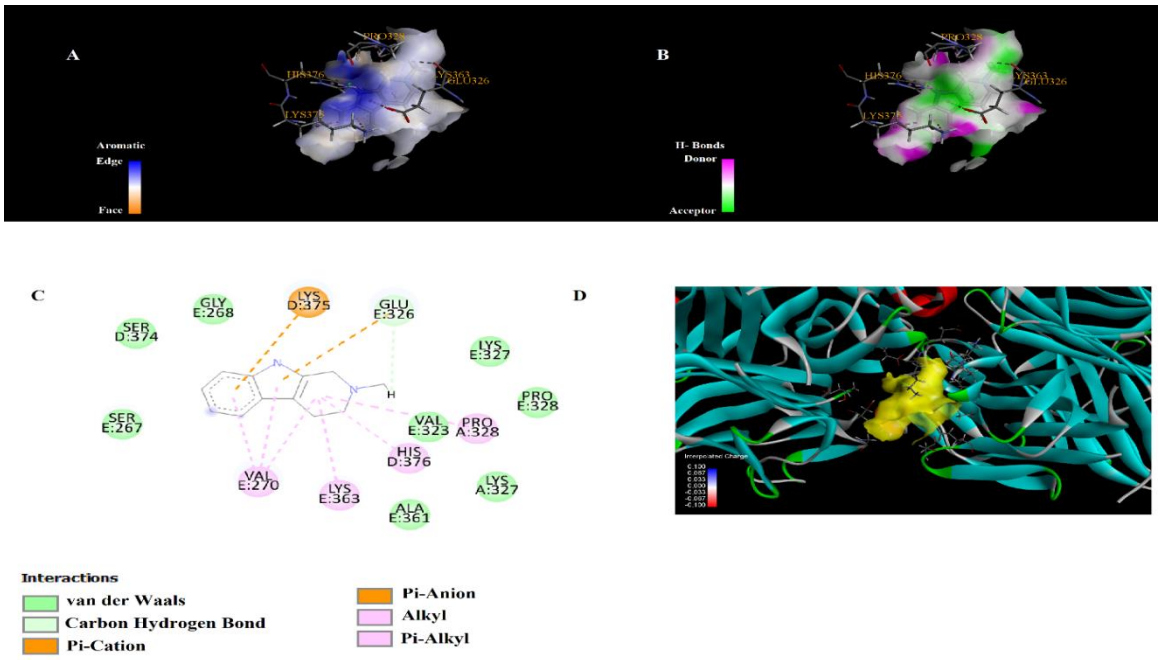

Figure 16. Interactions of 2-Methyl-1,2,3,4-tetrahydro-beta-carboline with target 1RJ8: A) Aromatic surface representation B) H-Bond distribution, C) 2D ligand interaction, D) 3D representation of docked poses.

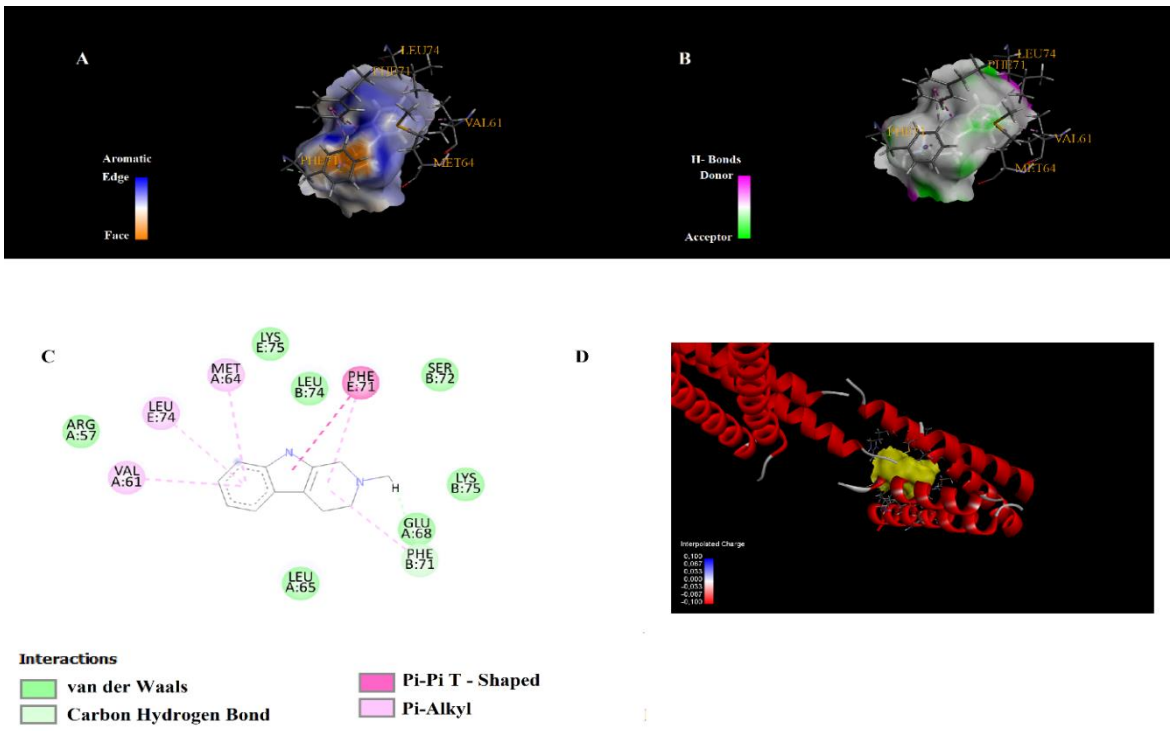

Figure 17. Interactions of 2-Methyl-1,2,3,4-tetrahydro-beta-carboline with target 4AUV: A) Aromatic surface representation B) H-Bond distribution, C) 2D ligand interaction, D) 3D representation of docked poses.

This study successfully bridges computational prediction with experimental validation to elucidate the anti-inflammatory potential of *A. articulata* alkaloids. The integrated results

from molecular docking, ADMET analysis and biological assays provide a compelling, multi-layered explanation for the potent anti-inflammatory effects observed, particularly in Fraction C.

The investigation began by computationally profiling six major alkaloids. The ADMET analysis revealed that all compounds possess favorable drug-like properties, including high gastrointestinal absorption and the ability to cross the blood-brain barrier. This suggests they would be effectively absorbed if administered orally and could potentially target neuroinflammation. Their molecular characteristics fell within optimal ranges for bioavailability, and most showed a low risk for problematic drug-drug interactions, with only selective inhibition of certain CYP enzymes. This foundational data confirmed that these natural products are not only active but also possess promising pharmacokinetic profiles for drug development.

The molecular docking results provided the crucial mechanistic link to the experimental findings. The strong inhibition of COX-2 (PDB: 5IKQ) by several alkaloids directly explains the exceptional performance in the BSA denaturation assay. This test models the ability of a compound to prevent protein unfolding, a process often driven by inflammation. The computational data shows that the alkaloids, particularly 2-Methyl-1,2,3,4-tetrahydro-β-carboline and Dehydrosalsolidine, achieve this by forming a stable, multi-faceted complex within the COX-2 active site. They utilize a network of hydrogen bonds and hydrophobic interactions with key amino acids, effectively stabilizing the protein and inhibiting its prostaglandin-producing activity. This is precisely why Fraction C, rich in these compounds, demonstrated 99.5% inhibition and was 8-fold more potent than the standard drug diclofenac.
Furthermore, the anti-inflammatory activity was not limited to a single target. The strong binding of compounds like Dehydrosalsolidine and Salsoline to TNF-α (PDB: 1RJ8)—with Salsoline forming an exceptionally short hydrogen bond—suggests a concurrent ability to modulate this key inflammatory signaling pathway. This multi-target mechanism is the most plausible explanation for the outstanding results in the *in vivo* carrageenan-induced paw edema test.

The carrageenan model unfolds in two phases: an early histamine/serotonin-mediated phase and a later prostaglandin and free radical-driven phase. The ability of Fraction C to achieve 86.99% inhibition, outperforming Diclofenac, indicates it acts on both phases. The computational evidence suggests this is achieved through a synergistic combination: blocking COX-2 to inhibit prostaglandin synthesis, modulating TNF-α to dampen the inflammatory

cascade, and, as supported by other experimental data, likely suppressing nitric oxide production and providing antioxidant activity.

In conclusion, the remarkable alignment between the computational predictions and the experimental results provides powerful validation. The binding energies and inhibition constants from docking directly correlated with the concentration-dependent activities seen *in vitro* and the potent efficacy observed *in vivo*. This integrated approach establishes that the anti-inflammatory power of *A. articulata* alkaloids, especially in Fraction C, stems from a synergistic, multi-target mechanism. They simultaneously engage several key players in the inflammatory process, making them highly effective therapeutic candidates at doses of 100-150 mg/kg, and offering a promising natural alternative for managing complex inflammatory conditions.

Conclusion and perspectives

This study is a contribution to the phytochemical study and biological evaluation of the crude ethanol extract and its fractions (acetone, hexane, chloroform, and alkaline aqueous) from the aerial part of *Anabasis articulata*, a plant used in traditional Algerian pharmacopoeia.

The phytochemical study revealed the richness of the plant in secondary metabolites, particularly flavonoids and alkaloids, which were detected in the crude extract and all its fractions. Bioguided screening and GC-MS analysis led to the identification of six major alkaloids in the chloroform fraction (Fraction C): carnegine, hordenine, dehydro-salsolidine, salsoline, gramine, and 2-methyl-1,2,3,4-tetrahydro-beta-carboline. The presence of these bioactive compounds is directly correlated with the observed biological activities.

The evaluation of antioxidant activity using multiple tests (DPPH, ABTS, FRAP, TAC) demonstrated remarkable potential, particularly in the alkaloid fraction (Fraction C), whose activity was superior to that of the crude extract and close to that of reference antioxidants in some tests.

The study of *in vitro* anti-inflammatory activity (inhibition of BSA denaturation) revealed an exceptional efficacy of Fraction C, with an activity approximately eight times more potent than that of diclofenac, a reference anti-inflammatory drug. This activity was confirmed *in vivo* on the carrageenan-induced paw edema model, where Fraction C showed a dose-dependent inhibition, reaching a maximum efficacy at a dose of 150 mg/kg, thus exceeding that of diclofenac.

The evaluation of antidiabetic activity showed that the crude extract has a strong α-amylase inhibitory power, with an efficacy comparable to that of acarbose, a reference drug.

In silico studies (molecular docking and ADMET prediction) provided mechanistic support for these results. They confirmed the strong binding affinity of the identified alkaloids with key protein targets of inflammation (such as COX-2/5IKQ and TNF-α/1RJ8), thereby explaining the observed anti-inflammatory activity. The predicted ADMET profiles indicated that these alkaloids possess good pharmacokinetic properties and a promising safety profile.

Finally, the acute toxicity test indicated that Fraction C is devoid of any toxic effects at the tested doses, confirming its safety for potential therapeutic use.

In summary, this study scientifically validates the traditional use of *Anabasis articulata* and demonstrates that its alkaloids, particularly concentrated in Fraction C, constitute natural and safe antioxidant, anti-inflammatory, and antidiabetic agents, likely acting through a multi-target mechanism.

These promising results represent only an initial step in the valorization of *Anabasis articulata*. To move forward, the following complementary studies are envisaged:

- **Isolation and further characterization:** It would be essential to proceed with the isolation and purification of the major alkaloids identified (salsoline, carnegine, 2-methyl-1,2,3,4-tetrahydro-beta-carboline) to evaluate their individual biological activity and any potential synergistic effects between them or in combination with conventional drugs.
- **Elucidation of mechanisms of action:** More in-depth *in vitro* and *in vivo* studies are necessary to elucidate the precise cellular and molecular signaling pathways (NF-κB pathway, pro-inflammatory cytokines, etc.) through which these alkaloids exert their anti-inflammatory and antidiabetic effects.
- ***In vivo* validation of activities:** It would be important to evaluate the efficacy of Fraction C and the pure alkaloids in animal models of chronic pathologies, such as rheumatoid arthritis for inflammation, or a long-term type 2 diabetes model for the antidiabetic activity, while also measuring oxidative stress markers.
- **Chronic toxicity studies:** Conducting subchronic and chronic toxicity studies is essential to confirm the safety of the extracts and pure compounds during prolonged administration and to determine the optimal therapeutic dose. In parallel, it is highly advised to carry out comprehensive cytotoxicity tests on a range of cell lines, with a special emphasis on cancer cell lines, to assess a potential antitumor profile.
- **Pharmaceutical development:** Finally, formulation studies should be initiated to develop delivery systems (for example, nanoparticles) to improve the bioavailability and stability of these natural active principles, with a view to therapeutic application.

References

- Abdallah, HM, Abdel-Naim, AB, Ashour, OM, Shehata, IA, Abdel-Sattar, EA. 2014. Anti-inflammatory activity of selected plants from Saudi Arabia. Z. Naturforsch. C J. Biosci, 69: 1–9.
- Abdulsahib, K, Abdulkareem, A, Ban Jumaa, Q, Hayder, S. 2016. Antiangiogenesis and antioxidant effect of *Anabasis articulata* stems extracts. Int. J. Pharm. Sci. Rev. Res, 41: 88-94.
- Abozeed, AE. 2014. Comparative study on the active chemical constituents of some chenopodiaceae plants. Bull. Fac. Agric, 65: 68-77.
- Afiomah, CS, Iwuozor, K. 2020. Nutritional and phytochemical properties of *Beta vulgaris* Linnaeus (Chenopodiaceae)--a review. Niger. J. Pharm. Appl. Sci. Res, 9: 38-44.
- Aftab, T, Khan, MMA, Naeem, M. 2025. Overexploitation and conservation strategies for medicinal and aromatic plants. In: Essential Oil-Bearing Plants. Academic Press, pp. 95-105.
- AG, H. BISCHOFF Bayer. 1994. Pharmacology of α-glucosidase inhibition. Eur. J. Clin. Invest, 24: 3-10.
- Alamzeb, M, Shah, SWA, Hussain, H, Zahoor, M, Ahmad, S, Mughal, EU, Ali, EA. 2024. Beneficial effects of natural alkaloids from *Berberis glaucocarpa* as antidiabetic agents: an *in vitro*, *in silico*, and *in vivo* approach. ACS Omega, 9: 9813–9822.
- Al-Joufi, FA, Jan, M, Zahoor, M, Nazir, N, Naz, S, Talha, M, Khan, FA. 2022. *Anabasis articulata* (Forssk.) Moq: A good source of phytochemicals with antibacterial, antioxidant, and antidiabetic potential. Molecules, 27: 3526.
- Altemimi, A, Lakhssassi, N, Baharlouei, A, Watson, DG, Lightfoot, DA. 2017. Phytochemicals: Extraction, isolation, and identification of bioactive compounds from plant extracts. Plants, 6: 42.
- Ameena, M, Arumugham, M, Ramalingam, K, Rajeshkumar, S, Shanmugam, R. 2023. Evaluation of the anti-inflammatory, antimicrobial, antioxidant, and cytotoxic effects of chitosan thiocolchicoside-lauric acid nanogel. Cureus, 15: e45289.
- Amssayef, A, Eddouks, M. 2023. Alkaloids as promising agents for the management of insulin resistance: a review. Curr. Pharm. Des, 29: 3123-3136.
- Amtaghri, S, Slaoui, M, Eddouks, M. 2025. The genus *Anabasis*: a review on pharmacological and phytochemical properties. Cardiovasc. Hematol. Agents Med. Chem, 23: 11-28.

- Aniszewski, T. 2007. Alkaloids-secrets of life: Alkaloid chemistry, biological significance, applications and ecological role. Elsevier.
- Antolovich, M, Prenzler, PD, Patsalides, E, McDonald, S, Robards, K. 2002. Methods for testing antioxidant activity. Analyst, 127: 183-198.
- Aouir, F, Chaibi, R, Benchettouh, A, Gouzi, H, Benaceur, F, Chenchouni, H. 2025. An ethnobotanical inventory and therapeutic potential of medicinal plants used in traditional practices in northeastern Algeria. Ethnobotany Res. Appl, 31: 1-19.
- Apak, R, Güçlü, K, Demirata, B, Özyürek, M, Çelik, SE, Bektaşoğlu, B, Özyurt, D. 2007. Comparative evaluation of various total antioxidant capacity assays applied to phenolic compounds with the CUPRAC assay. Molecules, 12: 1496-1547.
- Appley, MG, Chambers, MI, Musah, RA. 2022. Quantification of hordenine in a complex plant matrix by direct analysis in real time--high-resolution mass spectrometry: application to the "plant of concern" *Sceletium tortuosum*. Drug Test. Anal, 14: 604–612.
- Aryal, S, Baniya, MK, Danekhu, K, Kunwar, P, Gurung, R, Koirala, N. 2019. Total Phenolic Content, Flavonoid Content and Antioxidant Potential of Wild Vegetables from Western Nepal. Plants, 8: 96.
- Association, AD. 2021. 1. Improving care and promoting health in populations: Standards of Medical Care in Diabetes---2021. Diabetes Care, 44: S7-S14.
- Atanasov, AG, Waltenberger, B, Pferschy-Wenzig, EM, Linder, T, Wawrosch, C, Uhrin, P, Stuppner, H. 2015. Discovery and resupply of pharmacologically active plant-derived natural products: A review. Biotechnol. Adv, 33: 1582-1614.
- Azza, M, Mohga, A, Maha, R, El-Sayed, M, Abdel-Razik, F, El-Sharabasy, F, Aly, H, Mohamed, RM. 2014. Alleviation of Dimethylnitrosamine-induced liver injury and fibrosis by supplementation of *Anabasis articulata* extract in rats. Ind. J. Clin. Biochem, 29: 418–429.
- Bai, R, Yao, C, Zhong, Z, Ge, J, Bai, Z, Ye, X, Xie, T, Xie, Y. 2021. Discovery of natural anti-inflammatory alkaloids: Potential leads for the drug discovery for the treatment of inflammation. Eur. J. Med. Chem, 213: 113165.
- Bailey-Shaw, YA, Williams, LA, Green, CE, Rodney, S, Smith, AM. 2017. *In-vitro* evaluation of the anti-inflammatory potential of selected Jamaican plant extracts using the bovine serum albumin protein denaturation assay. Int. J. Pharm. Sci. Rev. Res, 47: 145-153.

- Bandala, C, Cárdenas-Rodríguez, N, Mendoza-Torreblanca, JG, Contreras-García, IJ, Martínez-López, V, Cruz-Hernández, TR, Carro-Rodríguez, J, Vargas-Hernández, MA, Ignacio-Mejía, I, Alfaro-Rodriguez, A, et al. 2023. Therapeutic potential of dopamine and related drugs as anti-inflammatories and antioxidants in neuronal and non-neuronal pathologies. Pharmaceutics, 15: 693.
- Bar, FMA, Sameti, M, Foudah, AI, Haque, A, Elsbaey, M. 2022. In vitro and in silico inhibition of COX-2 and 5-LOX by beta-carboline alkaloids from the seeds of *Peganum harmala* L. S. Afr. J. Bot, 147: 926-936.
- Batanouny, KH, Aboutabl, E, Shabana, M, Soliman, F. 1999. Wild medicinal plants in Egypt, Vol. 154. The Palm press, Cairo.
- Baziz, K, Maougal, RT, Amroune, A. 2020. An ethnobotanical survey of spontaneous plants used in traditional medicine in the region of Aures, Algeria. Eur. J. Ecol, 6: 51-68.
- Behl, T, Gupta, A, Albratty, M, Najmi, A, Meraya, AM, Alhazmi, HA, Bungau, SG. 2022. Alkaloidal phytoconstituents for diabetes management: exploring the unrevealed potential. Molecules, 27: 5851.
- Belhouala, K, Benarba, B. 2021. Medicinal plants used by traditional healers in Algeria: A multiregional ethnobotanical study. Front. Pharmacol, 12: 760492.
- Bellakhdar, J, Claisse, R, Fleurentin, J, Younos, C. 1991. Repertory of standard herbal drugs in the Moroccan pharmacopoea. J. Ethnopharmacol, 35: 123-143.
- Ben Menni, D, Belyagoubi-Benhammou, N, Abdelli, I, Bekkal Brikci, S, Benmahieddine, A, Ben Menni, H, Jafari, SM. 2024. Enzyme inhibitory, antioxidant and anti-inflammatory activities of *Anabasis articulata* phenolic-rich extract; *in vitro*, *in vivo*, and *in silico* studies. Plant Biosyst. Int. J. Deal. All Asp. Plant Biol, 158: 836-851.
- Ben Menni, D, Belyagoubi-Benhammou, N, Benmahieddine, A, Ben Menni, H, Gismondi, A, Monteleone, V, Di Marco, G, D'Agostino, A, Canini, A, Benamar, H, Atik-Bekkara, F. 2022. Identification of Sterols from *Anabasis articulata* (Forssk.) Moq. (Chenopodiaceae) Growing in Algeria and Study of Their Potential Bioactivity. Waste Biomass Valoriz, 13: 3283–3295.
- Benaiche, H, Bouredja, N, Alioua, A. 2019. Ethnobotanic study of medicinal plants used in Oran, Algeria. Bangladesh J. Bot, 48: 1163-1173.

- Benamar, H, Tomassini, L, Venditti, A, Marouf, A, Bennaceur, M, Serafini, M, Nicoletti, M. 2016. Acetylcholinesterase inhibitory activity of pyrrolizidine alkaloids from *Echium confusum* Coincy. Nat. Prod. Res, 31: 1-9.
- Benarba, B, Belabid, L, Righi, K, amine Bekkar, A, Elouissi, M, Khaldi, A, Hamimed, A. 2015. Ethnobotanical study of medicinal plants used by traditional healers in Mascara (North West of Algeria). J. Ethnopharmacol, 175: 626-637.
- Benhammou N, Belyagoubi L, Gismondi A, Di Marco G, Canini A, Atik-Bekkara F. 2019. GC/MS analysis, and antioxidant and antimicrobial activities of alkaloids extracted by polar and apolar solvents from the stems of Anabasis articulata. Med Chem Res. 28(5):754–767.
- Benhammou, N, Ghembaza, N, Benabdelkader, S, Atik-Bekkara, F, Kadifkova Panovska, T. 2013. Phytochemicals and antioxidant properties of extracts from the root and stems of *Anabasis articulata*. Int. Food Res. J, 20: 2057–2063.
- Benkrief, R, Brum-Bousquet, M, Tillequin, F, Koch, M. 1990. Alcaloïdes et flavonoïde des parties aériennes de *Hammada articulata* ssp. *scoparia* Alkaloids and flavonoid from aerial parts of *Hammada articulata* ssp. *scoparia*. Ann. Pharm. Fr, 48: 219–224.
- Benzie, IF, Strain, JJ. 1996. The ferric reducing ability of plasma (FRAP) as a measure of "antioxidant power": the FRAP assay. Anal. Biochem, 239: 70-76.
- Benzineb, E, Kambouche, N, Hamiani, A, Bellahouel, S, Zitouni, H, Toumi, H. 2019. Phenolics compounds and biological activity of leaves of *Anabasis articulata*, an Algerian medicinal Plant. Int. J. Pharm. Res. Allied Sci, 8: 1–5.
- Bhakkiyalakshmi, E, Sireesh, D, Ramkumar, KM. 2018. Redox sensitive transcription via Nrf2-Keap1 in suppression of inflammation. In: Immunity and Inflammation in Health and Disease. Academic Press, pp. 149-161.
- Bindu, S, Mazumder, S, Bandyopadhyay, U. 2020. Non-steroidal anti-inflammatory drugs (NSAIDs) and organ damage: A current perspective. Biochem. Pharmacol, 180: 114147.
- BIOVIA, DS. 2015. BIOVIA Discovery Studio Modeling Environment Release 4.5. Dassault Systèmes, San Diego.
- Bogucka-Kocka, A, Zalewski, D. 2017. Qualitative and quantitative determination of main alkaloids of *Chelidonium majus* L. using thin-layer chromatographic-densitometric method. Acta Chromatogr, 29: 385-397.

- Bouafia, M, Amamou, F, Gherib, M, Benaissa, M, Azzi, R, Nemmiche, S. 2021. Ethnobotanical and ethnomedicinal analysis of wild medicinal plants traditionally used in Naâma, southwest Algeria. Vegetos, 34: 654-662.
- Bouaziz, A, Mhalla, D, Zouari, I, Jlaiel, L, Tounsi, S, Jarraya, R, Trigui, M. 2016. Antibacterial and antioxidant activities of *Hammada scoparia* extracts and its major purified alkaloids. S. Afr. J. Bot, 105: 89–96.
- Boudjelal, A, Henchiri, C, Sari, M, Sarri, D, Hendel, N, Benkhaled, A, Ruberto, G. 2013. Herbalists and wild medicinal plants in M'Sila (North Algeria): An ethnopharmacology survey. J. Ethnopharmacol, 148: 395-402.
- Boutrif, O, Belyagoubi-Benhammou, N, Benmahieddine, A, Abbou, F, Di Marco, G, D'Agostino, A, Gismondi, A. 2024. Antioxidant and in vivo anti-inflammatory properties of alkaloid-rich fractions from the aerial parts of the Algerian *Anabasis articulata*. Plant Biosyst. Int. J. Deal. All Asp. Plant Biol, 158: 1264-1274.
- Bracca, ABJ, Kaufman, TS. 2004. Synthetic approaches to carnegine, a simple tetrahydroisoquinoline alkaloid. Tetrahedron, 60: 10575–10610.
- Brand-Williams, W, Cuvelier, ME, Berset, C. 1995. Use of free radical method to evaluate antioxidant activity. Lebensm. Wiss. Technol, 28: 25–30.
- Cheeke, PR. 1989. Toxicants of plant origin, Alkaloids (V.1). CRC Press, Boca Raton, p. 172.
- Chen, Q, Ruan, D, Shi, J, Du, D, Bian, C. 2023. The multifaceted roles of natural products in mitochondrial dysfunction. Front. Pharmacol, 14: 1093038.
- Cheng, F, Li, W, Zhou, Y, Shen, J, Wu, Z, Liu, G, Lee, PW, Tang, Y. 2012. AdmetSAR: A comprehensive source and free tool for assessment of chemical ADMET properties. J. Chem. Inf. Model, 52: 3099–3105.
- Cherrada, N, Elkhalifa Chemsa, A, Gheraissa, N, Zaater, A, Benamor, B, Ghania, A, Teferi Asres, D. 2024. Antidiabetic medicinal plants from the Chenopodiaceae family: a comprehensive overview. Int. J. Food Prop, 27: 194-213.
- Christodoulou, MI, Tchoumtchoua, J, Skaltsounis, AL, Scorilas, A, Halabalaki, M. 2019. Natural alkaloids intervening the insulin pathway: new hopes for anti-diabetic agents? Curr. Med. Chem, 26: 5982-6015.
- Corcuera, LJ. 1993. Biochemical basis of the resistance of the barley to aphids. Phytochemistry, 33: 741–747.

- Cuendet, M, Hostettmann, K, Potterat, O, Dyatmiko, W. 1997. Iridoid glucosides with free radical scavenging properties from *Fagraea blumei*. Helv. Chim. Acta, 80: 1144–1152.
- Cushnie, TT, Cushnie, B, Lamb, AJ. 2014. Alkaloids: An overview of their antibacterial, antibiotic-enhancing and antivirulence activities. Int. J. Antimicrob. Agents, 44: 377-386.
- Das, K, Iyer, KR, Orfali, R, Asdaq, SMB, Alotaibi, NS, Alotaibi, FS, Ghoneim, M. 2023. In silico studies and evaluation of in vitro antidiabetic activity of berberine from ethanol seed extract of *Coscinium fenestratum* (Gaertn.) Colebr. J. King Saud Univ. Sci, 35: 102666.
- De La Guardia, M, Armenta, S. 2011. Greening Sample Treatments. In: Comprehensive Analytical Chemistry. Elsevier, pp. 87–120.
- Dehimi, K, Djoudi, Z, Boulaouad, A, Maadadi, AR, Khennouf, S. 2020. A Contribution to the Valorization of Two Medicinal Plants: *Atriplex halimus* Sub. Sp. *schweinfurthii* and *Bunium incrassatum*, Growing in the Region of M'sila (North-East Algeria). Indian J. Novel Drug Deliv, 12: 208–216.
- Deng, JS, Chi, CS, Huang, SS, Shie, PH, Lin, TH, Huang, GJ. 2011. Antioxidant, analgesic, and anti-inflammatory activities of the ethanolic extracts of *Taxillus liquidambaricola*. J. Ethnopharmacol, 134: 1161–1171.
- Dhanani, T, Shah, S, Gajbhiye, NA, Kumar, S. 2017. Effect of extraction methods on yield, phytochemical constituents and antioxidant activity of *Withania somnifera*. Arab. J. Chem, 10: S1193–S1199.
- Djeridane, A, Hamdi, A, Bensania, W, Cheifa, K, Lakhdari, I, Yousfi, M. 2015. The *in vitro* evaluation of antioxidative activity, α-glucosidase and α-amylase enzyme inhibitory of natural phenolic extracts. Diabetes Metab. Syndr. Clin. Res. Rev, 9: 324–331.
- Du, H, Wang, Y, Yan, C, Zhou, LG, Hao, XJ. 2008. Alkaloids from *Anabasis aphylla* L. J. Asian Nat. Prod. Res, 10: 1093–1095.
- Ekor, M. 2014. Nephrotoxicity and nephroprotective potential of African medicinal plants. In: Toxicological Survey of African Medicinal Plants. Elsevier, pp. 357-393.
- El Dine, RS, Abdallah, HM, Kandil, ZA, Zaki, AA, Khan, SI, Khan, IA. 2019. PPARα and γ activation effects of new nor-triterpenoidal saponins from the aerial parts of *Anabasis articulata*. Planta Med, 85: 274-281.

- El-Haci, I, Atik-Bekkara, F, Mazari, W, Gherib, M. 2013. Phenolics content and antioxidant activity of some organic extracts of endemic medicinal plant *Anabasis aretioides* Coss. & Moq. From Algerian Sahara. Pharmacogn. J, 5: 108–112.
- ElNaggar, MH, Eldehna, WM, Abourehab, MA, Abdel Bar, FM. 2022. The old world salsola as a source of valuable secondary metabolites endowed with diverse pharmacological activities: a review. J. Enzyme Inhib. Med. Chem, 37: 2036-2062.
- El-Shazly, A, Wink, M. 2003. Tetrahydroisoquinoline and β-Carboline alkaloids from *Haloxylon articulatum* (Cav.) Bunge (Chenopodiaceae). Z. Naturforsch. C J. Biosci, 58: 477–480.
- Elwekeel, A, Hassan, MHA, Almutairi, E, AlHammad, M, Alwhbi, F, Abdel-Bakky, MS, Amin, E, Mohamed, EIA. 2023. Anti-inflammatory, anti-oxidant, GC-MS profiling and molecular docking analyses of non-polar extracts from five *Salsola* species. Separations, 10: 72.
- Fathoni, A, Hudiyono, S, Budianto, E, Cahyana, AH, Agusta, A. 2021. Metabolite detection and antibacterial activity of fungal endophytic extracts isolated from Brotowali (*Tinospora crispa*) plants using TLC-bioautography assay. In: IOP Conference Series: Materials Science and Engineering, Vol. 1011, p. 012041.
- Ferreira, LG, Dos Santos, RN, Oliva, G, Andricopulo, AD. 2015. Molecular docking and structure-based drug design strategies. Molecules, 20: 13384-13421.
- Ferreira, MJU. 2022. Alkaloids in future drug discovery. Molecules, 27: 1347.
- Floegel, A, Kim, DO, Chung, SJ, Koo, SI, Chun, OK. 2011. Comparison of ABTS/DPPH assays to measure antioxidant capacity in popular antioxidant-rich US foods. J. Food Comp. Anal, 24: 1043–1048.
- Forni, C, Facchiano, F, Bartoli, M, Pieretti, S, Facchiano, A, D'Arcangelo, D, Norelli, S, Valle, G, Nisini, R, Beninati, S, Tabolacci, C, Jadeja, RN. 2019. Beneficial role of phytochemicals on oxidative stress and age-related diseases. Biomed. Res. Int, 2019: 8748253.
- Furman, D, Campisi, J, Verdin, E, Carrera-Bastos, P, Targ, S, Franceschi, C, Slavich, GM. 2019. Chronic inflammation in the etiology of disease across the life span. Nat. Med, 25: 1822-1832.
- Gamal, G, Abo-El-Seoud, KA, Attia, G. 2021. Triterpenoids from the aerial parts of *Anabasis articulata* (Forssk) Moq: gastroprotective effect *in vivo* with *in silico* studies, cytotoxic and antimicrobial activities. Nat. Prod. Res, 36: 4076–4084.

- Gil, MI, Tomas-Barberan, FA, Hess-Pierce, B, Kader, AA. 2002. Antioxidant capacities, phenolic compounds, carotenoids, and vitamin C contents of nectarine, peach, and plum cultivars from California. J. Agric. Food Chem, 50: 4976–4982.
- Goura, K, Legrifi, I, Kallali, NS, Taoussi, M, Kenfaoui, J, Meddich, A, Lahlali, R. 2025. Beyond survival: The role of secondary metabolites in plant defense mechanisms. J. Crop Health, 77: 121.
- Haida, S, Kribii, A, Daoud, NA, Belakhmima, RA, Kribii, A. 2022. Antioxidant activity of *Haloxylon scoparium* alkaloid extracts from Figuig region (southeastern of Morocco). Braz. J. Pharm. Sci, 58: 1–13.
- Hammiche, V, Maiza, K. 2006. Traditional medicine in Central Sahara: pharmacopoeia of Tassili N'ajjer. J. Ethnopharmacol, 105: 358–367.
- Hannoodee, S, Nasuruddin, DN. 2024. Acute inflammatory response. In: StatPearls [Internet]. StatPearls Publishing.
- Harborne, JB. 1998. Phytochemical Methods: A guide to modern techniques of plant analysis. 3rd ed. Chapman and Hall, London, p. 303.
- Hashmi, MA, Khan, A, Farooq, U, Khan, S. 2018. Alkaloids as cyclooxygenase inhibitors in anticancer drug discovery. Curr. Protein Pept. Sci, 19: 292-301.
- Hayat, J, Akodad, M, Moumen, A, Baghour, M, Skalli, A, Ezrari, S, Belmalha, S. 2020. Phytochemical screening, polyphenols, flavonoids and tannin content, antioxidant activities and FTIR characterization of *Marrubium vulgare* L. from 2 different localities of Northeast of Morocco. Heliyon, 6: e05609.
- Heinrich, M, Mah, J, Amirkia, V. 2021. Alkaloids used as medicines: Structural phytochemistry meets biodiversity---An update and forward look. Molecules, 26: 1836.
- Hemmami, H, Seghir, BB, Zeghoud, S, Ben Amor, I, Kouadri, I, Rebiai, A, Atanassova, M. 2023. Desert endemic plants in Algeria: A review on traditional uses, phytochemistry, polyphenolic compounds and pharmacological activities. Molecules, 28: 1834.
- Hmidani, A, Bouhlali, EDT, Khouya, T, Ramchoun, M, Filali-zegzouti, Y, Benlyas, M, Alem, C. 2019. Effect of extraction methods on antioxidant and anticoagulant activities of *Thymus atlanticus* aerial part. Sci. Afr, 5: e00143.

- Hostettmann, K. 1999. Strategy for the biological and chemical evaluation of plant extracts. Invited lecture presented at the International Conference on Biodiversity and Bioresources: Conservation and Utilization. Phuket, Thailand; p. 23–37.
- Hostettmann, K, Terreaux, C, Marston, A, Potterat, O. 1997. The role of planar chromatography in the rapid screening and isolation of bioactive compounds from medicinal plants. Planar Chromatogr, 10: 251.
- Huang, D, Ou, B, Prior, RL. 2005. The chemistry behind antioxidant capacity assays. J. Agric. Food Chem, 53: 1841-1856.
- Hussain, T, Tan, B, Yin, Y, Blachier, F, Tossou, MC, Rahu, N. 2016. Oxidative stress and inflammation: what polyphenols can do for us? Oxid. Med. Cell. Longev, 2016: 7432797.
- Ibrayev, MK, Nurkenov, OA, Rakhimberlinova, ZB, Takibayeva, AT, Palamarchuk, IV, Turdybekov, DM, Kelmyalene, AA, Kulakov, IV. 2022. Synthesis, structure and molecular docking of new 4,5-dihydrothiazole derivatives based on 3,5-dimethylpyrazole and cytisine and salsoline alkaloids. Molecules, 27: 7598.
- Jan, M, Shah, AB, Al-Joufi, FA, Zahoor, M, Esa, M, Rashid, H, Shahzad, MS. 2025. Isolation, characterization, antidiabetic and antityrosinase potentials of compounds isolated from *Anabasis articulata*. Appl. Food Res, 5: 100949.
- Jarraya, RM, Bouaziz, A, Hamdi, B, Ben Salah, A, Damak, M. 2008. N-Methylisosalsoline from *Hammada scoparia*. Acta Crystallogr. Sect. E, 64: o1714–o1714.
- Jayaprakash, PT, Srinivasan, GJ, Amravaneswaran, MG. 2001. Cranio-facial morphoanalysis: a new method for enhancing reliability while identifying skulls by photo superimposition. Forensic Sci. Int, 117: 121–143.
- Ji, J, Yuan, M, Ji, RR. 2023. Inflammation and pain. In: Neuroimmune interactions in pain: mechanisms and therapeutics. Cham: Springer International Publishing, pp. 17-41.
- Kahn, SE. 2003. The relative contributions of insulin resistance and beta-cell dysfunction to the pathophysiology of Type 2 diabetes. Diabetologia, 46: 3-19.
- Kambouche, N, Merah, B, Derdour, A, Bellahouel, S, Bouayed, J, Dicko, A, Younos, C, Soulimani, R. 2009. Hypoglycemic and antihyperglycemic effects of *Anabasis articulata* (Forssk) Moq (Chenopodiaceae), an Algerian medicinal plant. Afr. J. Biotechnol, 8: 5589–5594.

- Kandikattu, K, Kumar, PBR, Priya, RV, Kumar, KS, Rathore, RSB. 2013. Evaluation of anti-inflammatory activity of *Canthium parviflorum* by *in-vitro* method. Indian J. Res. Pharm. Biotechnol, 1: 729–731.
- Katzung, B, Trevor, AJ. 2014. Basic and Clinical Pharmacology. 13th ed. Mc Graw Hill Education, Lange, p. 1216.
- Kaur, N, Kaur, N, Saggoo, MIS. 2022. Conservation strategies for medicinal plants in the face of environmental challenges. In: Environmental challenges and medicinal plants: Sustainable production solutions under adverse conditions. Cham: Springer International Publishing, pp. 461-485.
- Kitchen, DB, Decornez, H, Furr, JR, Bajorath, J. 2004. Docking and scoring in virtual screening for drug discovery: methods and applications. Nat. Rev. Drug Discov, 3: 935-949.
- Kulp, M, Bragina, O, Kogerman, P, Kaljurand, M. 2011. Capillary electrophoresis with led-induced native fluorescence detection for determination of isoquinoline alkaloids and their cytotoxicity in extracts of *Chelidonium majus* L. J. Chromatogr. A, 1218: 5298-5304.
- Kumar, S, Narwal, S, Kumar, V, Prakash, O. 2011. α-glucosidase inhibitors from plants: A natural approach to treat diabetes. Pharmacogn. Rev, 5: 19.
- Kumar, S, Sharma, S, Vasudeva, N. 2013. Screening of antidiabetic and antihyperlipidemic potential of oil from *Piper longum* and piperine with their possible mechanism. Expert Opin. Pharmacother, 14: 1723-1736.
- Kumari, K, Adhikari, P, Pandey, A, Samant, SS, Lal, M, Pande, V. 2024. Influence of Solvent Polarity on Phytochemicals, Antioxidants, and Antimicrobial Properties of *Delphinium denudatum*: A Medicinal Herb from Sainj Valley, Himachal Pradesh, India. Bioactivities, 2: 30-40.
- Kuznetsova, NN, Abdullaeva, LK, Sadikov, AA. 2005. Comparative action of salsoline, salsolidine, and related compounds on KML tissue culture and animal tumor strains. Chem. Nat. Compd, 41: 234–235.
- Laine, L, Curtis, SP, Cryer, B, Kaur, A, Cannon, CP. 2007. Assessment of upper gastrointestinal safety of etoricoxib and diclofenac in patients with osteoarthritis and rheumatoid arthritis in the Multinational Etoricoxib and Diclofenac Arthritis Long-term (MEDAL) programme: a randomised comparison. Lancet, 369: 465-473.

- Laine, L, White, WB, Rostom, A, Hochberg, M. 2008. COX-2 selective inhibitors in the treatment of osteoarthritis. In: Seminars in arthritis and rheumatism, Vol. 38, No. 3, pp. 165-187. WB Saunders.
- Lauterbach, M, Veranso-Libalah, MC, Sukhorukov, AP, Kadereit, G. 2019. Biogeography of the xerophytic genus *Anabasis* L.(Chenopodiaceae). Ecol. Evol, 9: 3539-3552.
- Lee, J, Chung, H, Chang, PS, Lee, J. 2007. Development of a method predicting the oxidative stability of edible oils using 2, 2-diphenyl-1-picrylhydrazyl (DPPH). Food Chem, 103: 662-669.
- Leite, FC, Ribeiro-Filho, J, Costa, HF, Salgado, PRR, Calheiros, AS, Carneiro, AB, Piuvezam, MR. 2014. Curine, an alkaloid isolated from *Chondrodendron platyphyllum* inhibits prostaglandin E2 in experimental models of inflammation and pain. Planta Med, 80: 1072-1078.
- Leong, LP, Shui, G. 2002. An investigation of antioxidant capacity of fruits in Singapore markets. Food Chem, 76: 69–75.
- Li, WX, Li, YF, Zhai, YJ, Chen, WM, Kurihara, H, He, RR. 2013. Theacrine, a purine alkaloid obtained from *Camellia assamica* var. *kucha*, attenuates restraint stress-provoked liver damage in mice. J. Agric. Food Chem, 61: 6328-6335.
- Lombardi, T, Bertacchi, A, Pistelli, L, Pardossi, A, Pecchia, S, Toffanin, A, Sanmartin, C. 2022. Biological and agronomic traits of the main halophytes widespread in the Mediterranean region as potential new vegetable crops. Horticulturae, 8: 195.
- Luo, Y, Liu, M, Yao, X, Xia, Y, Dai, Y, Chou, G, Wang, Z. 2009. Total alkaloids from Radix Linderae prevent the production of inflammatory mediators in lipopolysaccharide-stimulated RAW 264.7 cells by suppressing NF-κB and MAPKs activation. Cytokine, 46: 104-110.
- Maatalah, MB, Bouzidi, NK, Bellahouel, S, Merah, B, Fortas, Z, Soulimani, R, Saidi, S, Derdour, A. 2012. Antimicrobial activity of the alkaloids and saponin extracts of *Anabasis articulata*. E3 J. Biotechnol. Pharm. Res, 3: 54–57.
- Magalhães, LM, Segundo, MA, Reis, S, Lima, JL. 2008. Methodological aspects about *in vitro* evaluation of antioxidant properties. Anal. Chim. Acta, 613: 1-19.

- Mahomoodally, MF, Aumeeruddy, MZ, Legoabe, LJ, Dall'Acqua, S, Zengin, G. 2022. Plants' bioactive secondary metabolites in the management of sepsis: Recent findings on their mechanism of action. Front. Pharmacol, 13: 1046523.
- Makhlouf, Y, Bouaziz, A, Benazi, N, Djidel, S, Bentahar, A, Barghout, N, Dahamna, S. 2024. Assessment of antioxidant and antiinflammatory activities and acute toxicity of the aqueous extract from a mixture of leaves and flowers of *Anabasis articulata* (Forssk.) Moq. Arch. Biol. Sci, 76: 161-174.
- Makhlouf, Y, Bouaziz, A, Benyah lou, ZD, Boussebaa, W, Benazi, N, Yahiaoui, S, Saliha, D. 2024. LC-MS/MS ANALYSIS, *IN VITRO, IN VIVO* AND *IN SILICO* ANTI-INFLAMMATORY EVALUATION OF *ANABASIS ARTICULATA* (FORSSK.) MOQ. EXTRACTS. Cellul. Chem. Technol, 58: 1099-1112.
- Makhlouf, Y, Bouaziz, A, Hasnaoui, C, Zourgui, L, Dab, H, Yahia, B, Dahamna, S. 2025. Mechanisms of gastroprotective effects of *Anabasis articulata* (Forssk.) Moq. decoction against ethanol-induced gastric mucosal injury in rats. Arch. Biol. Sci, (00): 9-9.
- Markom, M, Hasan, M, Daud, W, Singh, H, Jahim, J. 2007. Extraction of hydrolysable tannins from *Phyllanthus niruri* Linn.: Effects of solvents and extraction methods. Sep. Purif. Technol, 52: 487–496.
- Matsuura, HN, Fett-Neto, AG. 2015. Plant alkaloids: main features, toxicity, and mechanisms of action. In: Plant toxins. Springer, Dordrecht, pp. 1-15.
- Medzhitov, R. 2008. Origin and physiological roles of inflammation. Nature, 454: 428-435.
- Meng, XY, Zhang, HX, Mezei, M, Cui, M. 2011. Molecular docking: a powerful approach for structure-based drug discovery. Curr. Comput. Aided Drug Des, 7: 146-157.
- Metrouh-Amir, H, Amir, N. 2018. Evaluation *in vivo* of anti-inflammatory and analgesic properties of *Matricaria pubescens* alkaloids. S. Afr. J. Bot, 116: 168-174.
- Miller, NJ, Rice-Evans, CA. 1997. Factors influencing the antioxidant activity determined by the ABTS + radical cation assay. Free Radic. Res, 26: 195–199.
- Mirkov, I, Stojković, D, Aleksandrov, AP, Ivanov, M, Kostić, M, Glamočlija, J, Soković, M. 2020. Plant extracts and isolated compounds reduce parameters of oxidative stress induced by heavy metals: an up-to-date review on animal studies. Curr. Pharm. Des, 26: 1799-1815.

- Mittal, M, Siddiqui, MR, Tran, K, Reddy, SP, Malik, AB. 2014. Reactive oxygen species in inflammation and tissue injury. Antioxid. Redox Signal, 20: 1126-1167.
- Mohammed, HA, Alshalmani, SK, Abdellatif, AG. 2013. Antioxidant and quantitative estimation of phenolic and flavonoids of three halophytic plants growing in Libya. J. Pharmacog. Photochem, 2: 89-94.
- Mondal, M, Hossain, MM, Rahman, MA, Saha, S, Uddin, N, Hasan, MR, Mubarak, MS. 2019. Hepatoprotective and antioxidant activities of *Justicia gendarussa* leaf extract in carbofuran-induced hepatic damage in rats. Chem. Res. Toxicol, 32: 2499-2508.
- Monteleone, V, Menni, DB, Belyagoubi-Benhammou, N, Di Marco, G, Canini, A, Gismondi, A. 2024. *Anabasis articulata* (Forssk.) Moq. food aqueous extract triggers oxidative stress-induced senescence and reduces metastatic power in MDA-MB-231 cells. J. Funct. Foods, 116: 106203.
- Morteza-Semnani, K. 2015. A Review on *Chenopodium botrys* L.: traditional uses, chemical composition and biological activities. Pharm. Biomed. Res, 1: 1-9.
- Munir, U, Perveen, A, Qamarunnisa, S. 2014. Comparative Pharmacognostic evaluation of some species of the genera *Suaeda* and *Salsola* leaf (Chenopodiaceae). Pak. J. Pharm. Sci, 27: 1363-1370.
- Ncube, B, Nair, JJ, Rárová, L, Strnad, M, Finnie, JF, Van Staden, J. 2015. Seasonal pharmacological properties and alkaloid content in *Cyrtanthus contractus* NE Br. S. Afr. J. Bot, 97: 69-76.
- Newman, DJ, Cragg, GM. 2016. Natural products as sources of new drugs from 1981 to 2014. J. Nat. Prod, 79: 629-661.
- Nirmala, AR, Permatasari, L, Muliasari, H, Deccati, RF. 2023. analysis of optimal conditions of bovine serum albumin (BSA) protein denaturation inhibition method in anti-inflammatory activity testing of various plant leaf extracts. J. Agritechnol. Food Process, 3: 101-113.
- O'leary, JW, Glenn, EP. 2021. Global distribution and potential for halophytes. In: Halophytes as a Resource for Livestock and for Rehabilitation of Degraded Lands. Springer Netherlands, Dordrecht, pp. 7-17.
- Okhale, SE, Egharevba, HO, Ona, EC, Kunle, OF. 2012. Phytochemicaland proximate analyses and thin layer chromatography fingerprinting of the aerial part of

Chenopodium ambrosioides Linn.(Chenopodiaceae). J. Med. Plants Res, 6: 2289-2294.

- Oray, M, Abu Samra, K, Ebrahimiadib, N, Meese, H, Foster, CS. 2016. Long-term side effects of glucocorticoids. Expert Opin. Drug Saf, 15: 457-465.
- Oyaizu, M. 1986. Studies on products of browning reaction: antioxidative activity of products of browning reaction prepared from glucosamine. Jpn. J. Nutr. Diet, 44: 307–315.
- Ozenda, P. 2004. Flore et végétation du Sahara. 3ème édition, CNRS Editions, Paris.
- Parbuntari, H, Prestica, Y, Gunawan, R, Nurman, MN, Adella, F. 2018. Preliminary phytochemical screening (qualitative analysis) of cacao leaves (*Theobroma cacao* L.). Eksakta Berkala Ilmiah Bidang MIPA, 19: 40-45.
- Pascual, ME, Carretero, ME, Slowing, KV, Villar, A. 2002. Simplified Screening by TLC of Plant Drugs. Pharm. Biol, 40: 139–143.
- Phaniendra, A, Jestadi, DB, Periyasamy, L. 2015. Free radicals: properties, sources, targets, and their implication in various diseases. Indian J. Clin. Biochem, 30: 11-26.
- Prieto, P, Pineda, M, Aguilar, M. 1999. Spectrophotometric quantitation of antioxidant capacity through the formation of a phosphomolybdenum complex: specific application to the determination of vitamin E. Anal. Biochem, 269: 337–341.
- Prior, RL, Wu, X, Schaich, K. 2005. Standardized Methods for the Determination of Antioxidant Capacity and Phenolics in Foods and Dietary Supplements. J. Agric. Food Chem, 53: 4290–4302.
- Pulido, R, Bravo, L, Saura-Calixto, F. 2000. Antioxidant activity of dietary polyphenols as determined by a modified ferric reducing/antioxidant power assay. J. Agric. Food Chem, 48: 3396-3402.
- Rahman, N, Muhammad, I, Khan, H, Aschner, M, Filosa, R, Daglia, M. 2019. Molecular docking of isolated alkaloids for possible α-glucosidase inhibition. Biomolecules, 9: 544.
- Rates, SMK. 2001. Plants as source of drugs. Toxicon, 39: 603-613.
- Re, R, Pellegrini, N, Proteggente, A, Pannala, A, Yang, M, Rice-Evans, C. 1999. Antioxidant activity applying an improved ABTS radical cation decolorization assay. Free Radic. Biol. Med, 26: 1231–1237.

- Reddi, KK, Li, H, Li, W, Tetali, SD. 2021. Berberine, a phytoalkaloid, inhibits inflammatory response induced by LPS through NF-kappaβ pathway: possible involvement of the IKKα. Molecules, 26: 4733.
- Rocha, JA, Rego, NC, Carvalho, BT, Silva, FI, Sousa, JA, Ramos, RM, Lima, FC. 2018. Computational quantum chemistry, molecular docking, and ADMET predictions of imidazole alkaloids of *Pilocarpus microphyllus* with schistosomicidal properties. PLoS One, 13: e0198476.
- Sadykov, AS, Tumur, B. 1960. The alkaloids of *Anabasis aphylla* var. *iljinii*. Doklady Akad. Nauk Uz. SSR Proc Acad Sci Uzbek SSR, 1: 27–29.
- Saeedi, P, Petersohn, I, Salpea, P, Malanda, B, Karuranga, S, Unwin, N, IDF Diabetes Atlas Committee. 2019. Global and regional diabetes prevalence estimates for 2019 and projections for 2030 and 2045: Results from the International Diabetes Federation Diabetes Atlas. Diabetes Res. Clin. Pract, 157: 107843.
- Saini, A, Seni, K, Chawla, PA, Chawla, V, Ganti, SS. 2024. An insight into recent updates on analytical techniques for bioactive alkaloids. Phytochem. Anal, 35: 423-444.
- Salehi, B, Ata, A, V. Anil Kumar, N, Sharopov, F, Ramirez-Alarcon, K, Ruiz-Ortega, A, Sharifi-Rad, J. 2019. Antidiabetic potential of medicinal plants and their active components. Biomolecules, 9: 551.
- Sales, PM, Souza, PM, Simeoni, LA, Magalhães, PO, Silveira, D. 2012. α-Amylase inhibitors: a review of raw material and isolated compounds from plant source. J. Pharm. Pharm. Sci, 15: 141-183.
- Sathiyamoorthy, P, Lugasi-Evgi, H, Van-Damme, P, Abu-Rabia, A, Gopas, J, Golan-Goldhirsh, A. 1997. Larvicidal activity in desert plants of the Negev and Bedouin market plant products. Int. J. Pharmacogn, 35: 265–273.
- Scalbert, A, Manach, C, Morand, C, Rémésy, C, Jiménez, L. 2005. Dietary polyphenols and the prevention of diseases. Crit. Rev. Food Sci. Nutr, 45: 287–306.
- Seal, S, Kar, S, Pal, S, Datta, S, Debnath, A, Bannerji, S, Sinha, D. 2024. Alkaloids of Natural Origin with Promising Anti-Diabetic Properties. Adv. Pharmacogn. Phytochem. Diabetes, 61.
- Senhaji, S, Lamchouri, F, Toufik, H. 2020. Phytochemical content, antibacterial and antioxidant potential of endemic plant *Anabasis aretioides* Coss. & Moq. (Chenopodiaceae). Biomed. Res. Int, 2020: 1–16.

- Shegebayev, Z, Turgumbayeva, A, Datkhayev, U, Zhakipbekov, K, Kalykova, A, Kartbayeva, E, Beyatli, A, Tastambek, K, Altynbayeva, G, Dilbarkhanov, B, Akhelova, A, Anarbayeva, R, Orynbassarova, K. 2023. Pharmacological properties of four plant species of the genus *Anabasis* Amaranthaceae. Molecules, 28: 4454.
- Sies, H. 2015. Oxidative stress: a concept in redox biology and medicine. Redox Biol, 4: 180-183.
- Singh, PA, Dash, S, Choudhury, A, Bajwa, N. 2024. Factors affecting long-term availability of medicinal plants in India. J. Crop Sci. Biotechnol, 27: 145-173.
- Sobiech, M, Giebułtowicz, J, Luliński, P. 2020. Application of magnetic core-shell imprinted nanoconjugates for the analysis of hordenine in human plasma-preliminary data on pharmacokinetic study after oral administration. J. Agric. Food Chem, 68: 14502–14512.
- Sommer, T, Göen, T, Budnik, N, Pischetsrieder, M. 2020. Absorption, biokinetics, and metabolism of the dopamine D2 receptor agonist hordenine (N,N-dimethyltyramine) after beer consumption in humans. J. Agric. Food Chem, 68: 1998–2006.
- Sostres, C, Gargallo, CJ, Arroyo, MT, Lanas, A. 2010. Adverse effects of non-steroidal anti-inflammatory drugs (NSAIDs, aspirin and coxibs) on upper gastrointestinal tract. Best Pract. Res. Clin. Gastroenterol, 24: 121-132.
- Spiegel, M, Kapusta, K, Kołodziejczyk, W, Saloni, J, Żbikowska, B, Hill, GA, Sroka, Z. 2020. Antioxidant activity of selected phenolic acids--ferric reducing antioxidant power assay and QSAR analysis of the structural features. Molecules, 25: 3088.
- Sreevidya, N, Mehrotra, S. 2003. Spectrophotometric method for estimation of alkaloids precipitable with Dragendorff's reagent in plant materials. J. AOAC Int, 86: 1124-1127.
- Sultana, B, Anwar, F, Ashraf, M. 2009. Effect of extraction solvent/technique on the antioxidant activity of selected medicinal plant extracts. Molecules, 14: 2167-2180.
- Tavares, L, Pimpao, R, McDougall, G, Stewart, D, Ferreira, RB, Santos, CN. 2013. Elucidating Phytochemical Production in *Juniperus* sp.: Seasonality and Response to Stress Situations. J. Agric. Food Chem, 61: 4044-4052.
- Tefarikis, DT, Morales-Briones, DF, Yang, Y, Edwards, G, Kadereit, G. 2022. On the hybrid origin of the C2 *Salsola divaricata* agg. (Amaranthaceae) from C3 and C4 parental lineages. New Phytol, 234: 1876–1890.

- Teow, CC, Truong, VD, McFeeters, RF, Thompson, RL, Pecota, KV, Yencho, GC. 2007. Antioxidant activities, phenolic and b-carotene contents of sweet potato genotypes with varying flesh colours. Food Chem, 103: 829–838.
- Thalapaneni, NR, Chidambaram, KA, Ellappan, T, Sabapathi, ML, Mandal, SC. 2008. Inhibition of carbohydrate digestive enzymes by *Talinum portulacifolium* (Forssk) leaf extracts. J. Complement. Integr. Med, 5: 1-8.
- Thawabteh, A, Juma, S, Bader, M, Karaman, D, Scrano, L, Bufo, SA, Karaman, R. 2019. The biological activity of natural alkaloids against herbivores, cancerous cells and pathogens. Toxins, 11: 656.
- Tintu, I, Dileep, KV, Augustine, A, Sadasivan, C. 2012. An isoquinoline alkaloid, berberine, can inhibit fungal alpha amylase: enzyme kinetic and molecular modeling studies. Chem. Biol. Drug Des, 80: 554–560.
- Trease, GE, Evans, WC. 2002. Pharmacognosy. 15th ed. WB Saunders, Edinburgh, New York, p. 246–249, 391-393.
- Trott, O, Olson, AJ. 2010. AutoDock Vina: improving the speed and accuracy of docking with a new scoring function, efficient optimization, and multithreading. J. Comput. Chem, 31: 455-461.
- Tsai, DS, Huang, MH, Tsai, JC, Chang, YS, Chiu, YJ, Lin, YC, Wu, LY, Peng, WH. 2015. Analgesic and anti-Inflammatory activities of *Rosa taiwanensis* Nakai in mice. J. Med. Food, 18: 592-600.
- Tundis, R, Menichini, F, Conforti, F, Loizzo, MR, Bonesi, M, Statti, G, Menichini, F. 2009. A potential role of alkaloid extracts from *Salsola* species (Chenopodiaceae) in the treatment of Alzheimer's disease. J. Enzyme Inhib. Med. Chem, 24: 818–824.
- Van De Waterbeemd, H, Gifford, E. 2003. ADMET *in silico* modelling: towards prediction paradise? Nat. Rev. Drug Discov, 2: 192-204.
- Varela, C, Silva, F, Costa, G, & Cabral, C. 2023. Alkaloids: Their relevance in cancer treatment. In New insights into glioblastoma. Academic Press (pp. 361-401).
- Wang, YY, Yang, XR, Zheng, XQ, Li, J, Ye, CX, Song, XH. 2010. Theacrine, a purine alkaloid with anti-inflammatory and analgesic activities. Fitoterapia, 81: 627-631.
- Wijngaard, H, Hossain, MB, Rai, DK, Brunton, N. 2012. Techniques to extract bioactive compounds from food by-products of plant origin. Food Res. Int, 46: 505–513.

- Winter, CA, Risley, EA, Nuss, GW. 1962. Carrageenan-induced edema in hind paw of the rat as an assay for anti-inflammatory drugs. Proc. Soc. Exp. Biol. Med, 111: 544-547.
- World Health Organization. 2013. WHO traditional medicine strategy 2014--2023. World Health Organization.
- Xu, M, Xiao, Y, Yin, J, Hou, W, Yu, X, Shen, L, Jia, W. 2014. Berberine promotes glucose consumption independently of AMP-activated protein kinase activation. PLoS One, 9: e103702.
- Yang, H, Lou, C, Sun, L, Li, J, Cai, Y, Wang, Z, Tang, Y. 2019. admetSAR 2.0: web-service for prediction and optimization of chemical ADMET properties. Bioinformatics, 35: 1067-1069.
- Yang, M, Wang, Y, Fan, Z, Xue, Q, Njateng, GSS, Liu, Y, Cheng, G. 2021. Chemical constituents and anti-inflammatory activity of the total alkaloid extract from *Melodinus cochinchinensis* (Lour.) Merr. and its inhibition of the NF-κB and MAPK signaling pathways. Phytomedicine, 91: 153684.
- Yin, J, Gao, Z, Liu, D, Liu, Z, Ye, J. 2008. Berberine improves glucose metabolism through induction of glycolysis. Am. J. Physiol. Endocrinol. Metab, 294: E148-E156.
- Youcef, H, Lamine, BM, Hocine, B, Rabah, M, Ali, L, Mohamed, B. 2012. Diversity of halophyte desert vegetation of the different saline habitats in the valley of Oued Righ, Low Sahara Basin, Algeria. Res. J. Environ. Earth Sci, 4: 308-315.
- Yubin, JI, Miao, Y, Bing, W, Yao, Z. 2014. The extraction, separation and purification of alkaloids in the natural medicine. J. Chem. Pharm. Res, 6: 338-345.
- Zakharov, VP, Aslanov, KA, Ishbaev, AI, Sadykov, AS, Yankovskii, BA. 1974. The separation of the alkaloids of *Anabasis aphylla*. Chem. Nat. Compd, 10: 474–476.
- Zhang, M, An, C, Gao, Y, Leak, RK, Chen, J, Zhang, F. 2013. Emerging roles of Nrf2 and phase II antioxidant enzymes in neuroprotection. Prog. Neurobiol, 100: 30-47.
- Zhao, F, Gao, Z, Jiao, W, Chen, L, Chen, L, Yao, X. 2012. *In vitro* anti-inflammatory effects of beta-carboline alkaloids, isolated from *Picrasma quassioides*, through inhibition of the iNOS pathway. Planta Med, 78: 1906–1911.

Appendices

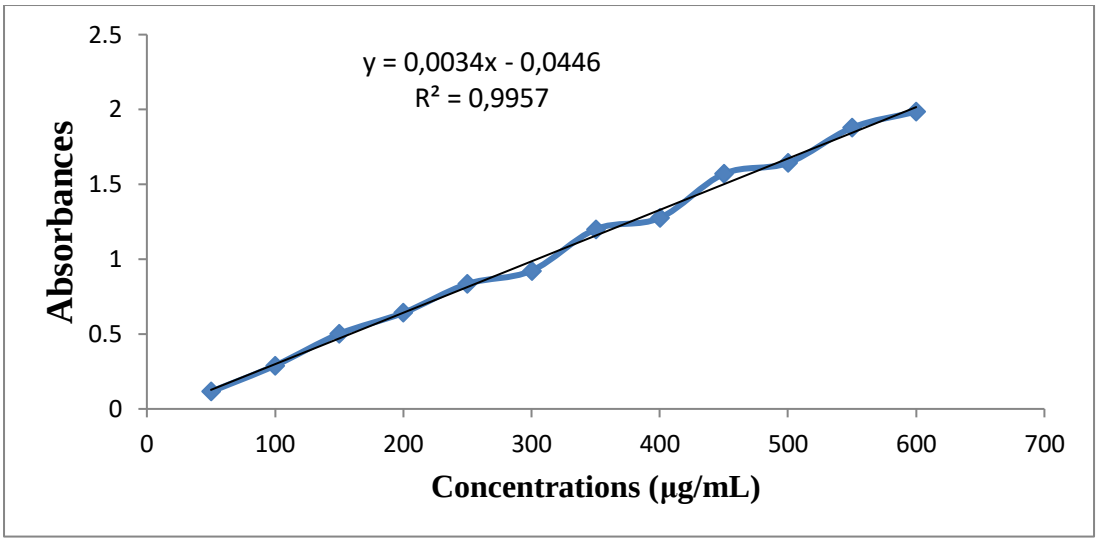

Appendice 1. Calibration curve of ascorbic acid for the total antioxidant capacity.

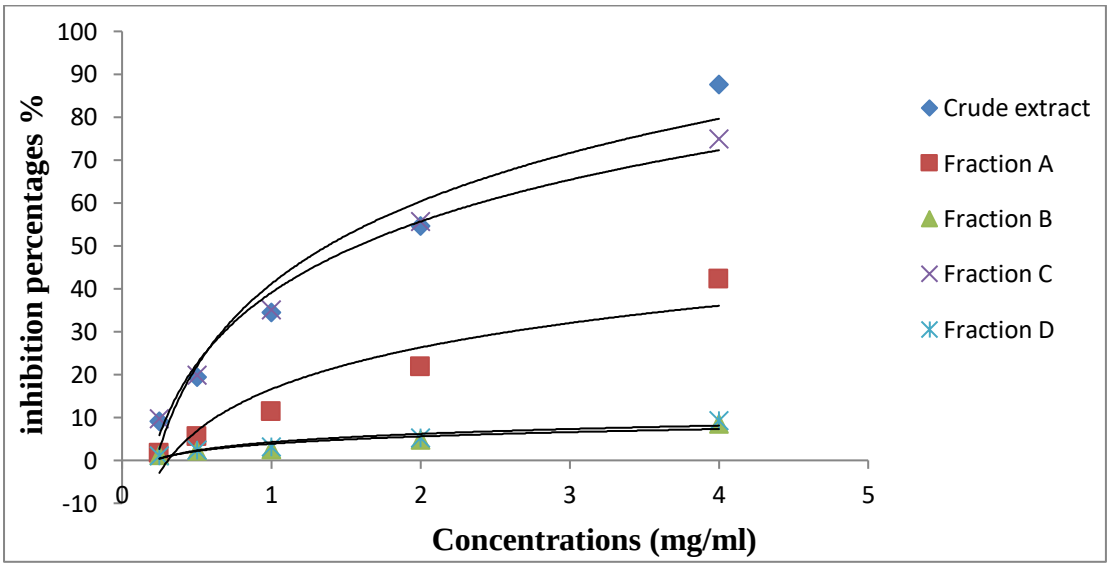

Appendice 2. Percentages of inhibition of DPPH˙ free radical as a function of the concentrations.

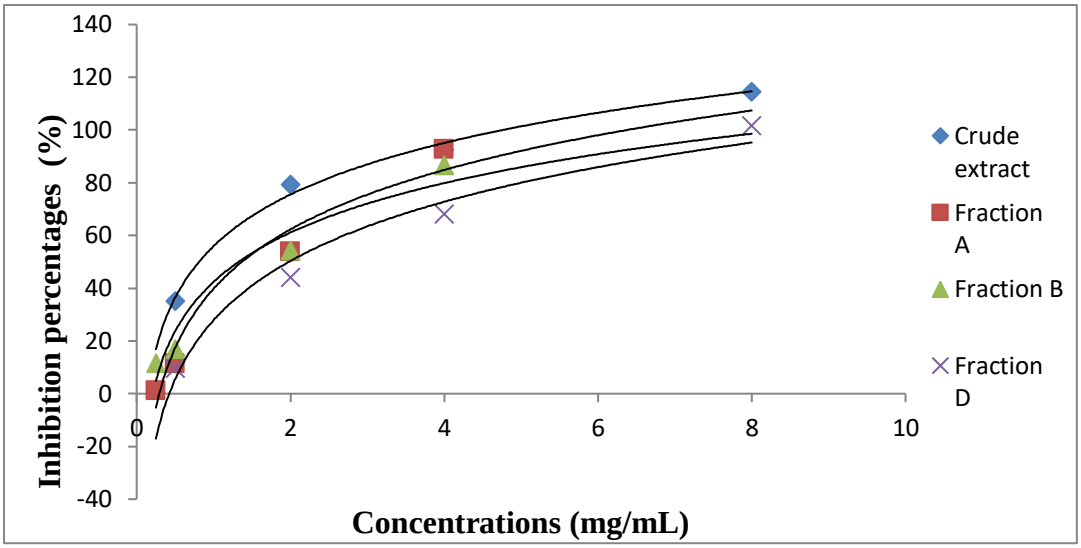

Appendice 3. Percentages of inhibition of $ABTS^{\bullet+}$ free radical as a function of the concentrations of the crude extract of *Anabasis atriculata* and fractions A, B and D.

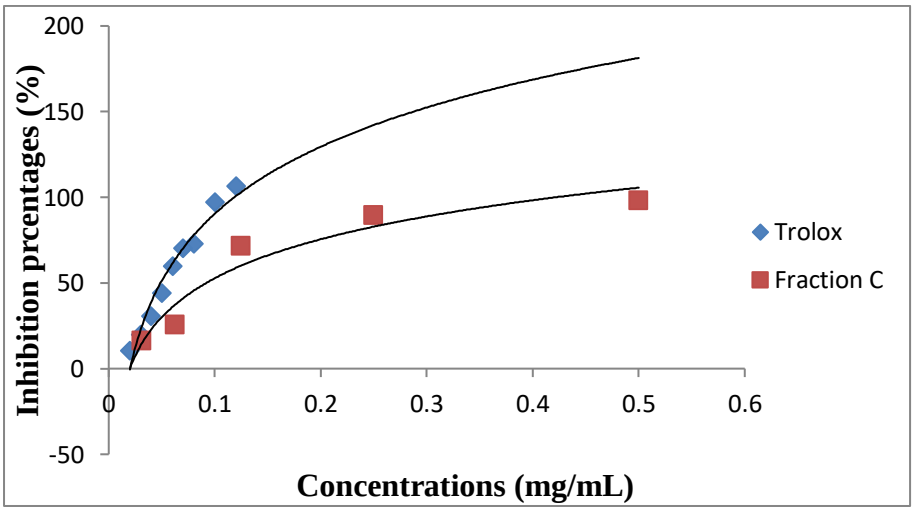

Appendice 4. Percentages of inhibition of $ABTS^{\bullet+}$ free radical of the fraction C of *Anabasis atriculata* compared to Trolox.

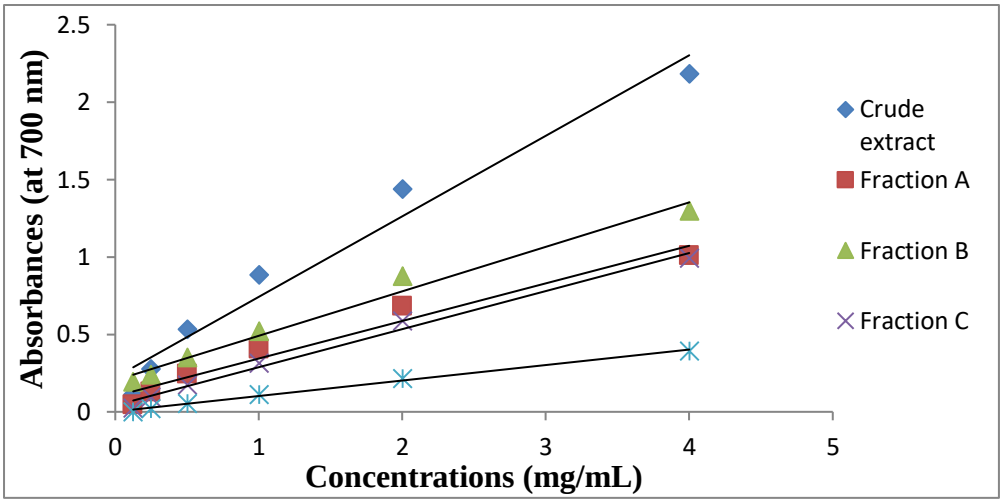

Appendice 5. Ferric reducing power absorbance as a function of the concentrations of the crude extract and its fractions of *A. articulata*.

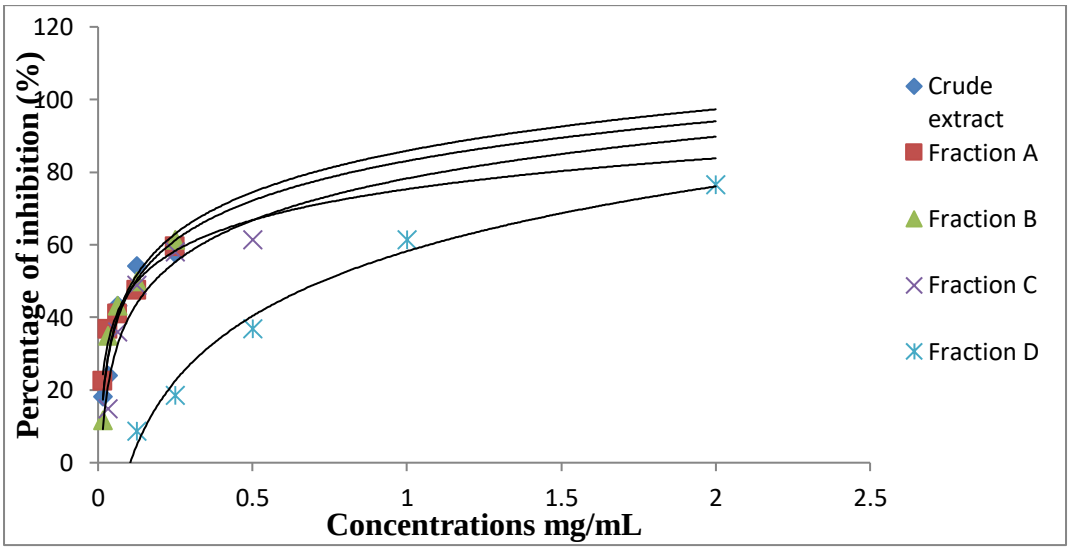

Appendice 6. Percentages of inhibition of α-amylase as a function of different concentrations of the crude extract and its fractions of the aerial part of *A. articulata*.